

Rochester Institute of Technology

**RIT Digital Institutional Repository**

---

Theses

---

1974

## **Development and applications of a quadratic isoparametric finite element for axisymmetric stress and deflection analysis**

F. X. Janucik

Follow this and additional works at: <https://repository.rit.edu/theses>

---

### **Recommended Citation**

Janucik, F. X., "Development and applications of a quadratic isoparametric finite element for axisymmetric stress and deflection analysis" (1974). Thesis. Rochester Institute of Technology. Accessed from

This Thesis is brought to you for free and open access by the RIT Libraries. For more information, please contact [repository@rit.edu](mailto:repository@rit.edu).

DEVELOPMENT AND APPLICATIONS OF A QUADRATIC ISOPARAMETRIC  
FINITE ELEMENT FOR AXISYMMETRIC STRESS AND DEFLECTION ANALYSIS

by

F. X. Janucik

A Thesis Submitted  
in  
Partial Fulfillment  
of the  
Requirements for the Degree of  
MASTER OF SCIENCE  
in  
Mechanical Engineering

Approved by:

Prof. Neville Rieger  
Thesis Advisor  
Dr. Robert McCalley Jr.  
(External Reviewer)  
Prof. B. Karlekar  
Prof. Richard B. Hetnarski  
Prof. Robert M Desmond  
(Department Head)

DEPARTMENT OF MECHANICAL ENGINEERING  
ROCHESTER INSTITUTE OF TECHNOLOGY  
ROCHESTER, NEW YORK

June, 1974

692062

## ACKNOWLEDGEMENTS

The author would like to express his appreciation to those who have assisted him during the course of this investigation and in particular:

To Professor N. F. Rieger, his thesis advisor, for his interest and guidance of the author's thesis research and for the profound effect that association with him has had on the author's professional career.

To Dr. R. B. McCalley, Jr., external thesis examiner, for his continued interest, insight, and encouragement in the author's thesis research.

To Dr. J. F. Loeber and Mr. T. Glasser, Knolls Atomic Power Laboratory, for their insight, suggestions, and assistance concerning this investigation.

To Professors B. Karlekar, R. Hetnarski, W. Halbleib, M. Sherman, and W. Walters, Rochester Institute of Technology, Mechanical Engineering Department, for their interest, suggestions, and encouragement concerning this thesis research.

To the author's wife Barbara for her encouragement and patience.

To Mrs. B. Engle for her superior job in typing the final manuscript of this investigation.

## ABSTRACT

The theory and computer program for an axisymmetric finite element for static stress and deflection analysis is presented. The element is an eight noded isoparametric quadrilateral based on the displacement method which is capable of representing quadratic variation of element boundaries and displacements. Element stiffness properties are developed for linear elastic small displacement theory using homogeneous isotropic material. Test cases are compared with theoretical solutions from the theory of elasticity to identify program capabilities and limitations.

Ability to analyse axisymmetric problems and to represent curved element boundaries has been demonstrated. Example problems including a cylindrical pressure vessel, a disk of uniform thickness subjected to centrifugal body force, and stress concentrations in a cylindrical rod due to a spherical inclusion are presented. In each of these cases program predicted deflection and stress values were within 2% of theoretical values.

Limitations which have been identified include the prediction of discontinuous stresses at adjacent element boundaries, failure to match original element boundary stress conditions in substructure analyses, and the necessity of double precision calculations to correctly analyse

problems whose theoretical solutions obey small displacement plate theory. Analysis of a spherical pressure vessel resulted in predicted displacements within 4% of theoretical values while stresses on element boundaries varied by 60% from theoretical values. Substructure analysis for the spherical inclusion problem resulted in prediction of boundary stresses which were incompatible with those originally obtained. Techniques to overcome this difficulty are proposed but are not tested. The inability to obtain reasonable results for flexural problems was found to be due to round off error in the single precision technique used for solving the structure equilibrium relations. Use of double precision calculations resulted in displacements and stresses within .25% and 4.% respectively of theory for the case of a clamped circular plate loaded by a uniform pressure normal to its surface.

## TABLE OF CONTENTS

	PAGE
i List of Figures	i
iii List of Tables	iii
iv Nomenclature	iv
1.0 INTRODUCTION	1
2.0 LITERATURE SURVEY	3
3.0 BASIC STEPS OF THE FINITE ELEMENT DISPLACEMENT METHOD	7
4.0 DEVELOPMENT OF THE QUADRATIC AXISYMMETRIC FINITE ELEMENT	9
4.1 Interpolation Formula and Isoparametric Concept	9
4.2 Strain-Displacement Relations	17
4.3 Stress-Strain Relations	21
4.4 Force-Displacement Relations	23
4.5 Distribution of Element Loads to Nodal Points	27
5.0 STRUCTURAL EQUILIBRIUM RELATIONS-THE STRUCTURAL STIFFNESS MATRIX	30
6.0 SOLUTION FOR STRUCTURAL NODAL POINT DISPLACEMENTS	32
7.0 DETERMINATION OF ELEMENT STRESSES	34
8.0 EXAMPLE PROBLEMS	39
8.1 Stresses and Deflections in a Cylindrical Pressure vessel	40

	PAGE
8.2 Stresses in a Uniform Disk Due to Centrifugal Loads	49
8.3 Stress Concentrations in a Cylindrical Rod Due to a Spherical Inclusion	53
8.4 Stresses and Deflections in a Spherical Pressure Vessel	60
8.5 Circular Plate Bending Investigation	69
9.0 DISCUSSION OF RESULTS	81
10.0 CONCLUSIONS	86
11.0 RECOMMENDATIONS	88
12.0 REFERENCES	89
13.0 APPENDIX A - NUMERICAL QUADRATURE	92
14.0 APPENDIX B - COMPUTER PROGRAM ISOAXI	97

## LIST OF FIGURES

<u>Figure</u>	<u>Title</u>	<u>Page</u>
1	Element Mapping	11
2	Location of Element Nodal Points	12
3	Allocation of Surface and Body Forces for a Regular Quadrilateral	29
4	A Banded Structural Stiffness Matrix	31
5	Quadrature Sampling Points and Element Nodal Point Locations	38
6	Thick Cylindrical Pressure Vessel (TC 1)	42
7	TC 1 Finite Element Idealization	43
8	TC 1 Stress and Displacement Results	44
9	Uniformly Thick Disk Subjected to Centrifugal Loading	51
10	TC 2 Radial and Hoop Stress Results	52
11	Cylindrical Rod With Spherical Inclusion (TC 3)	56
12	TC 3 Finite Element Idealization of Spherical Inclusion in Cylindrical Rod	57
13	TC 3 Variation of Axial Stress	59
14	TC 3 Refined Idealization	58
15	Spherical Pressure Vessel Subjected to Internal Pressure (TC 4)	63
16	TC 4 Finite Element Idealization	64
17	TC 4 Volumetric Expansion Versus Radius	66

<u>Figure</u>	<u>Title</u>	<u>Page</u>
18	TC 4 Principal Hoop Stress Versus Radius	67
19	TC 4 Principal Radial Stress Versus Radius	68
20	Circular Plate Subjected to Uniform Pressure-Problem and Idealization	77
21	Circular Plate Axial Deflection Results	78
22	Circular Plate Subjected to Uniform Load - Radial Stress Versus Radius	79
23	Circular Plate Subjected to Uniform Load - Hoop Stress Versus Radius	80

## LIST OF TABLES

<u>Table</u>	<u>Title</u>	<u>Page</u>
I.	Element Shape Functions	16
II.	Midside Node Stress Matrices	38
III.	TC 1 Summary of Results	47
IV.	TC 4 Summary of Displacement Results	62
V.	Abscissas and Weight Factors for Gaussian Integration	96
VI.	Comparison of Results of Thesis Versus Those of Linear and Quadratic Triangular Elements	48

## NOMENCLATURE

### Scalars

$r, z, \theta$	Cylindrical coordinates (radial, axial, circumferential)
$P, Q$	Local normalized curvilinear coordinates
$A$	Area
$V$	Volume
$u, v$	Displacement components in the radial and axial directions respectively
$F_{ir}, F_{iz}$	Components of force acting in the radial and axial directions respectively at nodal point $i$
$e_r, e_\theta, e_z$	Normal components of strain in the $r, \theta, z$ directions
$\gamma_{rz}$	Shearing strain in cylindrical coordinates
$\sigma_r, \sigma_\theta, \sigma_z$	Normal stress components in the $r, \theta, z$ directions
$\tau_{rz}$	Shearing stress in the $rz$ plane
$U$	Strain energy
$E$	Young's modulus of elasticity
$\nu$	Poisson's ratio
$\phi$	An arbitrary parameter varying within an element (e.g. displacement, geometry)
$\phi_i$	Value of unknown at element nodal point $i$
$N_i$	Element shape function associated with nodal point $i$
$\alpha$	Unknown polynomial coefficient

## Vectors and Matrices

$\{ \}$	Row or column vector
$[ ]$	Matrix
$[ ]^T, \{ \}^T$	Matrix or vector transposed
$[ ]^{-1}$	Inverse of a matrix
$\det[ ]$	Determinant of a matrix
$\{r_n\}$	Column vector of radial coordinates for element nodal points
$\{z_n\}$	Column vector of element nodal point axial coordinates
$\{u_n\}$	Column vector of element node radial displacement components
$\{v_n\}$	Column vector of element node axial displacement components
$\{W_o\}$	Column vector containing both radial and axial displacement components of the element nodes
$\{N\}$	Row vector of element shape functions
$\{e\}$	Column vector of strain components
$\{\sigma\}$	Column vector of stress components
$[B]$	Matrix relating displacement to strain
$[J]$	Jacobian matrix
$[G]$	Matrix relating element nodal point locations to the Jacobian matrix
$[X_o]$	Matrix of element nodes spatial coordinates
$[D]$	Matrix relating stress to strain
$[K]$	Element stiffness matrix

## Vectors and Matrices

$\{F_o\}$	Column vector listing element nodal point forces
$\{\delta W\}$	Column vector of virtual displacements in radial and axial direction of an element's nodal points
$\{\bar{B}\}$	Column vector of element body force components
$\{\bar{P}\}$	Column vector of element surface force components
$[N']$	Matrix of shape functions
$\{\Delta\}$	Column vector of structure nodal point displacement components
$[K]^S$	Structural stiffness matrix
$\{R\}$	Column vector of structure nodal point force components
$[S]$	Matrix relating stress to displacement

## 1.0 INTRODUCTION

All linear elastic static stress and deflection problems of axially symmetric continua are, in theory, capable of being solved using the finite element method. (e.g. pressure vessels, cooling towers, rocket nozzles). Limitations to the finite element method occur when numerous elements are required to achieve a desired degree of accuracy thus resulting in large computer core requirements and/or excessive cost.

Prior to 1968, finite elements having only linear variation of boundaries were available. Thus, when a curved geometric boundary was to be modelled, one was forced to introduce large numbers of elements to achieve acceptable results. This required the solution of a greatly increased number of equilibrium equations and was recognized as a limiting factor in the application of the finite element method to this type of problem.

Introduction of the isoparametric concept by Ergatoudis [8] enabled development of elements with polynomial variation of boundaries and led to a reduction in the number of elements necessary to idealize curved boundaries.

The objective of this thesis is to present details of an isoparametric finite element for axisymmetric stress analysis which is capable of representing quadratic variation of element boundaries exactly. The development of the element, a computer program, and demonstrative applications are presented.

The element developed is an eight-noded quadrilateral based on the isoparametric element concept. Its material properties are isotropic and linear. Element force-displacement relations are obtained using the displacement method of minimum potential energy.

## 2.0 LITERATURE SURVEY

For the case of axisymmetric bodies subjected to axially symmetric boundary conditions, Timoshenko shows that the three dimensional equations of elasticity in cylindrical coordinates  $(r, \theta, z)$ , reduce to equations in two dimensions  $(r, z)$  [1]\*, [2].

Two papers exist which are considered the classic presentations of finite element development based on this theory.

Clough and Rashid[3] present a straight sided plane triangular element whose displacements are assumed linear functions of element spatial coordinates  $r$  and  $z$ . Element stresses are constant and are assumed to be average values acting at the element's centroid. Element property expressions (e.g. stiffness matrix, load vectors), are developed in integral form based on the principle of virtual work and are recognized as being complicated and lengthy. Three example problems are presented: two dealing with pressure vessel analyses, and a third with the response of an elastic half space to a point load. Highly refined finite element models involving large numbers of elements are used in all examples which appear to agree quite well with theory. Results are presented in graphic form. No specific comparisons of predicted to theoretical values are given.

Wilson[4] presents additional development and modifications for the Clough and Rashid element which increases its

---

\*Numbers in square brackets refer to the references listed in Section 12.0.

ability to analyse a broader class of structural problems. Presented is the development for determining steady state thermal effects and a procedure for analysing axisymmetric bodies experiencing asymmetric loads. The technique for the latter consists of introducing harmonic displacement functions and summing a series of two dimensional analyses.<sup>1</sup> Wilson notes the advantage of quadrilateral elements for automated mesh generation and presents development for a quadrilateral element which is actually degenerated into four linear displacement triangles. Factors which prohibit direct formulation of quadrilateral elements are not considered.

Superiority of the linear displacement trapezoidal element over its triangular counterpart has been demonstrated based on strain energy considerations by Parsons and Wilson [32]. The internal work done by one trapezoid is shown to be lower than that of two corresponding triangular elements experiencing similar boundary conditions and the implication is made that more and smaller triangular elements are necessary to achieve results which are as accurate as those obtained with quadrilaterals. Among the disadvantages discussed is the difficulty to integrate for the stiffness matrix for shapes other than trapezoidal and introduction of inter-element displacement incompatibility when adjacent elements are not rectangular.

---

1. For additional information, see Crose [5] or Ergatoudis [8]

The concept of an isoparametric element capable of overcoming the above disadvantages is credited to Taig by Irons[7] and Ergatoudis[8]. The technique of introducing a local curvilinear coordinate system is due to Taig[8] but was also developed independently, including consideration of curved element edge formulation and numerical integration convergence criteria, by Irons[7].

Ergatoudis, working in collaboration with Irons and Zienkiewicz, was the first to present plane quadrilateral elements based on the isoparametric concept[31]. Elements for two dimensional stress analysis were developed assuming linear, quadratic, and cubic boundary and displacement variations. Numerous example problems were presented and compared with solutions from the theory of elasticity. The necessity of numerical integration is noted but not discussed in depth. Conclusions are drawn favoring isoparametric quadrilateral elements having assumed variation functions of higher than first order. Subsequent work by Ergatoudis[8] includes the formulation of isoparametric, axisymmetric quadrilaterals having quadratic, cubic, and quintic displacement and boundary variations. Example problems of pressure vessels, circular plates, and rotating shafts in which excellent results were obtained are presented. Justification for the choice of particular elements in some examples is not provided.

The basic theory for deriving isoparametric elements is available in numerous texts. Theory is presented by Desai and Abel[17] and Martin and Carey[34] but the most comprehensive treatment of the concept is presented by Zienkiewicz[9] - [12].

Irons establishes the efficiency of numerical integration[7] and presents efficient integration techniques for the experienced analyst[13] - [15]. A recent paper by Gupta and Mohraz[16] presents an efficient technique for the numerical integration of element stiffness matrices which may readily be placed in a programmable form. Also included is a second technique which minimizes the number of mathematical computations necessary and hence computer time. A comparison of computer times between the two shows the proposed technique to be more efficient.

Example problems which demonstrate the increased efficiency of higher ordered isoparametric elements are presented by Dario and Bradley[21] for triangular elements and Ergatoudis[8], [31] for quadrilaterals.

### 3.0 BASIC STEPS OF THE FINITE ELEMENT DISPLACEMENT METHOD

Finite element development for stress and deflection analysis may be based on either of two variational principles; i) principle of minimum potential energy or ii) complementary energy theorem. The principle of minimum potential energy states that the true deformations of a body are those which make its potential energy a minimum. Application of this principle results in algebraic equations of equilibrium. The complementary potential energy theorem may be used to obtain algebraic equations of compatibility. The more commonly used principle is that of minimizing potential energy since it facilitates assemblage of structural equilibrium relations. This technique is referred to as the displacement method of finite element analysis.

Models comprised of finite elements based on the displacement method tend to be stiffer than actual structures. This fact is due to the restraint introduced in prescribing intra-element displacement variation. Refinement of idealizations or the use of higher order elements minimizes this effect and provides convergence to true displacement shapes.

The six basic steps of the finite element technique based on the displacement method are:

1. Discretization of a continuum into an equivalent system of finite elements which are interconnected at nodal points.

2. Selection of a interpolation formula to approximate the variation of displacement on and within element boundaries.
3. Derivation of element stiffness matrices giving equilibrium relations between the forces and displacements at each element nodal point.
4. Assembly of the element stiffness matrices based on nodal point force equilibrium and displacement compatibility to obtain structural equilibrium relations.
5. Solution of the structural equilibrium relations for unknown displacements.
6. Solution of element stresses based on element nodal point displacements.

These steps are applicable for development of all finite element types (e.g. plane stress/strain, axisymmetric, three dimensional solid). Development of a specific element type requires further consideration of the governing elasticity equations. The foregoing steps will now be applied to the development of an isoparametric finite element for axisymmetric static stress analysis.

## 4.0 DEVELOPMENT OF THE QUADRATIC-AXISYMMETRIC FINITE ELEMENT

### 4.1 Interpolation Formula and Isoparametric Concept

The selection of an interpolation formula describing the variation of some unknown  $\phi$  (e.g. radial or axial displacement) within an element is of foremost importance in developing a finite element based on the displacement method. This formula is generally expressed as:

$$\phi = \sum_{i=1}^n N_i \phi_i \quad (1)$$

where  $N_i$  is a normalized "shape function" of polynomial form in spatial coordinates  
 $\phi_i$  is the value of the unknown function  $\phi$  at element node  $i$   
 $n$  is the number of nodes used to define the element

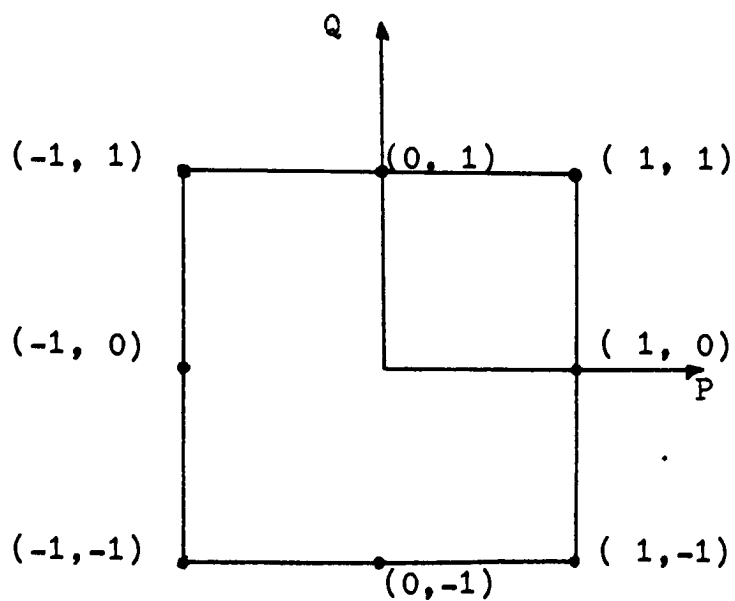
The shape functions in Eq. 1 may not be chosen arbitrarily if monotonic convergence is to be expected[10]. In order that finite element solutions converge to true solutions, shape functions must be chosen which:

1. Are of such order and form that continuity of unknown  $\phi$  occurs between elements.
2. Allow any arbitrary linear form of  $\phi$  to be taken to represent constant derivatives.

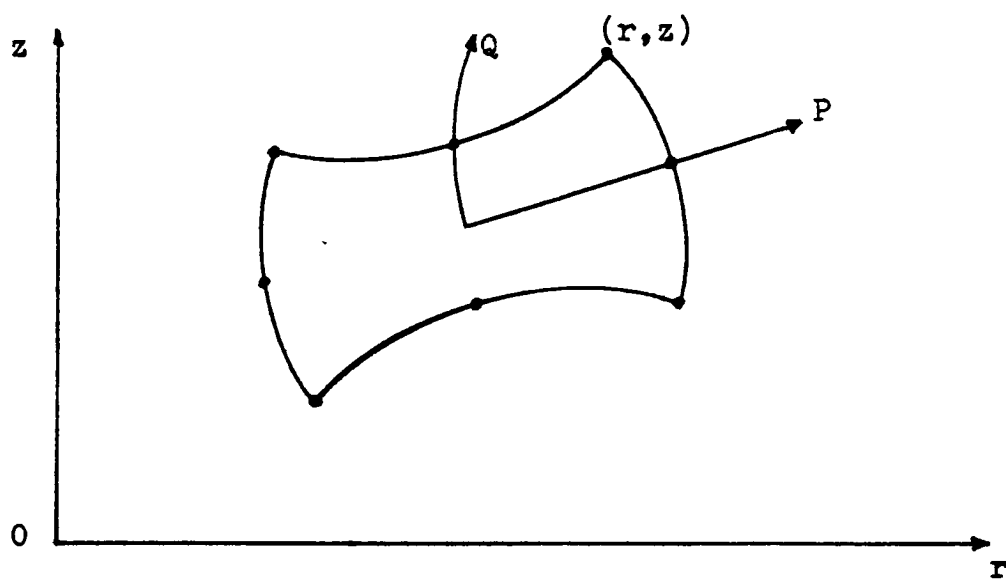
With respect to element displacement, these requirements imply that no gaps or overlapping of adjacent

element boundaries occur and that states of constant strain may be represented.

Although the quadrilateral element has been shown by Wilson and Parsons[32] to be superior to its triangular counterpart, the use of cartesian polynomials to define element shape functions is not suitable since convergence criteria can only be satisfied for the limited cases of elements being rectangles or parallelograms. The isoparametric concept enables specification of shape functions which will satisfy convergence criteria and also allow arbitrary element shapes which are consistent with assumed spatial variation. In the isoparametric concept, element shape functions are obtained for a square normalized element in a local coordinate system  $(P,Q)$ . This coordinate system has its origin at the centroid of the element. Element boundaries have limits of  $-1$  and  $1$  as shown in Fig. 1a. This normalized element and its shape functions are then associated with the curved element in spatial coordinates  $(r,z)$  shown in Fig. 1b. Therefore, coordinate system  $(P,Q)$  becomes curvilinear and both curved element displacement and geometry is expressed in terms of  $P$  and  $Q$  through Eq. 1.



a) local coordinate system



b) global coordinate system

## Element Mapping

FIGURE 1

Zienkiewicz[12] suggested that shape functions which obey convergence properties may be obtained by inspection providing:

1. They have value of unity at the nodal point they refer to and zero at all other element nodes.
2. They have such an order of variation on element interfaces that the parameters specified on such interfaces uniquely define the function there.

Shape functions for a quadratic element which satisfy these criteria are presented in Table 1. The order in which these functions appear corresponds to the counterclockwise sequencing of nodal points shown in Figure 2.

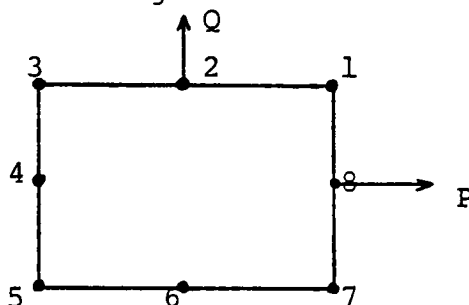


Figure 2. Location of Element Nodal Points and Associated Shape Functions

As stated previously, the order of the element interpolation formula (Eq.1) can be related to the number of nodes used to describe the element. Only six nodes would be required to specify a

complete quadratic function in two variables. To maintain symmetry of the element, eight nodes are used. Expansion of Eq. 1 in terms of P and Q, using the above shape functions, the interpolation formula will be found to contain two terms of cubic order,  $PQ^2$  and  $P^2Q$ . Therefore, although the element is referred to as quadratic, actual element variations are assumed which are higher order.

The axisymmetric problem in cylindrical coordinates may be completely specified in two dimensions.

When axisymmetric boundary conditions exist, strain relations are completely specified in radial and axial coordinates  $(r, z)$ , independent of  $\theta$ . Thus, only two-dimensional finite elements in the  $r$ - $z$  plane need be considered.

From Eq. 1, the variation of displacement within an element may be expressed as:

$$u = [N] \{u_n\} \quad (2)$$

$$v = [N] \{v_n\} \quad (3)$$

where  $u$  and  $v$  are radial and axial displacement components respectively at any point within the element.

[N] is a matrix of element shape functions:

$$[N] = [N_1, N_2, N_3, \dots, N_8]$$

$\{u_n\}, \{v_n\}$  are column vectors of element nodal point displacement components.

$$\{u_n\}^T = \{u_1, u_2, u_3, \dots, u_8\}$$

$$\{v_n\}^T = \{v_1, v_2, v_3, \dots, v_8\}.$$

By definition, element geometry is also defined by Eq. 1 and may be expressed as:

$$r = [N] \{r_n\} \quad (4)$$

$$z = [N] \{z_n\} \quad (5)$$

where  $r$  and  $z$  are element spatial coordinates in the radial and axial directions.  $\{r_n\}, \{z_n\}$  are column vectors of element nodal point coordinates.

$$\{r_n\}^T = \{r_1, r_2, r_3, \dots, r_8\}$$

$$\{z_n\}^T = \{z_1, z_2, z_3, \dots, z_8\}$$

To demonstrate the element's ability to represent quadratic varying boundaries, consider Eqs. 4 and 5 for the case  $P = 1$  which corresponds to the element edge defined by nodes 1, 7, and 8 in Fig. 2. From Table 1, shape functions  $N_2$

through  $N_6$  are zero and Eqs. 4 and 5 simplify to:

$$r = r_8 + \frac{1}{2}(r_1 - r_7)Q + \frac{1}{2}(r_1 + r_7 - 2r_8)Q^2$$

$$z = z_8 + \frac{1}{2}(z_1 - z_7)Q + \frac{1}{2}(z_1 + z_7 - 2z_8)Q^2$$

which represents a quadratic variation of element boundary.

These element displacement and geometry relations will now be used to establish element strain and stiffness properties.

TABLE I

ELEMENT SHAPE FUNCTIONS

<u>i</u>	<u><math>N_i</math></u>	<u><math>\frac{\partial N_i}{\partial P}</math></u>	<u><math>\frac{\partial N_i}{\partial Q}</math></u>
1	$\frac{1}{4}(1+P)(1+Q)(-1+P+Q)$	$\frac{1}{4}(1+Q)(2P+Q)$	$\frac{1}{4}(1+P)(2Q+P)$
2	$\frac{1}{2}(1-P^2)(1+Q)$	$-P(1+Q)$	$\frac{1}{2}(1-P^2)$
3	$\frac{1}{4}(1-P)(1+Q)(-1-P+Q)$	$\frac{1}{4}(1+Q)(2P-Q)$	$\frac{1}{4}(1-P)(2Q-P)$
4	$\frac{1}{2}(1-P)(1-Q^2)$	$-\frac{1}{2}(1-Q^2)$	$-Q(1-P)$
5	$\frac{1}{4}(1-P)(1-Q)(-1-P-Q)$	$\frac{1}{4}(1-Q)(2P+Q)$	$\frac{1}{4}(1-Q)(2Q+P)$
6	$\frac{1}{2}(1-P^2)(1-Q)$	$-P(1-Q)$	$-\frac{1}{2}(1-P^2)$
7	$\frac{1}{4}(1+P)(1-Q)(-1+P-Q)$	$\frac{1}{4}(1-Q)(2P-Q)$	$\frac{1}{4}(1+P)(2Q-P)$
8	$\frac{1}{2}(1+P)(1-Q^2)$	$\frac{1}{2}(1-Q^2)$	$-Q(1+P)$

## 4.2 Strain-Displacement Relationships

As developed by Timoshenko[1], the linear strain-displacement relations for an axisymmetric body experiencing axisymmetric boundary conditions reduce to the following in cylindrical coordinates:

$$\begin{aligned}
 e_r &= \frac{\partial u}{\partial r} \\
 e_\theta &= \frac{u}{r} \\
 e_z &= \frac{\partial v}{\partial z} \\
 \gamma_{rz} &= \frac{\partial u}{\partial z} + \frac{\partial v}{\partial r}
 \end{aligned}
 \tag{6}$$

where  $u$  and  $v$  are displacement components in the radial and axial directions respectively. Substituting Eqs. 2 and 3 into Eq. 6, the element strain may be expressed in matrix form as:

$$\{e\} = [B]\{w_o\}
 \tag{7}$$

where  $\{e\}^T = \{e_r \quad e_\theta \quad e_z \quad \gamma_{rz}\}$

$$[B] = [B_1 \quad B_2 \quad B_3 \quad \dots \quad B_8]$$

$$[B_i] = \begin{bmatrix} \frac{\partial N_i}{\partial r} & 0 \\ \frac{N_i}{r} & 0 \\ 0 & \frac{\partial N_i}{\partial z} \\ \frac{\partial N_i}{\partial z} & \frac{\partial N_i}{\partial r} \end{bmatrix}$$

$$\text{and } \{W_o\}^T = \{u_1 \ v_1 \ u_2 \ v_2 \ \dots \ u_8 \ v_8\}$$

The coefficients of matrix [B] contain derivatives of the element shape functions with respect to cylindrical coordinates. The shape functions are defined in terms of normalized coordinates (P,Q).

A relationship may be established between derivatives of two coordinate systems by the introduction of the Jacobian matrix of transformation from (r,z) to (P,Q) [23].

Applying the chain rule and differentiating shape function  $N_i$  with respect to P or Q, one obtains:

$$\frac{\partial N_i}{\partial P} = \frac{\partial N_i}{\partial r} \frac{\partial r}{\partial P} + \frac{\partial N_i}{\partial z} \frac{\partial z}{\partial P}$$

$$\frac{\partial N_i}{\partial Q} = \frac{\partial N_i}{\partial r} \frac{\partial r}{\partial Q} + \frac{\partial N_i}{\partial z} \frac{\partial z}{\partial Q}$$

or in matrix form:

$$\begin{Bmatrix} \frac{\partial N_i}{\partial P} \\ \frac{\partial N_i}{\partial Q} \end{Bmatrix} = \begin{bmatrix} \frac{\partial r}{\partial P} \\ \frac{\partial r}{\partial Q} \end{bmatrix} \begin{bmatrix} \frac{\partial z}{\partial P} \\ \frac{\partial z}{\partial Q} \end{bmatrix} \begin{Bmatrix} \frac{\partial N_i}{\partial r} \\ \frac{\partial N_i}{\partial z} \end{Bmatrix}$$

where the matrix

$$\begin{bmatrix} \frac{\partial r}{\partial P} & \frac{\partial z}{\partial P} \\ \frac{\partial r}{\partial Q} & \frac{\partial z}{\partial Q} \end{bmatrix} = [J]$$

is called the Jacobian matrix.

Premultiplying both sides of the above equation by the inverse of the Jacobian, derivatives of the shape functions with respect to cylindrical coordinates may be expressed as:

$$\begin{Bmatrix} \frac{\partial N_i}{\partial r} \\ \frac{\partial N_i}{\partial z} \end{Bmatrix} = [J]^{-1} \begin{Bmatrix} \frac{\partial N_i}{\partial P} \\ \frac{\partial N_i}{\partial Q} \end{Bmatrix}$$

Determination of the Jacobian matrix is accomplished by differentiation of Eqs. 4 and 5 with respect to P and Q.

Applying the chain rule, the four coefficients of the Jacobian matrix become:

$$\frac{\partial r}{\partial P} = \sum_{i=1}^8 \frac{\partial N_i}{\partial P} r_i; \quad \frac{\partial z}{\partial P} = \sum_{i=1}^8 \frac{\partial N_i}{\partial P} z_i$$

$$\frac{\partial r}{\partial Q} = \sum_{i=1}^8 \frac{\partial N_i}{\partial Q} r_i; \quad \frac{\partial z}{\partial Q} = \sum_{i=1}^8 \frac{\partial N_i}{\partial Q} z_i$$

since the spatial coordinates of element nodes are constant.

These relations may be written in matrix form as:

$$[J] = [G] [X_0]$$

where

$$[G] = \begin{bmatrix} \frac{\partial N_1}{\partial P}, & \frac{\partial N_2}{\partial P}, & \frac{\partial N_3}{\partial P}, & \dots, & \frac{\partial N_8}{\partial P} \\ \frac{\partial N_1}{\partial Q}, & \frac{\partial N_2}{\partial Q}, & \frac{\partial N_3}{\partial Q}, & \dots, & \frac{\partial N_8}{\partial Q} \end{bmatrix}$$

$$[X_0]^T = \begin{bmatrix} r_1 & r_2 & r_3 & \dots & r_8 \\ z_1 & z_2 & z_3 & \dots & z_8 \end{bmatrix}$$

### 4.3 Stress-Strain Relations

Element stress-strain relations are presented for homogeneous, isotropic material.

For axially symmetric bodies, four components of stress exist. Normal stress components are in the axial, radial, and circumferential directions and shearing stress exists in the  $r z$  plane.

In the absence of initial strain, the relations between these element stresses and the element strains are:

$$\sigma_r = \frac{E(1-\nu)}{(1+\nu)(1-2\nu)} e_r + \left(\frac{\nu}{1-\nu}\right) (e_\theta + e_z)$$

$$\sigma_\theta = \frac{E(1-\nu)}{(1+\nu)(1-2\nu)} e_\theta + \left(\frac{\nu}{1-\nu}\right) (e_z + e_r)$$

$$\sigma_z = \frac{E(1-\nu)}{(1+\nu)(1-2\nu)} e_z + \left(\frac{\nu}{1-\nu}\right) (e_r + e_\theta)$$

$$\tau_{rz} = \frac{E}{2(1+\nu)} \gamma_{rz}$$

where  $E$  represents Young's modulus

$\nu$  represents Poisson's ratio

These relations may then be expressed in matrix form as:

$$\{\sigma\} = [D] \{e\} \quad (9)$$

where

$$\{ \sigma^T \} = \{ \sigma_r \quad \sigma_\theta \quad \sigma_z \quad \tau_{rz} \}$$

$$[D] = \frac{E(1-\nu)}{(1+\nu)(1-2\nu)} \begin{bmatrix} 1 & \left(\frac{\nu}{1-\nu}\right) & \left(\frac{\nu}{1-\nu}\right) & 0 \\ \left(\frac{\nu}{1-\nu}\right) & 1 & \left(\frac{\nu}{1-\nu}\right) & 0 \\ \left(\frac{\nu}{1-\nu}\right) & \left(\frac{\nu}{1-\nu}\right) & 1 & 0 \\ 0 & 0 & 0 & \left(\frac{1-2\nu}{2(1-\nu)}\right) \end{bmatrix}$$

#### 4.4 Force - Displacement Relations

Relations between element nodal point forces and displacements may be obtained by the use of Castigliano's theorem. The strain energy of an axis-symmetric element in a general state of stress may be expressed in matrix form as:

$$U = 1/2 \int_V \{\sigma\}^T \{e\} dV \quad (10)$$

From Eqs. 7 and 9,

$$\{e\} = [B] \{w_o\}$$

$$\{\sigma\} = [D] \{e\} = [D] [B] \{w_o\}$$

The volume integral in Eq. 10 is expressed in cylindrical coordinates as:

$$\int_V dV = \int_z \int_r \int_0^{2\pi} r d\theta dr dz = \int_z \int_r 2\pi r dr dz$$

From Eq. 4.

$$r = [N] \{r_o\}$$

Thus

$$\int_V dV = \int_z \int_r 2\pi [N] \{r_o\} dr dz$$

Substituting the above relations into Eq. 10, the strain energy may be written as:

$$U = \int_z \int_r \pi \{w_o\}^T [B]^T [D] [B] \{w_o\} [N] \{r_o\} dr dz \quad (11)$$

Using the above relation and Castigliano's Theorem, the equilibrium relations between nodal point forces and displacements may be found.

Castigliano's Theorem states, "If the strain energy  $U$  of an elastic element is represented as a function of statically independent displacements, the partial derivative of this function with respect to displacements will give the actual forces at the displaced points in the directions of the displacements". [1]

Or

$$\frac{\partial U}{\partial \{W_o\}} = \{F_o\}$$

where  $\{F_o\}$  refers to nodal point force components of an element.

$$\{F_o\}^T = \{F_{1r}, F_{1z}, F_{2r}, F_{2z}, \dots, F_{8r}, F_{8z}\}$$

Applying the above to Eq. 11 we obtain,

$$\{F_o\} = \left\langle \int_z \int_r 2\pi [B]^T [D] [B] [N] \{r_o\} dr dz \right\rangle \{W_o\}$$

or

$$\{F_o\} = [K] \{W_o\}$$

where

$$[K] = \int_z \int_r 2\pi [B]^T [D] [B] [N] \{r_o\} dr dz \quad (12)$$

and is the element stiffness matrix.

Evaluation of element stiffness by direct integration of Eq. 12 is not practical. Matrices  $[B]$  and  $[N]$  are expressed in curvilinear coordinates and would require transformation to cylindrical coordinates. Also, limits of integration are complicated by the curved boundaries shown in Fig. 1b.

These difficulties are overcome by transforming Eq. 12 to an integral in the local normalized coordinate system shown in Fig. 1a. This transformation is accomplished by recognizing that the determinant of the Jacobian matrix is equal to the ratio of differential areas in global ( $drdz$ ) and local ( $dPdQ$ ) coordinates [23].

$$drdz = \det[J]dPdQ$$

Applying this relation to Eq. 12 and changing limits of integration, the element stiffness matrix may be expressed as:

$$[K] = \int_{-1}^1 \int_{-1}^1 2\pi [B]^T [D] [B] [N] \{r_0\} \det[J] dPdQ \quad (13)$$

where all quantities within the integral are either constants or functions of  $P$  and  $Q$ .

Although limits of integration have been simplified, the quadratic form of the shape functions result

in an expression to be integrated which is complex in form and not practical to integrate analytically. For this reason, evaluation of Eq. 13 is most readily accomplished by numerical integration using the Gauss quadrature technique. Details of the procedure used herein are presented in Appendix A.

#### 4.5 Distribution of Element Loads to Nodal Points

In the finite element method, structural loading conditions are represented as point loads applied at the nodes of the idealized structure. In cases where distributed surface and body forces are present, these forces may be "intuitively" distributed to the nodal points, or a specific routine may be used.

In the case of higher order elements there is a departure from an easily conceived idealization and the allocation of distributed loads to nodal points by intuition may no longer be correct, [12]. However, nodal point loads, consistent with the assumed displacement functions, may be formulated for distributed loads by considering the Principal of Virtual Work, viz:

"If an element which is in equilibrium under a set of body forces ( $\{\bar{B}\}$ ) and surface forces ( $\{\bar{P}\}$ ), is given an arbitrary virtual displacement  $\{\delta W\}$ , which does not violate kinematic and geometrical boundary constraints, then the work done by the internal forces equals the work done by the applied loads during these displacements," [19].

This statement leads to the matrix equation:

$$\int_A \{\delta W\}^T \{\bar{P}\} dA + \int_V \{\delta W\}^T \{\bar{B}\} dV = \{\delta W_o\}^T \{F\} \quad (17)$$

where

$dA$  = differential surface area of an element  
boundary

$dV$  = differential volume within the element

$\{\delta W_o\}$  = virtual displacements of the element's nodes

$\{\delta W\}$  = virtual displacements within the element

Note also that  $\{\delta W\} = [N'] \{\delta W_o\}$  from assumed variation of intraelement displacement.

$$[N'] = \begin{bmatrix} N_1 & \circ & N_2 & \circ & N_3 & \circ & \dots & N_8 & \circ \\ \circ & N_1 & \circ & N_2 & \circ & N_3 & \dots & \circ & N_8 \end{bmatrix}$$

$F$  = force components at element nodal points

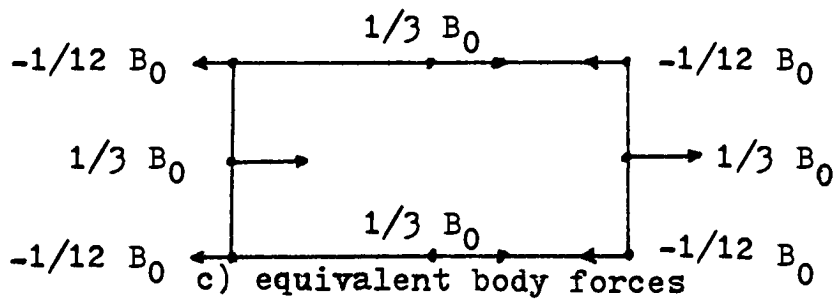
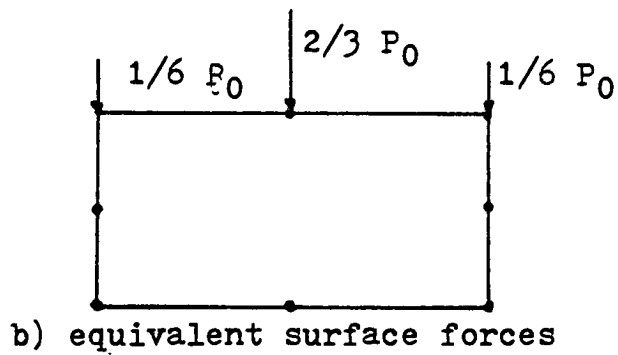
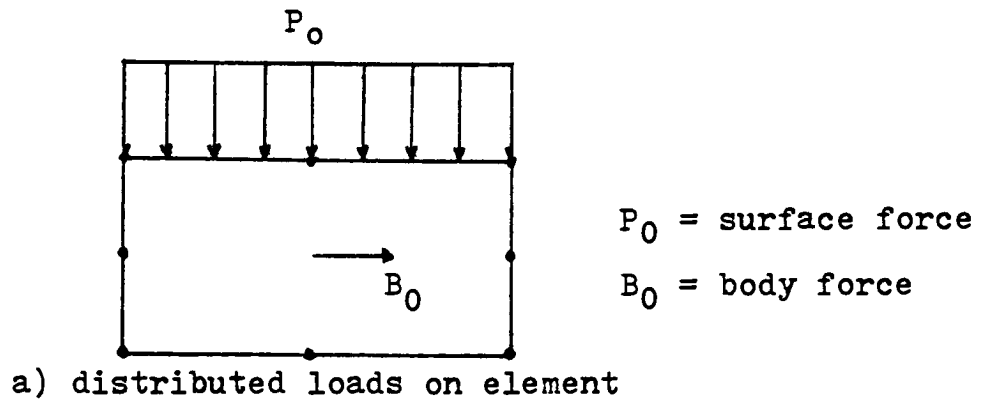
$$\text{As } \{\delta W\}^T = \{\delta W_o\}^T [N']^T$$

Eq. 17 becomes:

$$\int_A [N']^T \{P\} dA + \int_V [N']^T \{B\} dV = \{F\} \quad (18)$$

The increased flexibility introduced in defining element shapes in cylindrical coordinates complicated the limits of integration in Eq. 18. It is found convenient to transform these integrals to the local coordinate system and integrate numerically as was done with the element stiffness matrix.

The option to internally generate these consistent loads has not been developed in the program presented, but, wherever required, allocation of distributed loads has been made as shown in Fig. 3.



Allocation of Surface and Body Forces  
 For a Regular Quadrilateral

Figure 3

## 5.0 STRUCTURAL EQUILIBRIUM RELATIONS-THE STRUCTURAL STIFFNESS MATRIX

For the previously developed element stiffness matrix  $[K]$ , equilibrium equations relating element nodal point forces to displacements were obtained.

The next step of the displacement method is the determination of equilibrium relations between nodal point forces and displacements for the entire structure or, the structural stiffness matrix  $[K]^S$ .

The almost universally employed technique for obtaining this matrix is the direct stiffness method [17] which involves assembling the individual element stiffness matrices such that both displacement compatibility and force equilibrium are satisfied at the nodal points, as follows:

1. All elements adjacent to a particular node must have the same displacement components at that node.
2. The external forces acting at a nodal point must equal the sum of the internal forces contributed by the elements meeting at the node.

Using these criteria, the structural stiffness matrix  $[K]^S$  may be obtained by direct addition of the individual elements' stiffness coefficients to their appropriate locations in  $[K]^S$ .

These appropriate locations are determined by the nodal points defining each element.

Two important properties which the structural stiffness matrix possesses are

1. For linear elastic systems the element stiffness matrix is symmetric (i.e.  $[K] = [K]^T$ ) and the assembled structural stiffness matrix is also symmetric.
2. Sequencing of elements and nodal points such that the maximum difference between nodal point numbers defining an element is a minimum, the resulting structural stiffness matrix will be banded as shown in Fig. 4.

Proof of these properties may be found in either reference [12] or [17].

Although these properties may not appear significant, they play an important role in an efficient scheme for solution of the structural equilibrium equations which requires a minimum amount of computer core capacity.

$$[K]^S = \begin{bmatrix} X & X & X & 0 & 0 & 0 & 0 & 0 & 0 & 0 \\ X & X & X & X & 0 & 0 & 0 & 0 & 0 & 0 \\ X & X & X & X & X & 0 & 0 & 0 & 0 & 0 \\ 0 & X & X & X & X & X & 0 & 0 & 0 & 0 \\ 0 & 0 & X & X & X & X & X & 0 & 0 & 0 \\ 0 & 0 & 0 & X & X & X & X & X & 0 & 0 \\ 0 & 0 & 0 & 0 & X & X & X & X & X & 0 \\ 0 & 0 & 0 & 0 & 0 & X & X & X & X & X \\ 0 & 0 & 0 & 0 & 0 & 0 & X & X & X & X \end{bmatrix}$$

Figure 4

A Banded Structural Stiffness Matrix (x = non-zero terms)

## 6.0 SOLUTION FOR STRUCTURAL NODAL POINT DISPLACEMENTS

Having found the structural stiffness matrix  $[K]^S$ , the structural equilibrium relations may be written as:

$$\{R\} = [K]^S \{\Delta\} \quad (19)$$

where  $\{R\}$  = a vector of external force components acting at the nodes of the structure

$\{\Delta\}$  = a vector of displacement components of the nodal points of the structure

The external forces applied at nodal points may be added directly to their appropriate locations in vector  $\{R\}$ . Also required is a sufficient number of prescribed displacement components in the vector  $\{\Delta\}$  to prevent rigid body motion of the structure. Failure to constrain rigid body motions will result in matrix  $[K]^S$  being singular and not possessing an inverse.

Introduction of prescribed displacements to Eq. 19 is accomplished by modification of  $\{R\}$  and  $[K]^S$  such that vector  $\{\Delta\}$  will remain a vector of unknowns but yield the correct prescribed displacements when solved.

Having defined vector  $\{R\}$  and introduced prescribed displacements, Eq. 19 may be solved.

Computer subroutines for the assemblage of the structural stiffness matrix and solving structure equilibrium equations were taken from an existing finite

element computer program developed at the General Electric Research and Development Center by Levy[20] and used with only minor modifications for accomodation of the element developed.

Although no documentation of the above techniques is available in this report, the procedures used are similar to those presented by Cheung and King.[12]. The specific numerical technique used in finding displacements is a direct solution method using Gauss elimination for a tridiagonal matrix whose coefficients are themselves matrices.

Advantage of this technique is that a minimal amount of computer core required as all zero coefficients outside the bandwidth need not be retained. However, frequent accesses to peripheral storage devices during the Gauss elimination tends to increase total computer time. As a result of the minimizing of core requirements possible using this technique, the computer program given in this thesis is capable of handling 600 nodes or 1200 displacement degrees of freedom. Such a problem corresponds to  $[K]^S$  being of the order  $1200 \times 1200$  and would require  $1.44 \times 10^6$  words of computer storage with full retention of the structural stiffness matrix. The computer core required for the solution of this problem using the tridiagonal method is 10,100 words.

## 7.0 DETERMINATION OF ELEMENT STRESSES

Having determined nodal point displacements, it is then desirable to find stress components within the structure. Structural stress components are determined on a per-element basis and may be determined by a number of different techniques.

Three techniques currently used for obtaining element stress components, are:

1. Calculating stress components at element centroids and assuming these to be the average values of stress within each element. [17]
2. Assuming a polynomial variation of stress components and extrapolating these components to element boundaries. [20]
3. Calculation of consistent stress distributions based on the theory of conjugate approximations, [24] , [25].

Of these three techniques, the second has been employed.

The first technique was found to be too limited in stress information available while the third required sophistication beyond the scope of this thesis.

An advantage of the second technique is its ability to determine stresses on element boundaries, (where magnitudes are often a maximum) with a minimum of effort. Its disadvantage is that values of stress components calculated at a point similar to adjacent elements may

exhibit finite discontinuities between the elements.

This is demonstrated in section 8.4.

From Eq. 7, the matrix expression:

$$\{e\} = [B] \{w_o\}$$

was obtained which related element strain to its nodes' displacements.

From Eq. 9, the element stress vector was expressed as:

$$\{\sigma\} = [D] \{e\}$$

The relationship between stress and displacement is then:

$$\{\sigma\} = [D][B] \{w_o\}$$

where the matrix product  $[D][B]$  is often referred to as the stress matrix  $[S]$ .

Stress components may be found at the midside nodes of each element by considering the element in its local normalizing coordinates.

As shown in Appendix A, the product  $[D][B]$  is found at nine sampling points within an element when determining element stiffness. The locations of these sampling points are shown in Figure 5.

Since the locations and stress matrices of the sampling points are known, it is possible to extrapolate these matrices to the element's midside nodes.

Consider Fig. 5 for the case of  $P = 0$ . By definition, element nodes 2 and 6 lie on this line, and also sampling

points 4, 5, and 6.

Assuming quadratic variation of the stress matrix as a function of  $Q$ , the stress matrix  $[S(Q)]$  may be written as:

$$[S(Q)] = \alpha_1 + \alpha_2 Q + \alpha_3 Q^2$$

where  $\alpha_1$ ,  $\alpha_2$ , and  $\alpha_3$  are unknown coefficients to be determined.

The stress matrices at nodes 2 and 6 become:

$$[S] \text{ node 2} = \alpha_1 + \alpha_2 + \alpha_3$$

$$[S] \text{ node 6} = \alpha_1 + \alpha_2 + \alpha_3$$

Denoting  $[S]_i$  and  $a_i$  as the stress matrix and coordinate  $Q$  of sampling point  $i$  respectively, the following three equations are obtained.

$$[S]_4 = \alpha_1 + a_4 \alpha_2 + a_4^2 \alpha_3$$

$$[S]_5 = \alpha_1 + a_5 \alpha_2 + a_5^2 \alpha_3$$

$$[S]_6 = \alpha_1 + a_5 \alpha_2 + a_6^2 \alpha_3$$

The above represents 3 equations having 3 unknowns and may be solved for  $\alpha_1$ ,  $\alpha_2$ , and  $\alpha_3$ .

Using the same procedure for the case  $Q = 0$ , stress matrices at nodes 4 and 8 may be obtained in terms of the stress matrices at sampling points 2, 5, and 8.

Relationships between element midside node stress matrices and the stress matrices at the sampling points are presented in Table II.

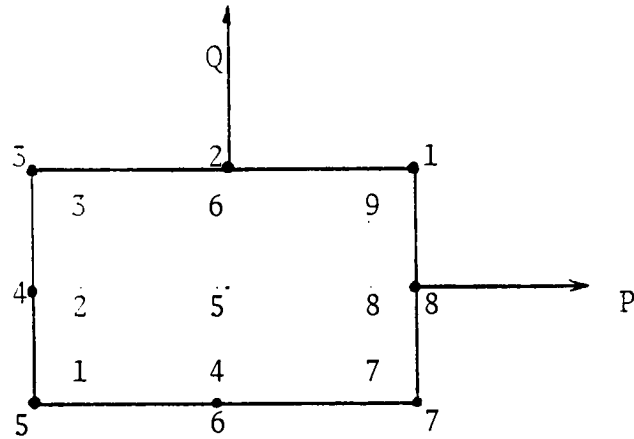


Figure 5. Quadrature Sampling Points and Element Nodal Point Locations

TABLE II

Midside Node Stress Matrices

$$[S] \text{ node } 2 = 0.1878 [S]_4 - .6666 [S]_5 + 1.4788 [S]_6$$

$$[S] \text{ node } 6 = 1.4788 [S]_4 - .6666 [S]_5 + 0.1878 [S]_6$$

$$[S] \text{ node } 4 = 1.4788 [S]_2 - .6666 [S]_5 + 0.1878 [S]_8$$

$$[S] \text{ node } 8 = 0.1878 [S]_2 - .6666 [S]_5 + 1.4788 [S]_8$$

## 8.0 EXAMPLE PROBLEMS

A computer program has been written based on the foregoing development.

Numerous test cases have been examined to verify the computer program developed. Five test cases are presented to demonstrate program capabilities. Although limited in geometric and loading complexities, they are sufficiently representative to provide insight into the capabilities and limitations of the program.

The five test cases in order of presentation are:

- TC 1. Cylindrical pressure vessel subjected to internal and external pressures.
- TC 2. Stresses in a circular disk of uniform thickness due to centrifugal loading.
- TC 3. Stress concentration in a cylindrical rod in tension due to a spherical inclusion.
- TC 4. Spherical pressure vessel subjected to internal pressure.
- TC 5. Bending of circular plates.

Results for cases similar to TC 1 and TC 3 have been published by Dario and Bradley [21] using quadratic triangular elements and results for cases similar to TC 2 and TC 5 using cubic and quartic quadrilateral elements have been presented by Ergatoudis [8].

All numerical results presented are in either tabular or graphical form as the actual computer output is too voluminous.

## 8.1 STRESSES AND DEFLECTIONS IN A CYLINDRICAL PRESSURE

### VESSEL TC 1

This case is presented to verify the ability of the program to solve axisymmetric problems and involves the classical thick cylinder problem from the theory of elasticity. The theoretical solution of this problem is due to Lamé and is presented by Timoshenko[1]. Cylinder geometry and loading is presented in Fig. 6. Of primary interest is radial stress, hoop stress, and radial displacement. The theoretical displacement solution contains  $1/r$  terms and stresses terms involving  $1/r^2$ . Refinement of finite element models is necessary to approximate true stresses and displacements since actual variations are of higher order than those assumed within an element. Three finite element idealizations are presented having 1, 5, and 30 elements respectively. These models are shown in Fig. 7 and their results summarized in Table III. Graphs of radial stress, hoop stress, and radial displacement are presented in Fig. 8 for the 5 and 30 element models comparing their results with theory. For the 30 element model, stresses and deflections have converged to within a maximum difference of 1.0% of theoretical values at all locations. Comparison information for the problem shown in Fig. 6 is available in a paper by Dario and Bradley[21] A

comparison between predicted stresses for the quadratic quadrilateral and linear and quadratic triangles is presented in Table VI, displacement information is not available. Superiority of the quadratic quadrilateral over the linear triangle is apparent. Advantage over its triangular counterpart is not as evident.

An unexpected result of this analysis was the prediction of displacements converging to the true solution from an upper bound. This contradicts the fact that elements based on the displacement method always prove too stiff. Two exceptions to this rule occur when either interelement displacement compatibility is not maintained or when element volume integration is approximate. Neither of these exceptions are believed to apply in this development. Also, similar displacement results were not obtained in other example problems. Explanation of this result is not available.

Results demonstrate functioning of the thesis program and also that the accuracy is a function of model refinement.

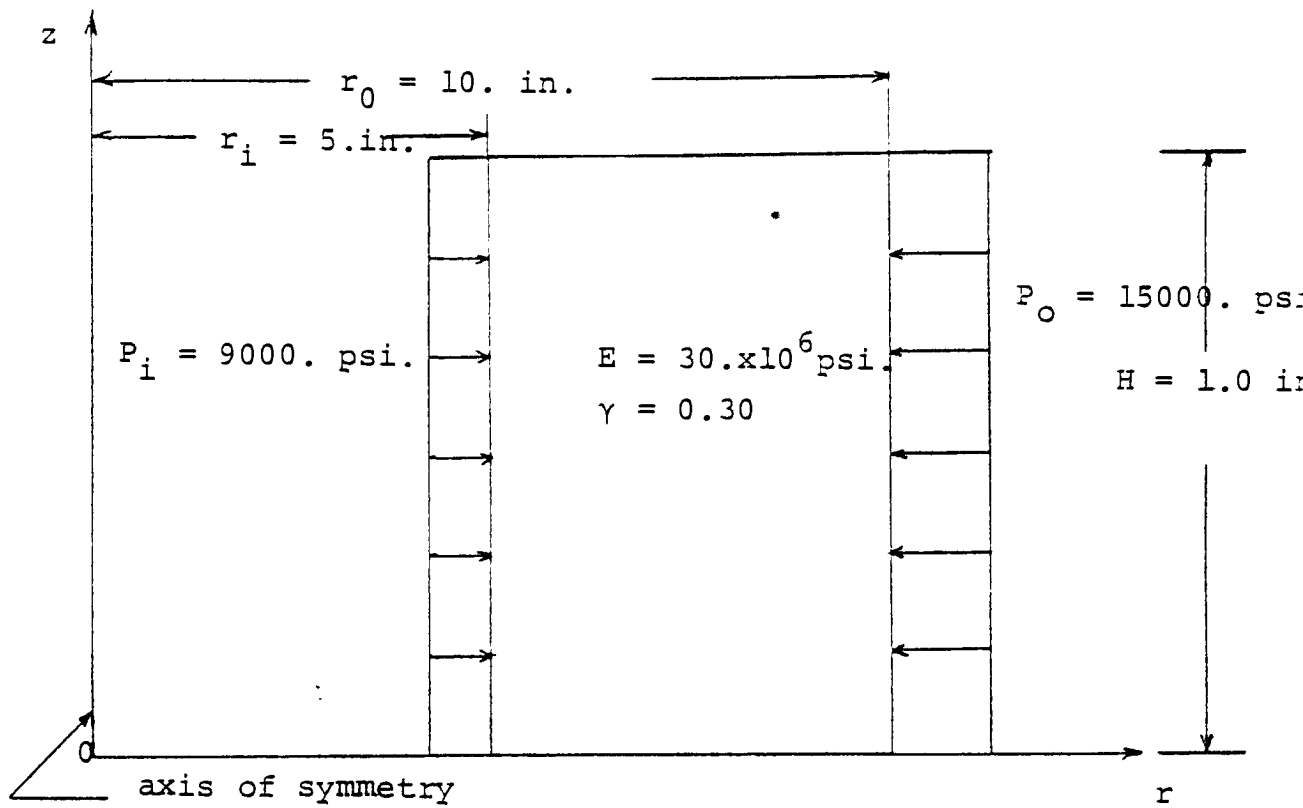
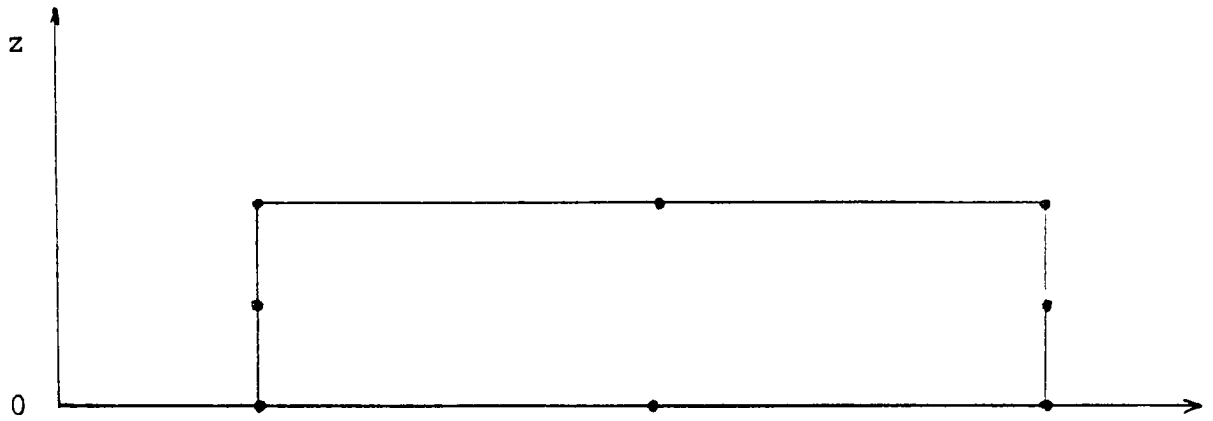
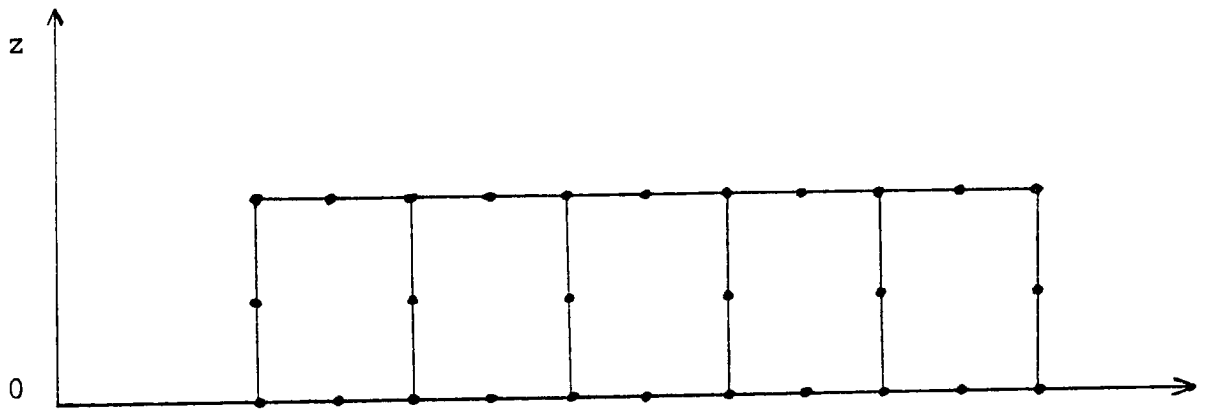


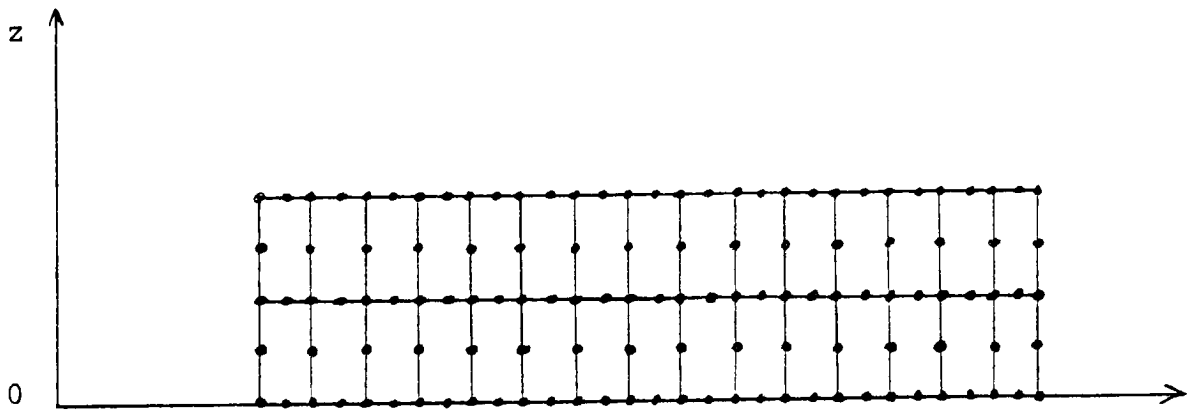
FIGURE 6  
 Thick Cylindrical Pressure Vessel



a) 14 unconstrained degrees of freedom



b) 54 unconstrained degrees of freedom



c) 248 unconstrained degrees of freedom

FIGURE 7

Finite Element Idealizations of TC 1

FIGURE 8  
RADIAL DISPLACEMENT VERSUS RADIUS TC 1

RADIAL  
DISPLACEMENT  
 $\times 10^{-3}$  in.

-5.0

-4.5

-4.0

5.

6.

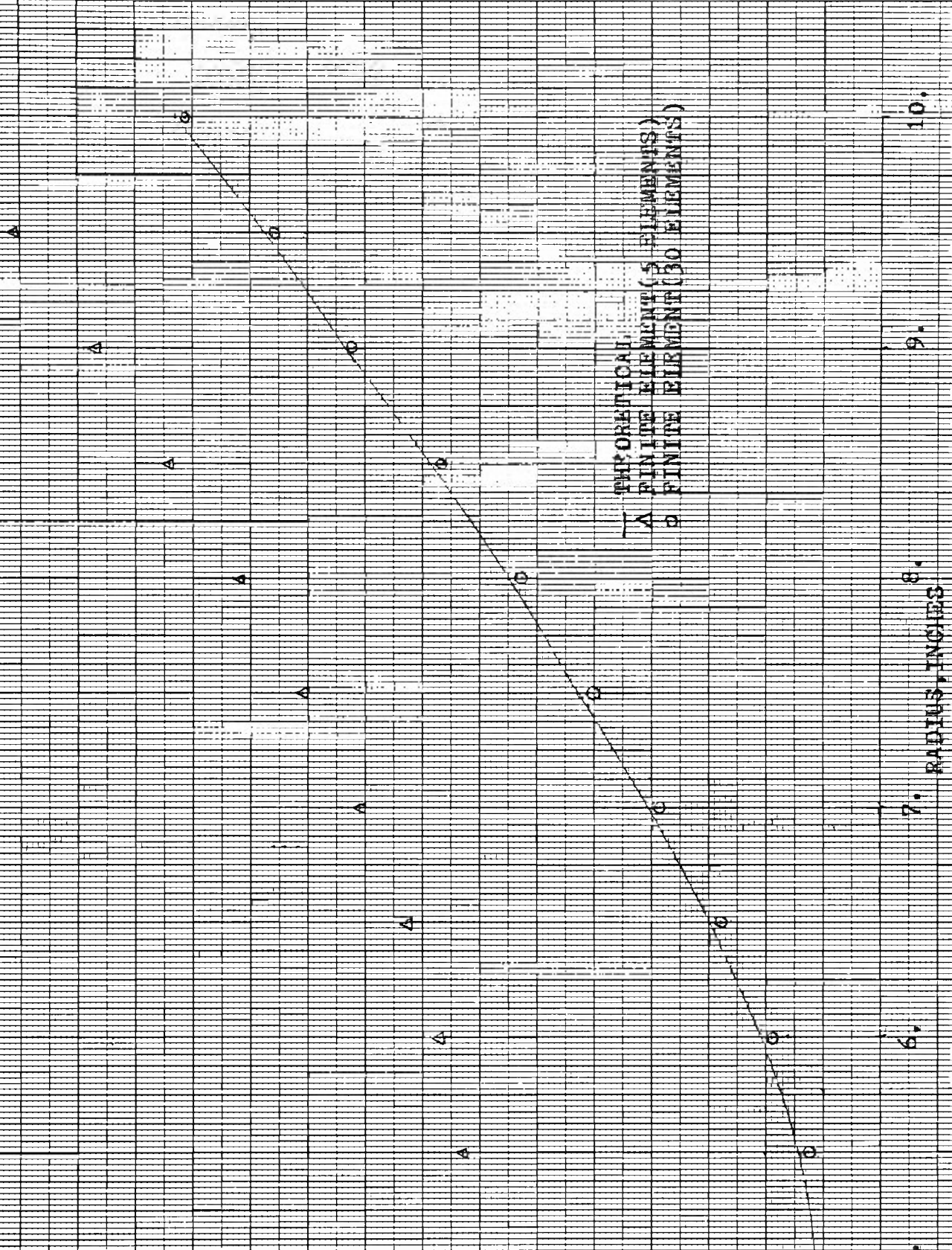
7.

8.

9.

10.

RADIUS, INCHES



THEORETICAL  
 A FINITE ELEMENT (5 ELEMENTS)  
 O FINITE ELEMENT (30 ELEMENTS)

PICTURE 8

RADIAL STRESS VERSUS RADIUS FOR

RADIAL STRESS  
 $\times 10^3$   
PSI

-14.0

-12.0

-10.0

-8.0

— THEORETICAL  
△ FINITE ELEMENT (5 ELEMENTS)  
○ FINITE ELEMENT (20 ELEMENTS)

RADIUS, INCHES

5. 6. 7. 8. 9. 10.

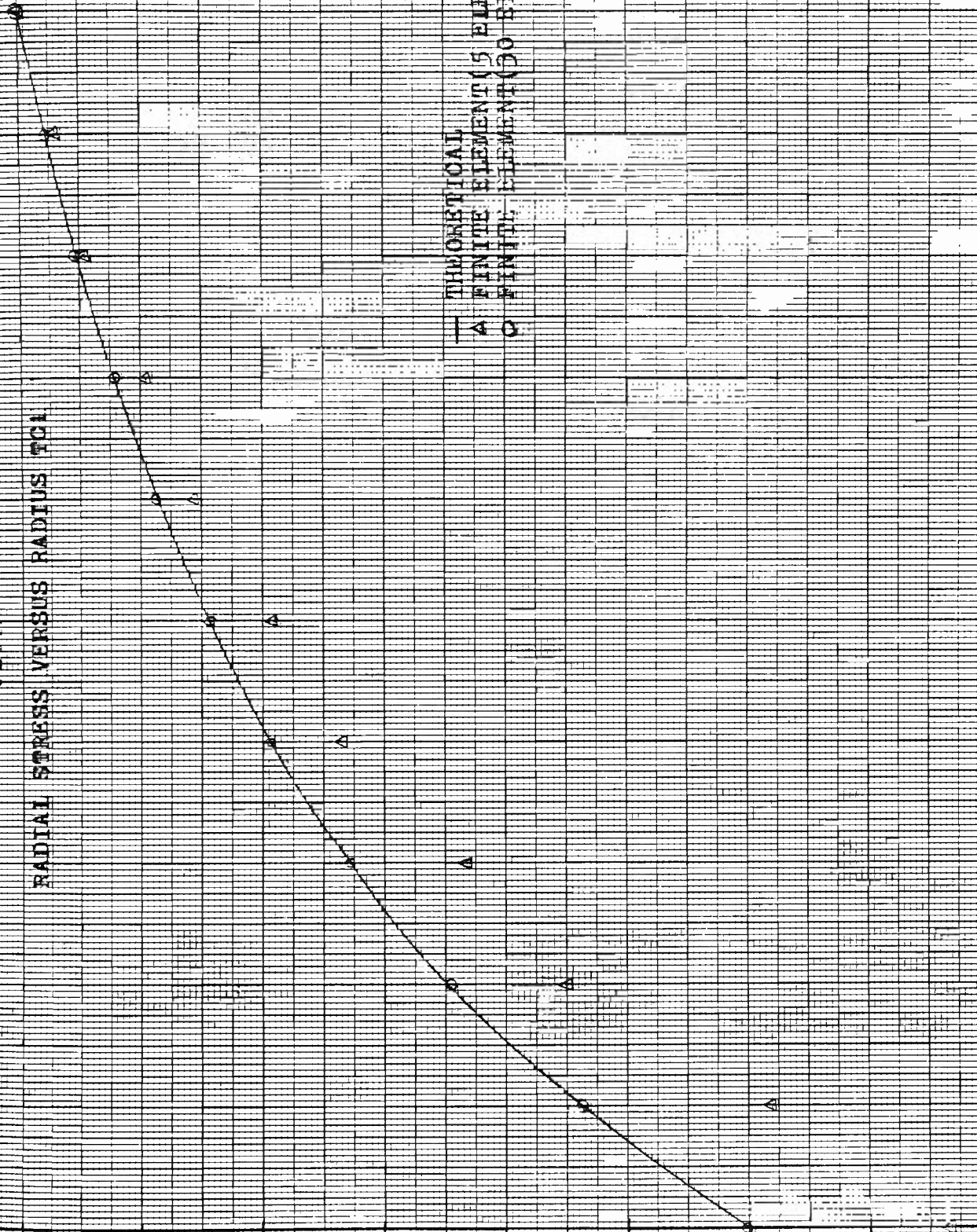
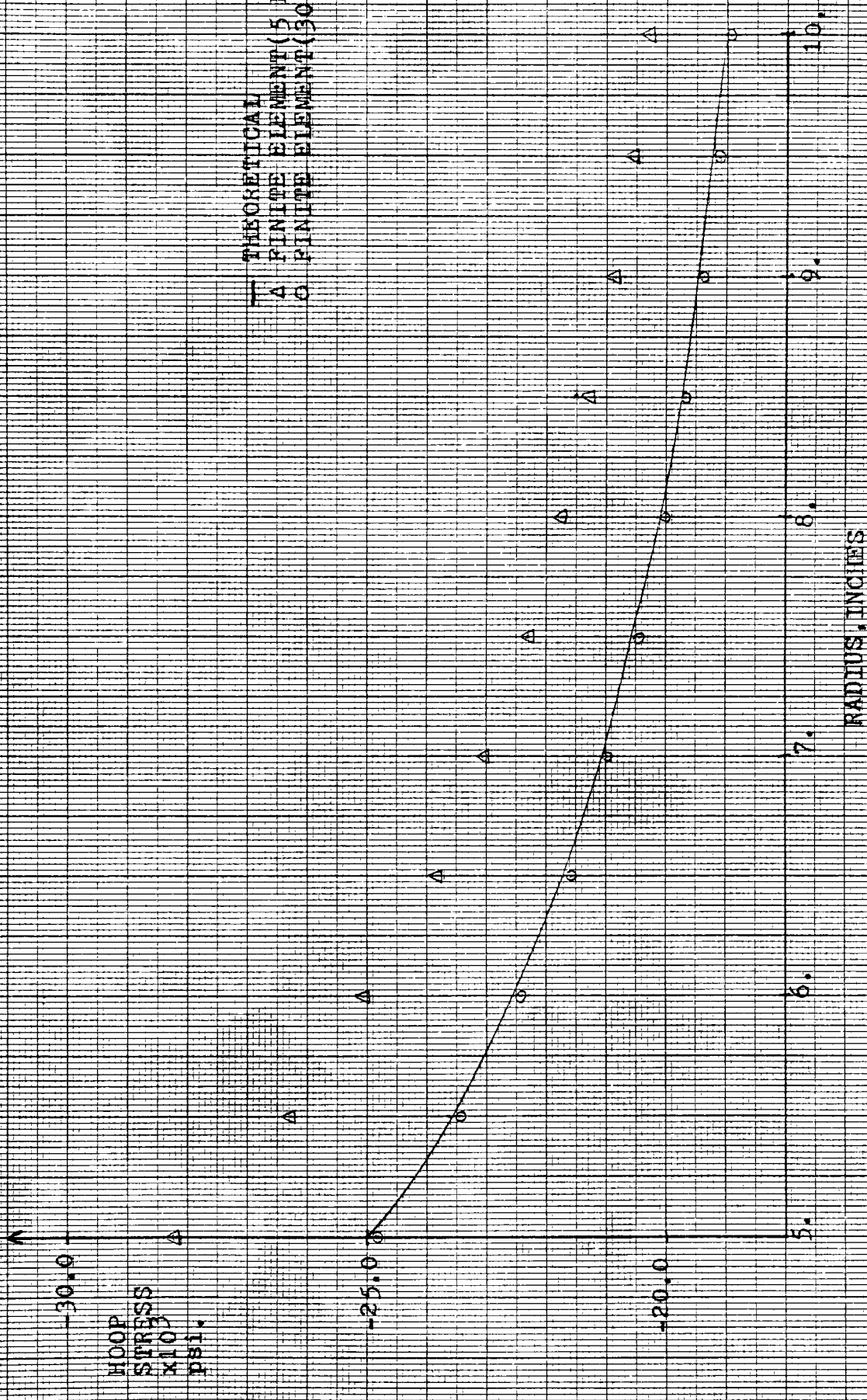


FIGURE 8  
HOOP STRESS VERSUS RADIUS TC1 (30 ELEMENTS)



HOOP STRESS x10<sup>3</sup> psi.

RADIUS, INCHES

THEORETICAL

△ FINITE ELEMENT (5 ELEMENT)

○ FINITE ELEMENT (30 ELEMENT)

TABLE III  
 TC 1 SUMMARY OF RESULTS

DEGREES OF FREEDOM	$\sigma_r$ MAX. psi.	% DIFF.	$\sigma_\theta$ MAX. psi.	% DIFF.	$U_r$ MAX. $\text{in} \times 10^{-3}$	% DIFF.
Theoretical	-15000.	---	-25000.	---	-4.83	---
14*	-16223.	8.15	-28376.	13.50	-5.25	8.49
54**	-15023.	0.16	-28249.	13.00	-5.26	8.90
248***	-15004.	0.03	-24820.	0.72	-4.81	0.41

\* 1 element

\*\* 5 elements

\*\*\* 30 elements

TABLE VI  
 COMPARISON OF RESULTS OF THESIS VERSUS THOSE OF  
 LINEAR AND QUADRATIC TRIANGULAR ELEMENTS

	<u>DARIO &amp; BRADLEY</u>	<u>DARIO &amp; BRADLEY</u>	<u>THESIS</u>
<u>Element shape:</u>	triangle	triangle	quadrilateral
<u>Displacement function:</u>	linear	quadratic	quadratic
<u>Model information</u>			
Number of nodes:	105	105	110
Number of elements:	160	40	30
<u>Maximum stress differences</u>			
Radial stress:	6.43%	0.46%	0.03%
Hoop stress:	0.7%	0.1%	0.72%

## 8.2 Stresses in a Uniformly Thick Disk Due to Centrifugal Load TC 2

The second test case is a classic problem in the theory of elasticity and involves the determination of radial and hoop stresses in a circular disk of uniform thickness subjected to centrifugal loading. Problem geometry and loading conditions are shown in Fig. 9a. The finite element model used contained 30 elements and 125 nodes and is shown in Fig. 9b. Theoretical solutions for stresses are presented by Timoshenko [1] and are quadratic in nature. Results from the finite element idealization are compared with their theoretical values in Fig. 10 and for all practical purposes may be considered exact.

Consideration in this analysis was not only determination of accurate stress values but also the work necessary in specifying the body force loading condition.

Body forces were calculated for each element and specified as external forces acting at the model nodal points, consistent with the allocation scheme shown in Fig. 3.

Using the above technique presents severe limitations in representing this type of problem which

include:

1. An excessive amount of time to calculate element body forces and distribute them to the nodal points.
2. A necessarily large amount of input data for specification for the external nodal point forces calculated.
3. In the case of elements with curved boundaries, allocation of element body force to its nodes is no longer obvious as in the case presented and requires additional consideration.

All of the above limitations may be alleviated by the introduction of a subroutine in the program to internally calculate and distribute body forces to nodal points on a per element basis. Also, the third limitation cited is greatly reduced by using quadrature techniques. The computer program developed does not contain this option which is left for future development.

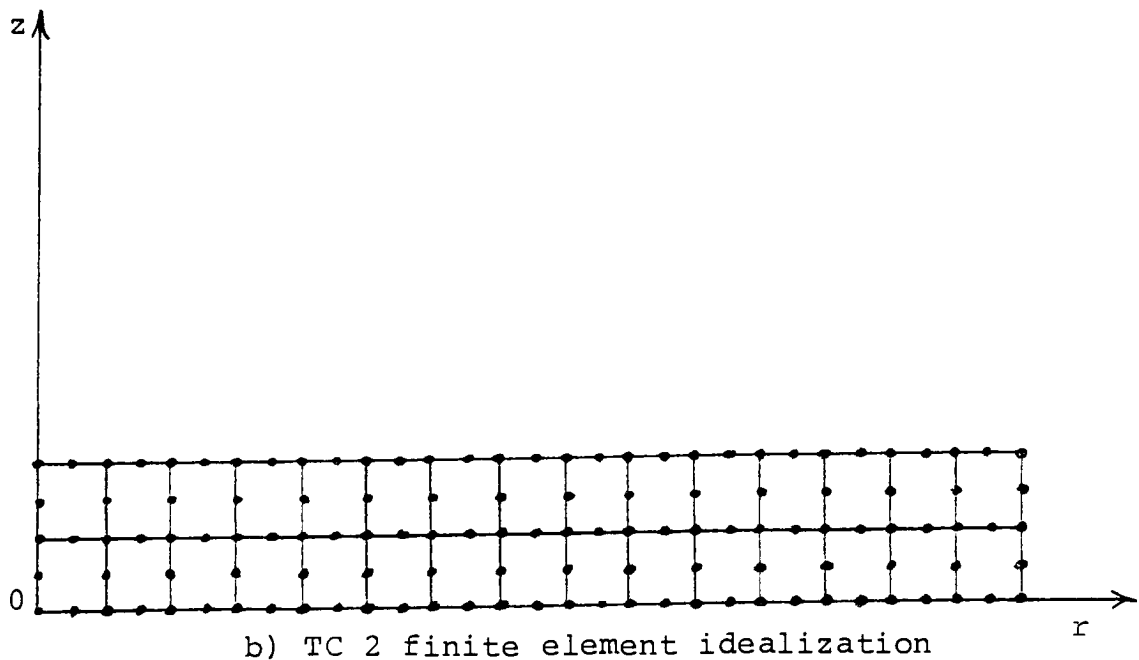
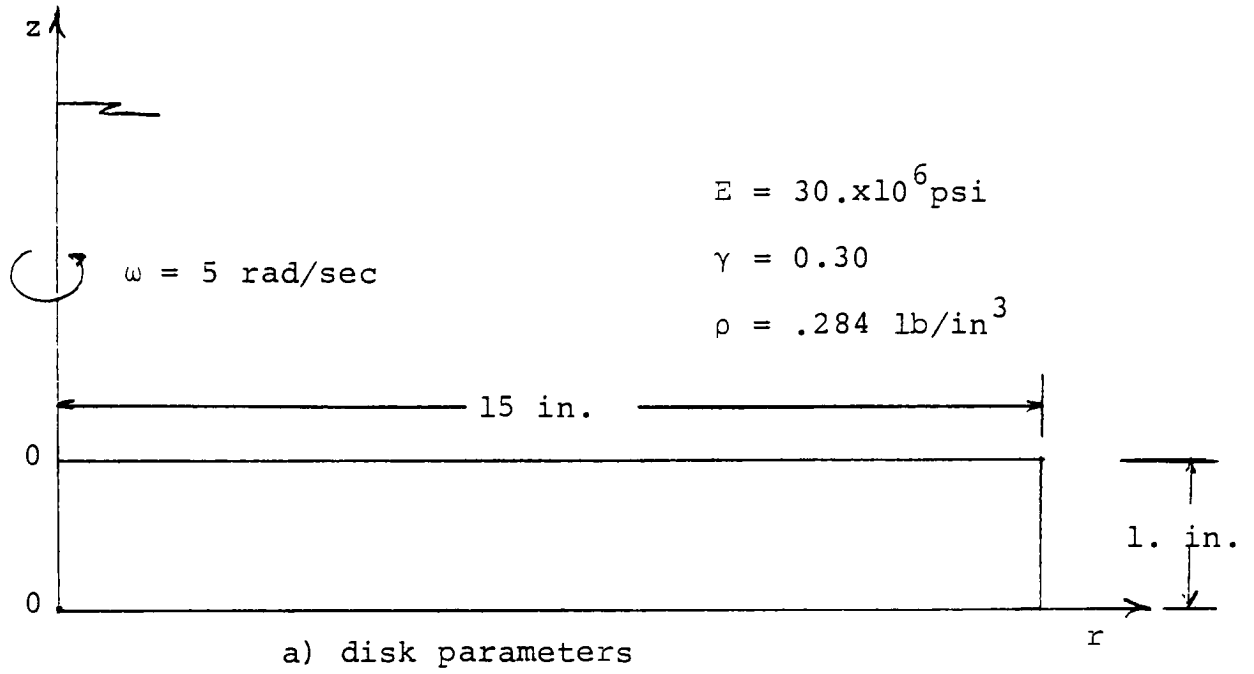


FIGURE 9  
Uniformly Thick Disk Subjected  
to Centrifugal Loading

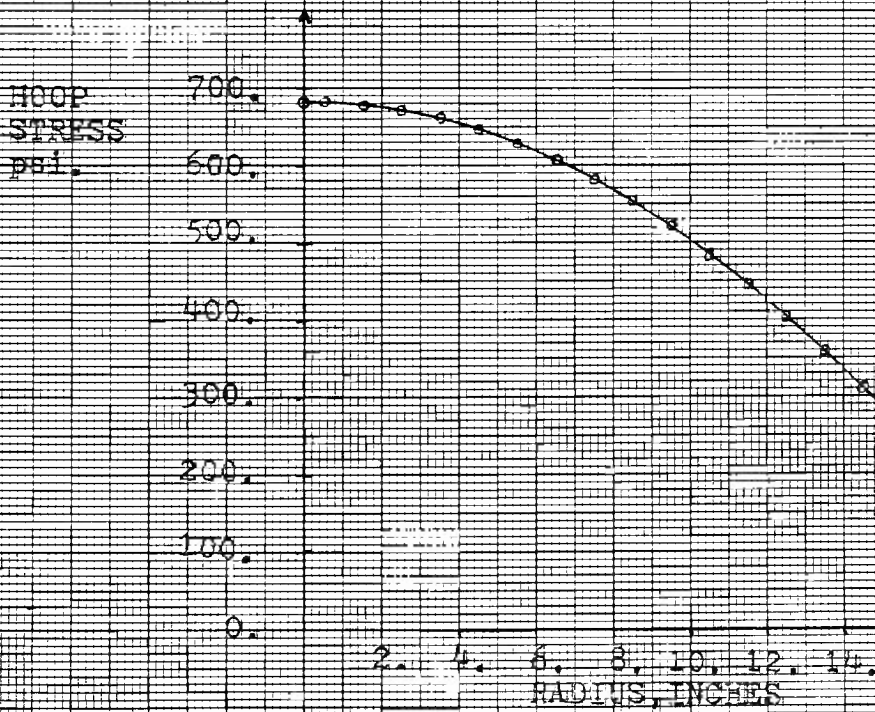
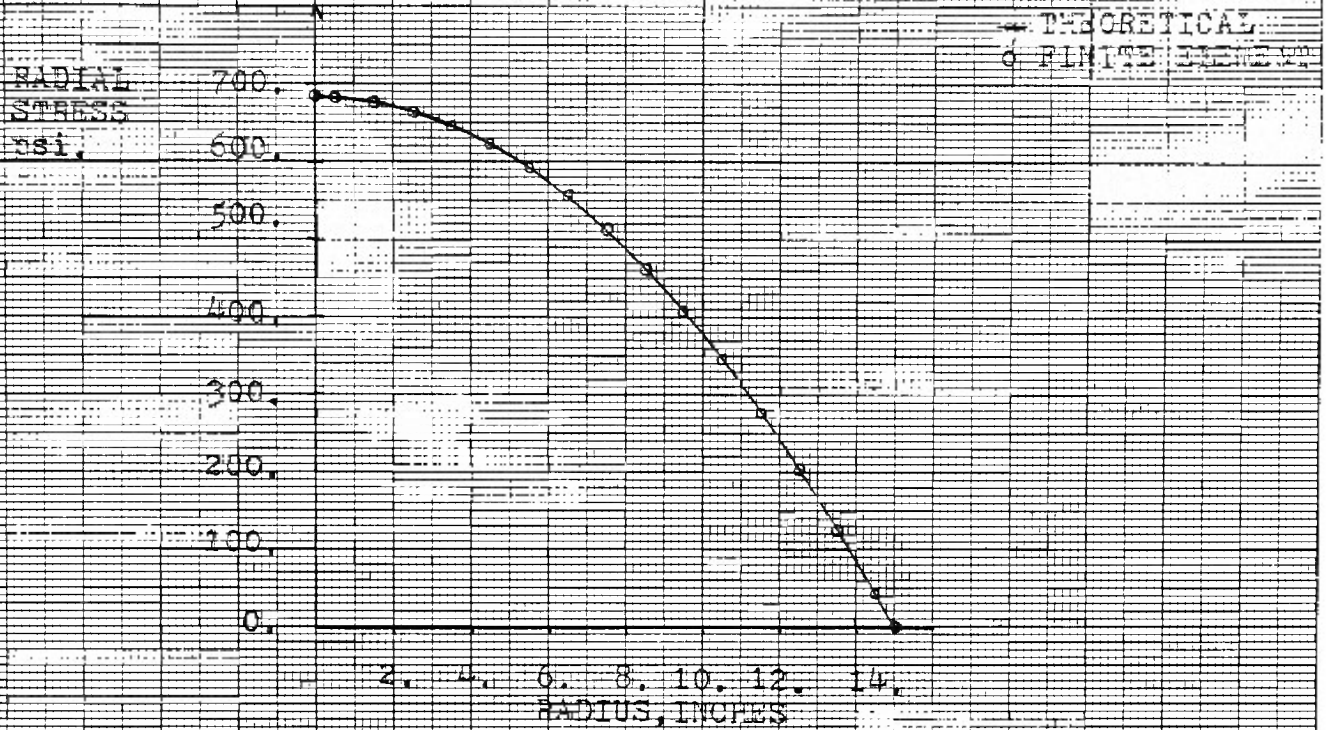


FIGURE 10  
 RADIAL AND HOOP STRESS RESULTS FOR TC 2

### 8.3 Stress Concentrations in a Cylindrical Rod Due to a Spherical Inclusion TC 3

The problem of axial stress concentration in a cylindrical rod containing a spherical inclusion was analysed as a test case to demonstrate the program's ability to represent curved boundaries and predict stress concentration values. The rod is subjected to a uniform tensile stress distribution as shown in Fig. 11.

The actual problem follows the notation of Dario and Bradley [21]. A closed form solution is presented by Timoshenko[1].

The finite element model developed, taking into account the symmetry of loading, is presented in Fig. 12. Only three elements are used to represent the inclusion boundary.

A graph comparing finite element to theoretical axial stress in the plane perpendicular to the z axis at  $z = 0$  is presented in Fig. 13. The maximum difference between predicted and theoretical stress values was found to be 1.06%.

In an attempt to obtain further stress information in the localized area of concern, a second model was developed simulating a region consisting of the four elements noted in Fig. 13.

These four elements were divided into the eight elements shown in Fig. 14. Nodal points corresponding to nodes of the original model are circled. New model boundary conditions were specified as enforced displacements at the circled nodes obtained in the initial idealization.

The results for axial stress ( $\sigma_z$ ) in the plane  $z = 0$  for this model produced no correlation with that previously obtained. However, stresses at element midside nodes just away from the boundary ( $z = .166$ in.) did exhibit convergence and are shown in Fig. 13. The reason for boundary discrepancies is believed to be due to the introduction of additional nodes on the refinement's boundaries. It is felt that these additional nodes whose displacements are not prescribed result in deformation of the idealization's boundaries which are incompatible with the deformations of the original model. Possible techniques to overcome these discrepancies are:

1. Use element displacement functions (Eqs. 2 and 3) to determine prescribed displacements for all nodes of the refined model (Fig. 14.). This would assure displacement compatibility between both models.

2. Determine stress element boundary values directly for each element of the original model using the relation:

$$\{\sigma\} = [D][B]\{w_o\}$$

Both of these techniques would require the development of an auxiliary program. The second technique appears to be more efficient since it would not require the formulation of additional structural models. Development of a program using the second technique cited has been initiated but is as yet unfinished. At present, discrepancies in boundary stresses of refined models are unresolved.

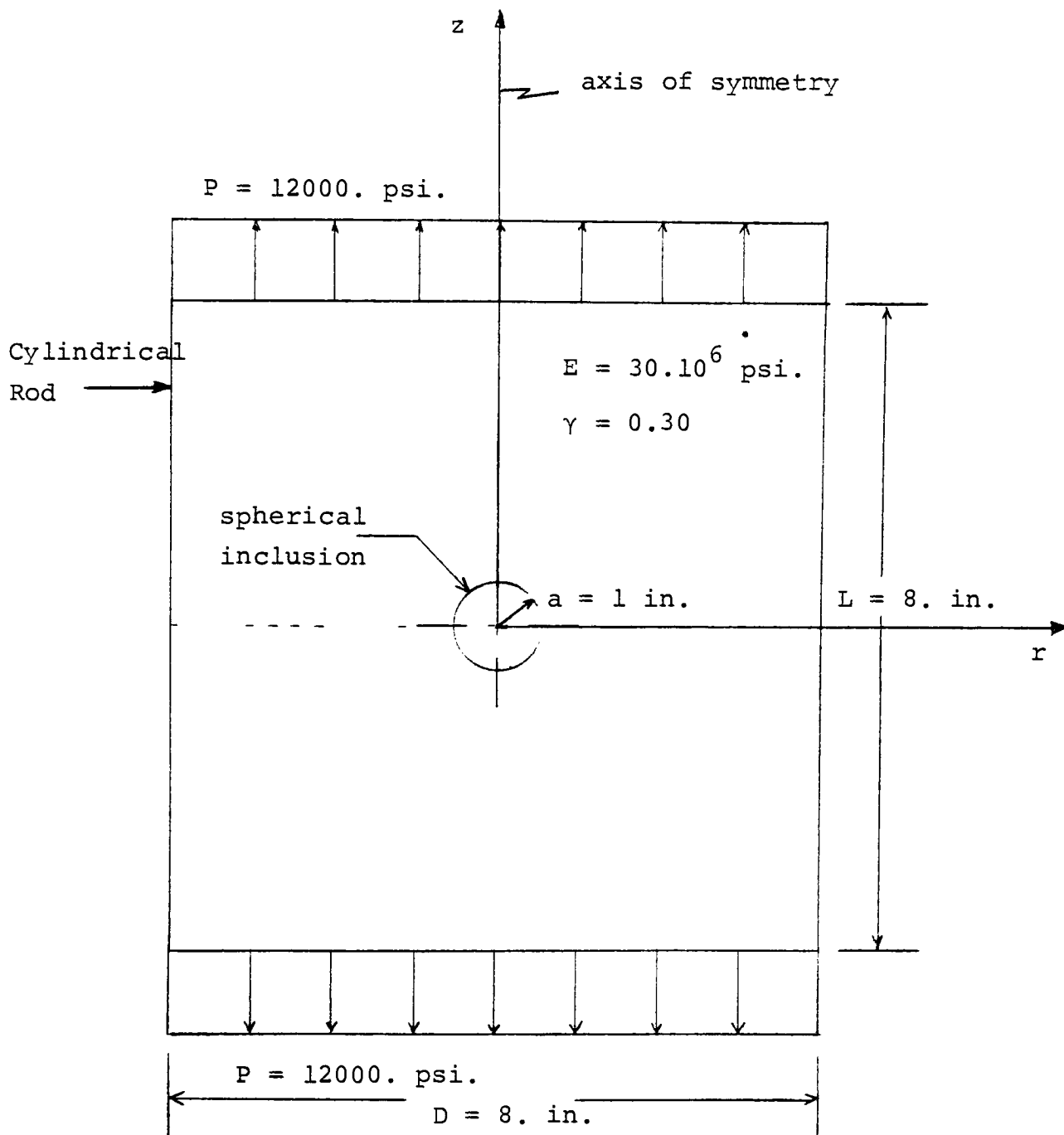


FIGURE 11

Cylindrical Rod Having a Spherical Inclusion

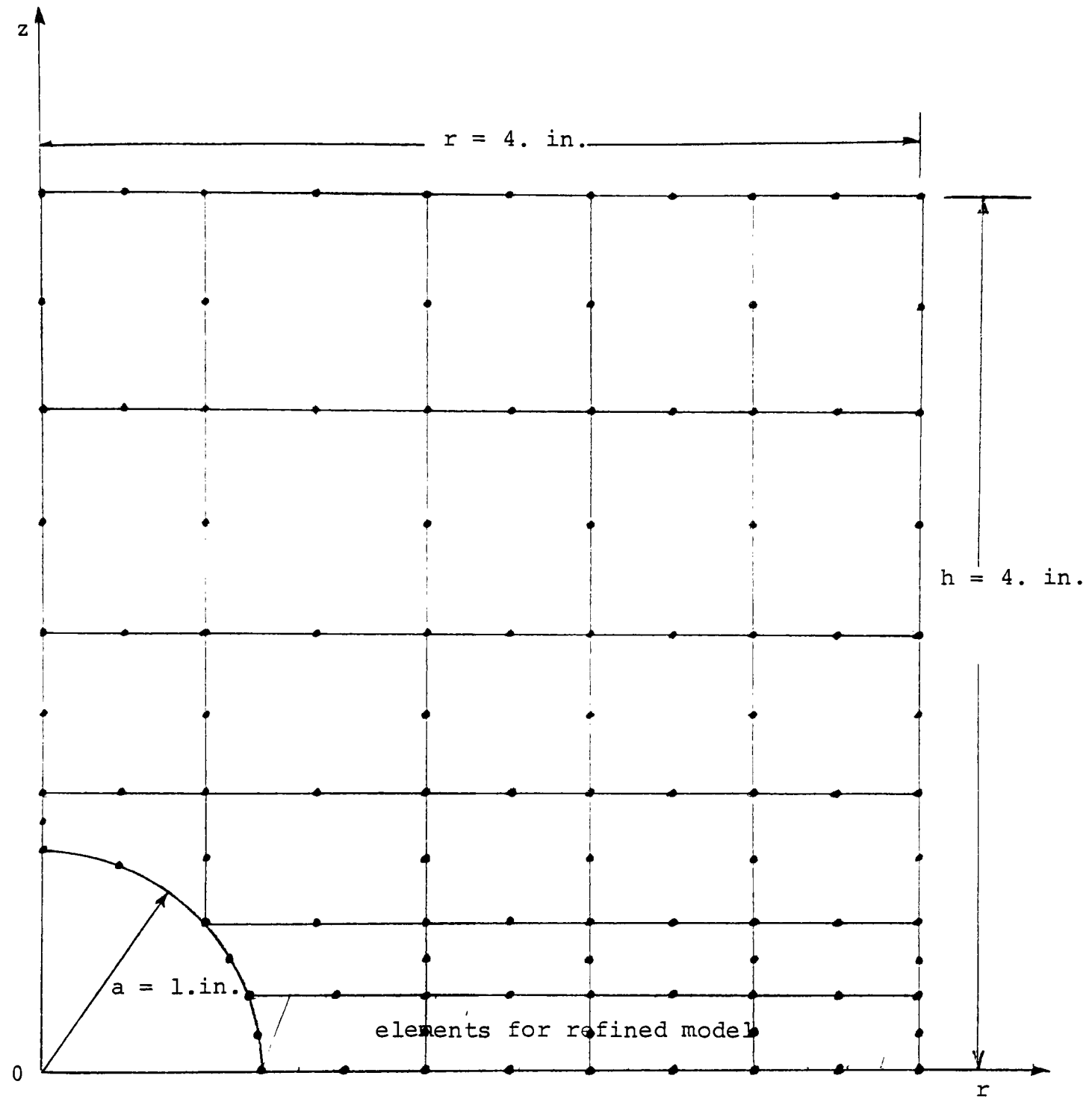


FIGURE 12

TC 3 Finite Element Idealization of  
Spherical Inclusion in Cylindrical Rod

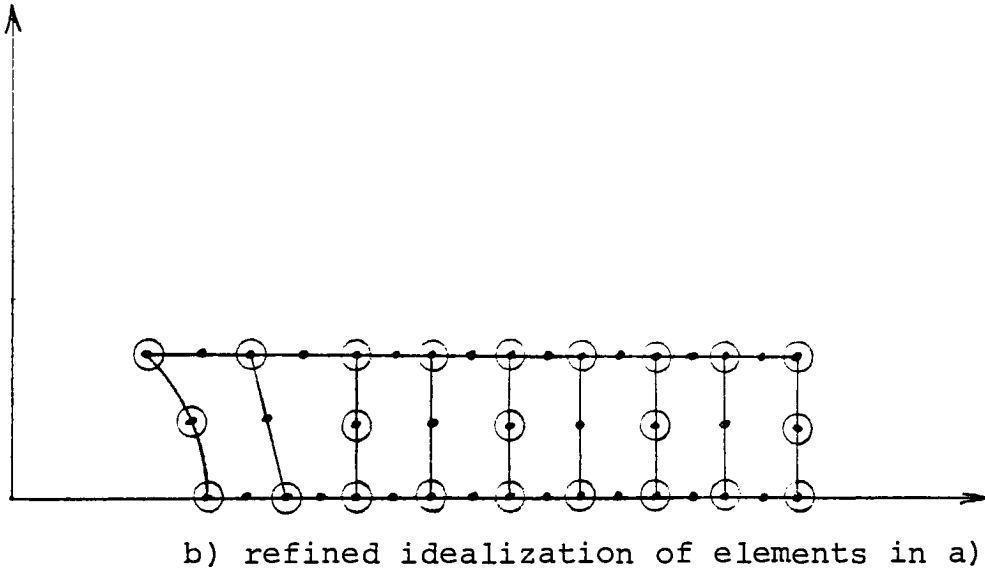
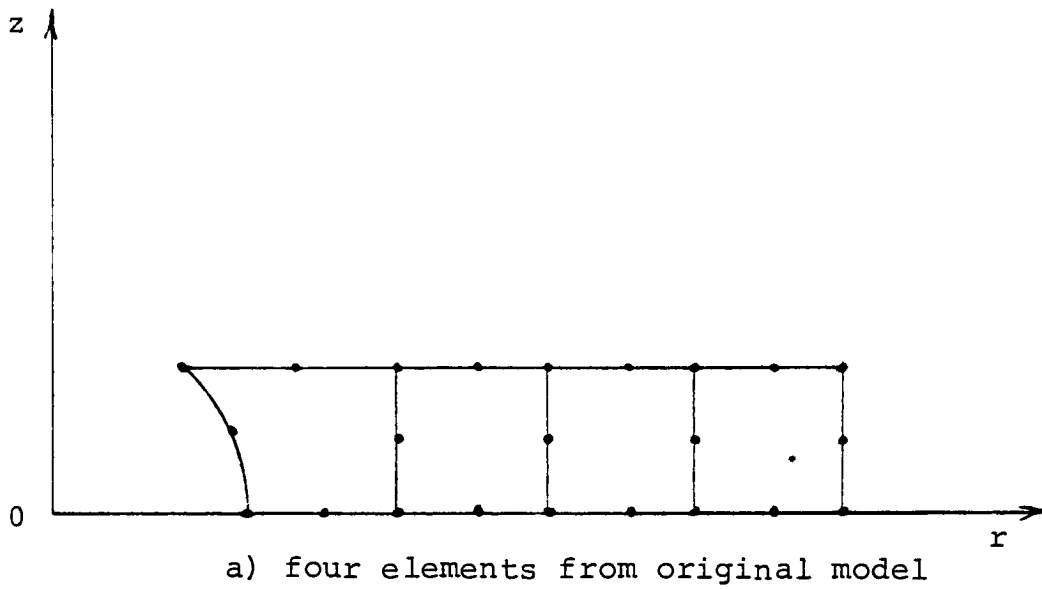


FIGURE 14

TC 3 Refined Idealization

FIGURE 13  
FIG 3 AXIAL STRESS RESULTS



## 8.4 Stresses and Deflections in a Spherical Pressure

### Vessel TC 4

The fourth test case presented involves the determination of principal stresses and volumetric expansion of a thick spherical pressure vessel subjected to an internal pressure as shown in Fig. 15.

Theoretical solutions for stress and displacement contain cubic and quartic functions of radius respectively. Of particular interest in this test case is the element's ability to represent the curved spherical surface.

Due to symmetry only half of the sphere was necessary in describing a finite element model.

Difficulties with principal stress predictions resulted in the formulation of the four finite element models shown in Fig. 16. In all four cases the volumetric expansions obtained showed good correlation with theoretical results. Comparisons of the theoretical maximum displacement with the results from the four test cases is presented in Table IV. A graph showing theoretical, TC 4A, and TC 4D radial displacement as a function of radius is presented in Fig. 17.

The order of the displacement function for the quadratic element results in linear intraelement

stress variation. In the case where actual stress is of higher than linear order, stresses computed for coarse finite element models will exhibit finite discontinuities at midside nodes of adjacent elements. This as pointed out by Desai and Abel[17], is due to the absence of force equilibrium in individual elements. Involving structural force equilibrium relations, the overall equilibrium of the body is approximated but not that of individual elements. Increased finite element refinement minimizes this effect.

TABLE IV

## TC 4 SUMMARY OF MAXIMUM DISPLACEMENT RESULTS

<u>MODEL</u>	<u>DEGREES OF FREEDOM</u>	<u>MAXIMUM DISPLACEMENT in. x 10<sup>-6</sup></u>	<u>PERCENT DIFFERENCE</u>
Theoretical	closed form solution	22.22	--
TC 4A	64	18.82	15.3
TC 4B	88	20.20	9.09
TC 4C	112	20.64	7.11
TC 4D	224	21.36	3.87

It was found that only the finest mesh (TC 4D) predicted stress values that were at all close to theoretical values. Graphs comparing the theoretical principal hoop and radial stresses and the interelement linear variations of stress for TC 4D are shown in Figs. 18 and 19.

As can be seen from these graphs, large discontinuities in stress between the first two adjacent elements through the thickness of the sphere are predicted. These stress values are quite unreliable. Both the large discontinuities and the gradient of the theoretical curves suggest that a more refined finite element simulation is required in this region to improve stress results. Also, the extrapolation technique for stresses proposed in section 8.3 might improve these values.

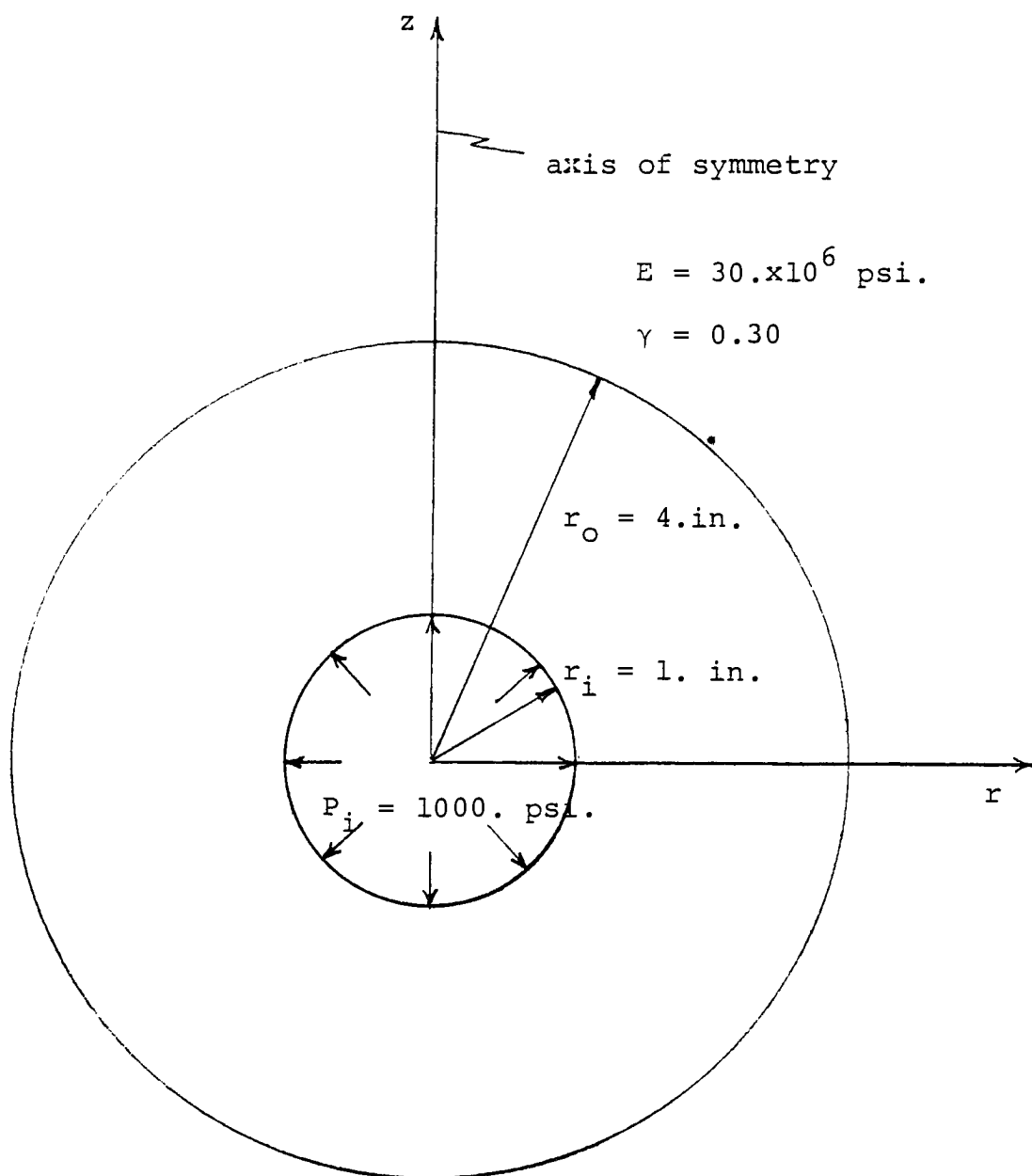
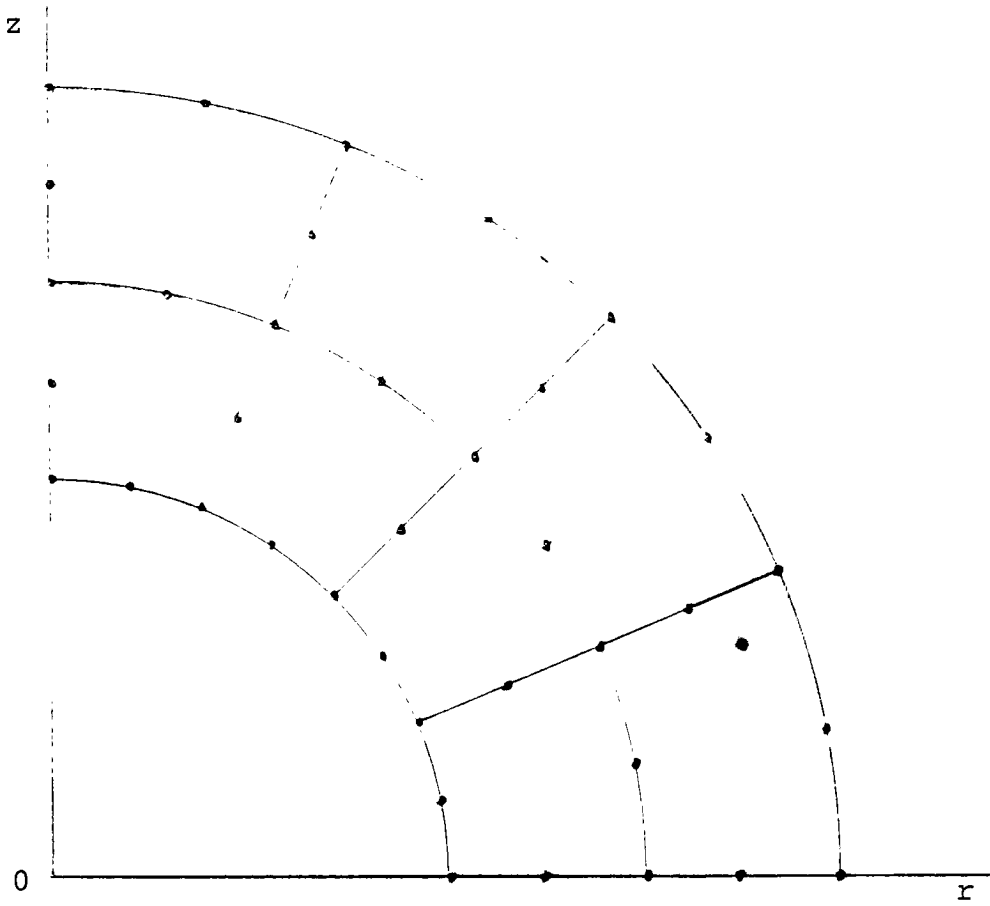
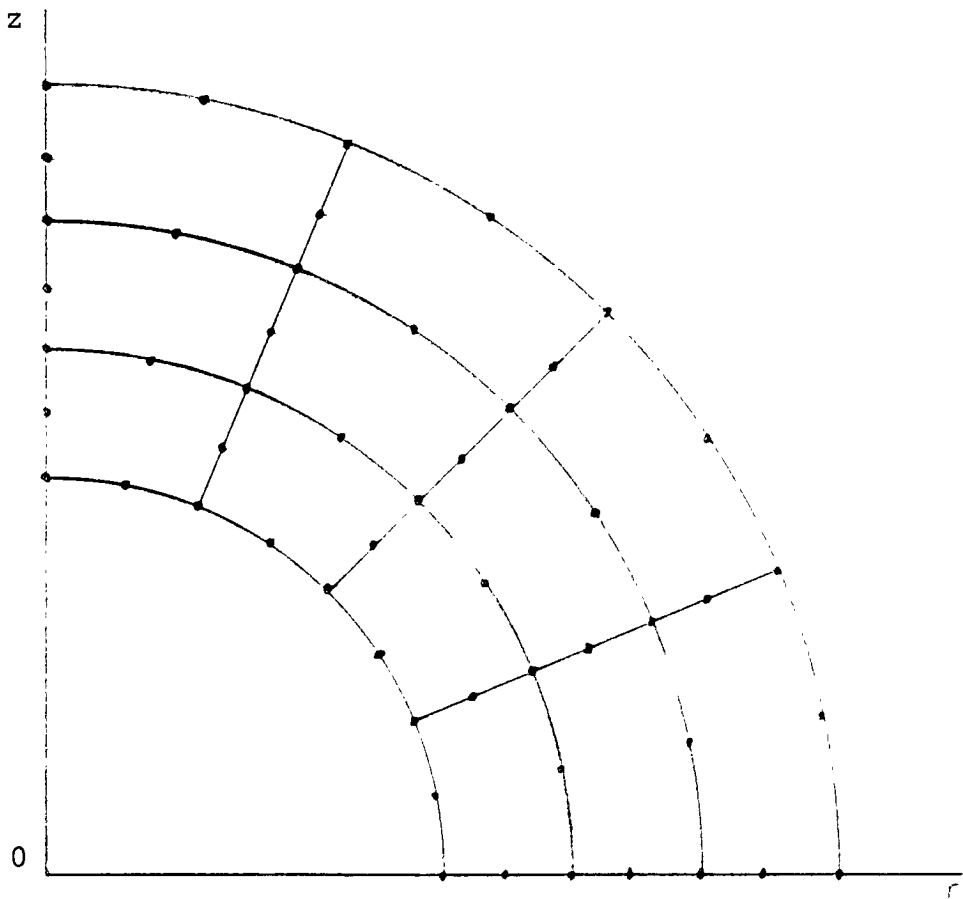


FIGURE 15

Spherical Pressure Vessel  
Subjected to Internal Pressure

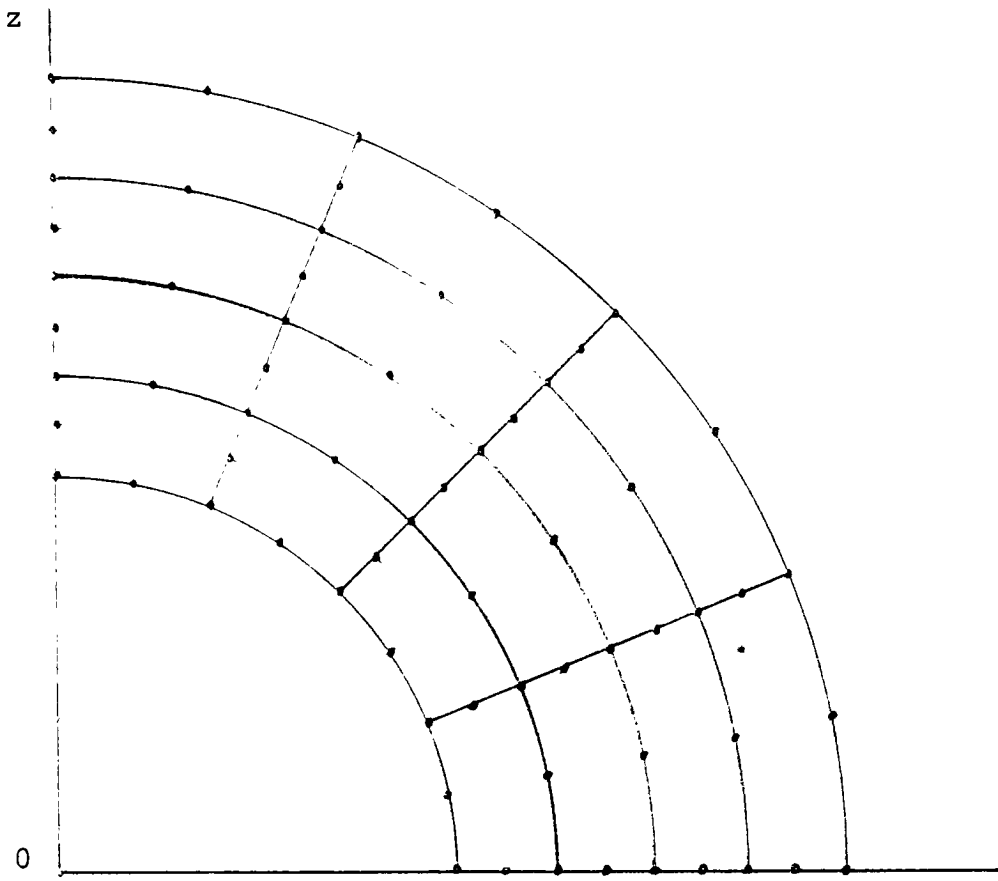


a) first finite element idealization TC 4A

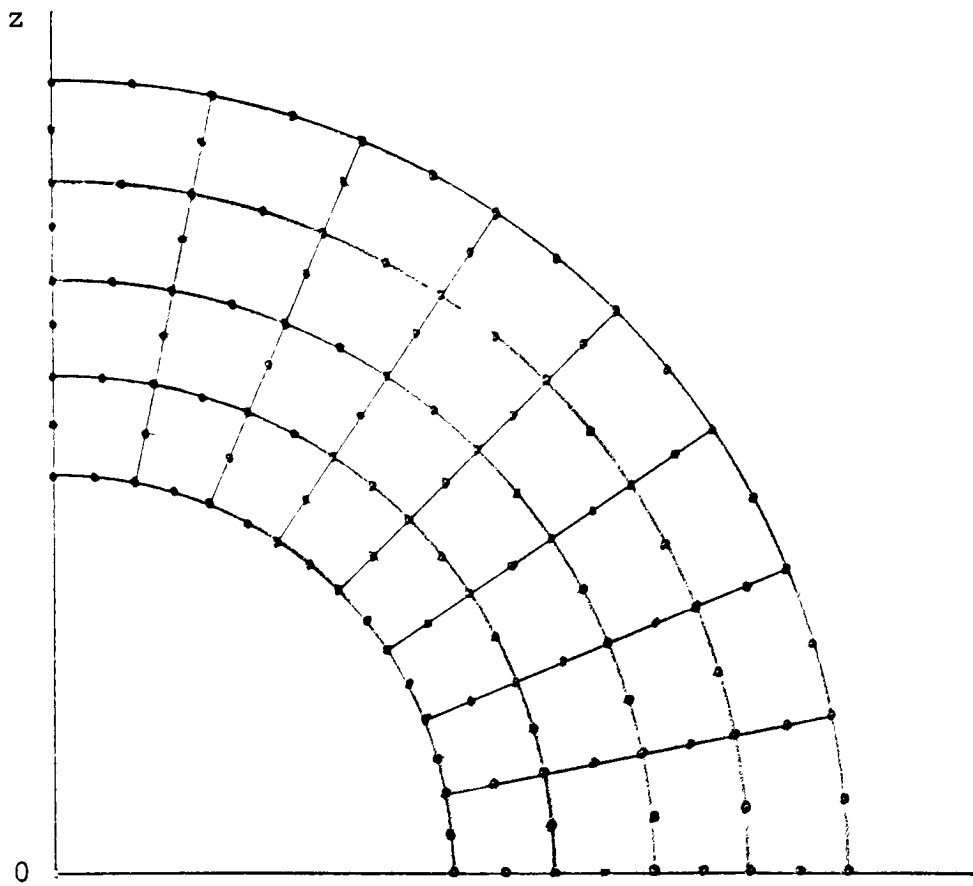


b) second idealization TC 4B

FIGURE 16  
Finite Element Idealizations of TC4



c) third idealization TC 4C



d) fourth idealization TC 4D

FIGURE 16 (Continued)

FIGURE 17  
 TC 4 VOLUMETRIC EXPANSION  
 VERSUS RADIUS

$U_D$   
 $\times 10^{-6}$

— THEORETICAL  
 O TC 4A  
 X TC 4D

1.0  
 2.0  
 3.0  
 4.0

RADIUS, INCHES

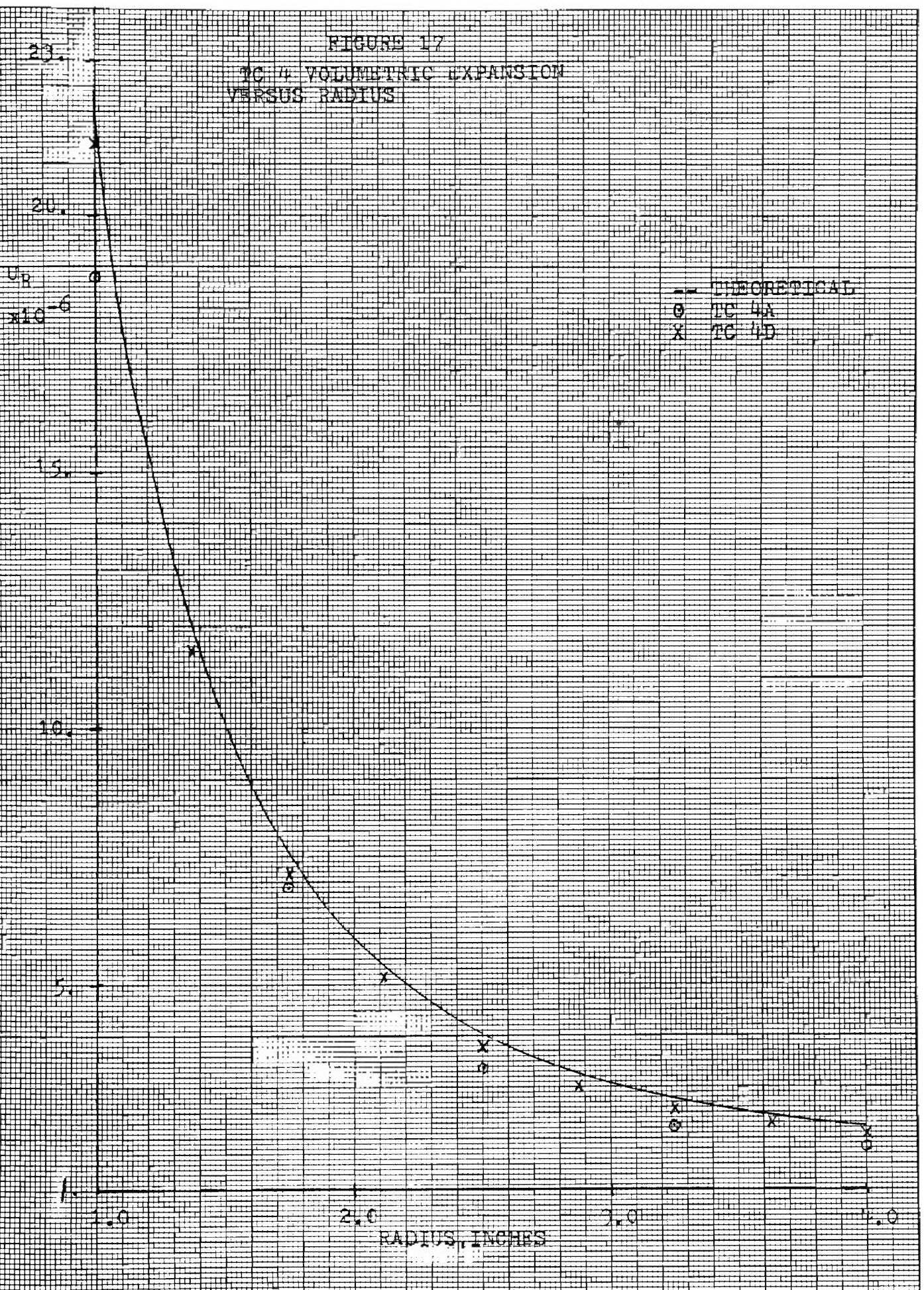


FIGURE 18  
PRINCIPAL HOOP STRESS  
VERSUS RADIUS

HOOP  
STRESS  
psi.

— THEORETICAL  
-•- FINITE ELEMENT  
(TC 4D)

600.

500.

400.

300.

200.

100.

1.0

2.0

3.0

4.0

RADIUS, INCHES

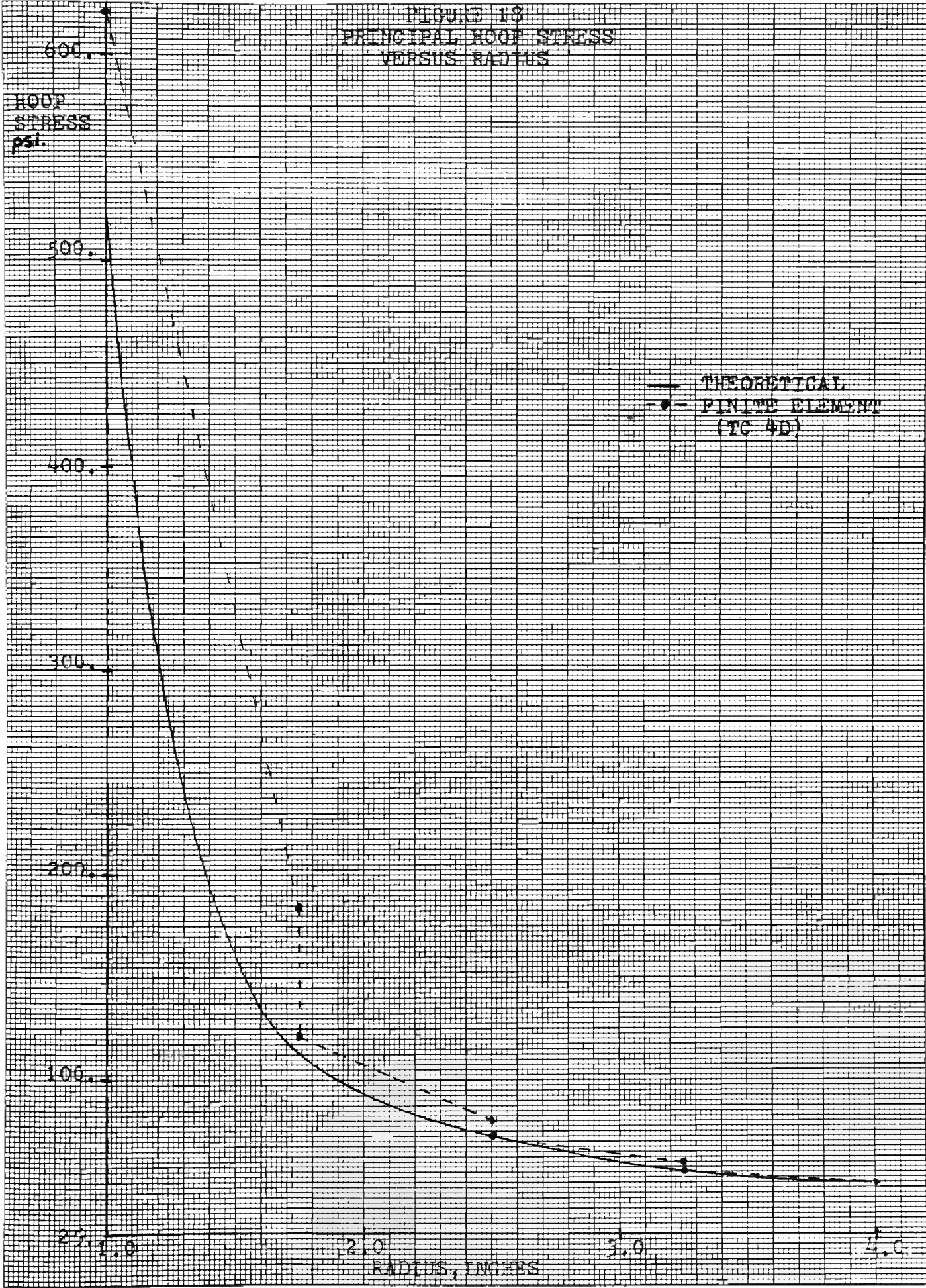
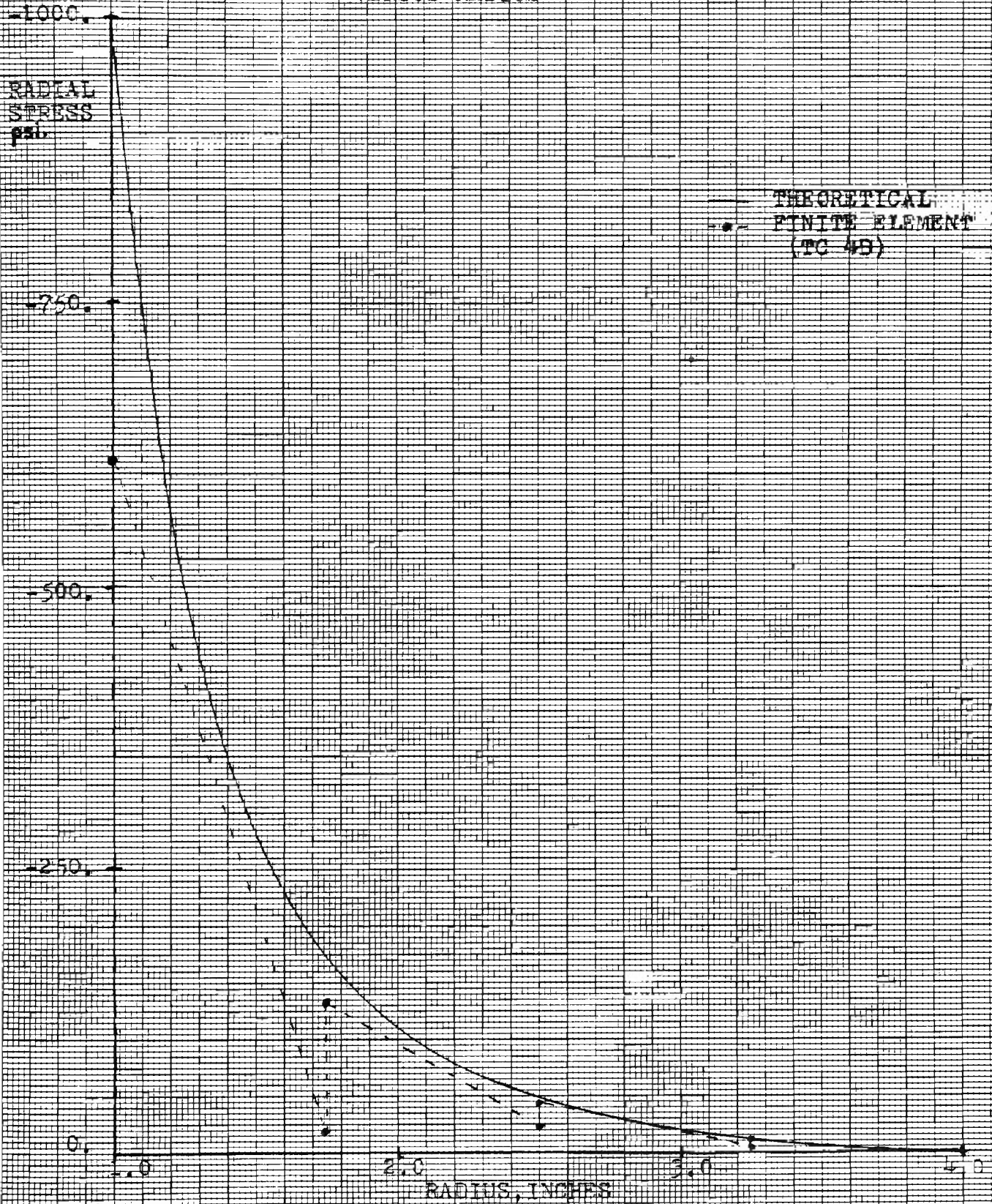


FIGURE 19  
PRINCIPAL RADIAL STRESS  
VERSUS RADIUS



### 8.5 Circular Plate Bending-Investigation TC 5

The objective of this investigation was to determine this quadratic element's ability to predict displacements and stresses in structures obeying small displacement plate theory. This theory involves approximations in order that a linear differential equation of equilibrium is obtained. The criteria which a structure must meet to qualify as a plate obeying small displacement theory are stated by Timoshenko and Woinowski-Krieger [28] as:

1. There is no in-plane deformation of the middle plane of the plate which remains neutral during bending.
2. Lines initially normal to the middle plane of the plate experience linear variation of stress and strain.
3. Normal stresses in the direction transverse to the plate may be disregarded.

These criteria are satisfied provided transverse displacements are small in comparison with plate thickness and plate thickness is much smaller than radius.

The particular problem chosen to analyse was that of a circular plate clamped along its outer radius and loaded with a uniform pressure normal to its

surface. Plate geometry and boundary conditions are shown in Fig. 20a.

A finite element idealization of this problem was developed for the case of a load intensity  $P_0 = 10$  psi. (Fig. 20b.) Structural displacement results were compared with the theoretical solution presented by Timoshenko and Woinowski-Krieger [28] and were found to be of unreasonable form and magnitude. This lack of correlation was discussed in detail with several knowledgeable individuals in the field of finite element analysis [25], [26], [27], [33]. These discussions and a survey of available literature resulted in identification of several areas as the potential sources of discrepancy. These areas and comments on their subsequent investigations are:

#### Potential Sources of Discrepancy

1. Errors in element development or computer programming.
2. Errors in stiffness calculations due to the singularity in hoop strain ( $e_\theta$ ) for elements lying on the axis of symmetry.
3. Inappropriate structural idealization.
4. Incorrect specification of structure boundary conditions.
5. Violation of plate theory assumptions.

#### Comments

- 1.a) Investigations of element development and computer program by McCalley [26], Rieger [33],

- and the author did not identify any errors.
- b) At the suggestion of McCalley, the eigenvalues and eigenvectors of a single element's stiffness matrix were calculated to verify element stiffness formulation. All principal stiffness values were found to be positive and the fundamental eigenvector was found to correspond to a rigid body axial translation. Both of these findings were consistent with a correctly formulated stiffness matrix.
  - c) It was established for a one element problem that structural force equilibrium was maintained.
2. The singularity in the hoop strain expression ( $e_{\theta} = \frac{u}{r}$ ) will not provide error in stiffness formulation.
- As noted by Ergatoudis [8], these expressions are evaluated at Gauss sampling points when stiffness matrices are evaluated numerically and these sampling points will not generally lie on element boundaries where  $r = 0$ . Also, results obtained in TC 2, TC 3, and TC 4 where elements were defined having an edge on the axis of symmetry did not exhibit similar difficulties.

- 3.a) The use of one element through plate thickness is justified by the second assumption of plate theory that lines initially normal to the middle plane of the plate experience linear variation of stress and strain. Since element displacement is quadratic, transverse stress and strain may vary linearly in the element. This fact is discussed by Griffin [30] for the case of beams in bending and also that a large number of elements are necessary along the length of a beam to account for curvature of axial fibers. Similar reasoning applies to the case of circular plates. However, increasing element refinement to 60 elements through the radius produced no appreciable difference in displacements.
- b) At the suggestion of Glasser [ 27 ], solutions were obtained for models having four elements through the plate thickness. Due to limitations of computer core, a maximum of 16 elements along the radial direction could be specified. Resulting elements had aspect ratios of radial length/thickness of 10 and predicted unreasonable displacements. These results were inconclusive.

4. A total of 30 computer runs were made having minor modifications in specified boundary conditions. Alterations of plate geometry, force distribution, and displacement constraints did not produce appreciable changes in predicted results.
5. The possibility of violating the plate theory assumption that the middle plane of a plate remains neutral in bending was suggested by Rieger [33]. By reducing the load intensity  $P_0$  in Fig. 20a, a significant improvement was obtained in deflection results.

Based on these observations, it was concluded that one discrepancy which existed was due to violation of the assumptions of small displacement plate theory. It was also decided that the structural idealization shown in Fig. 20b was appropriate. The load intensity was changed to 1 psi (Fig. 20a) to reduce deflection magnitudes.

Displacement results were obtained for three finite element models having 20, 30, and 40 elements through plate radius and 1 element through its thickness. Computer calculations were performed in single precision arithmetic. A comparison of predicted and theoretical displacement results is presented in Fig. 21. Predicted displacement shapes were reasonable

but their magnitudes did not exhibit lower bound convergence to theoretical values with model refinement.

These observations indicated additional error in either computer program or finite element idealization. In depth discussions with Halbleib [35] vindicated the finite element idealizations representing plate theory. Verification of a quadratic element's ability to represent flexural problems and the eventual determination of the source of error in the thesis program was made possible with the help of Loeber [25].

It was learned that a quadratic element similar to that developed was in use at the Knolls Atomic Power Laboratory (KAPL). In collaboration with Loeber, 20, 30, and 40 element idealizations similar to those run by the author were executed at KAPL. In all cases, displacement results were found to agree within 1% of theoretical values. Subsequent discussion with Loeber identified the major discrepancy between the thesis and KAPL programs as being the arithmetic precision of the computers involved. The Xerox Sigma 6 computer available to the author uses a 32 bit word in single precision arithmetic calculations while the CDC 7600 computer at KAPL uses a 60 bit word in single precision. It was

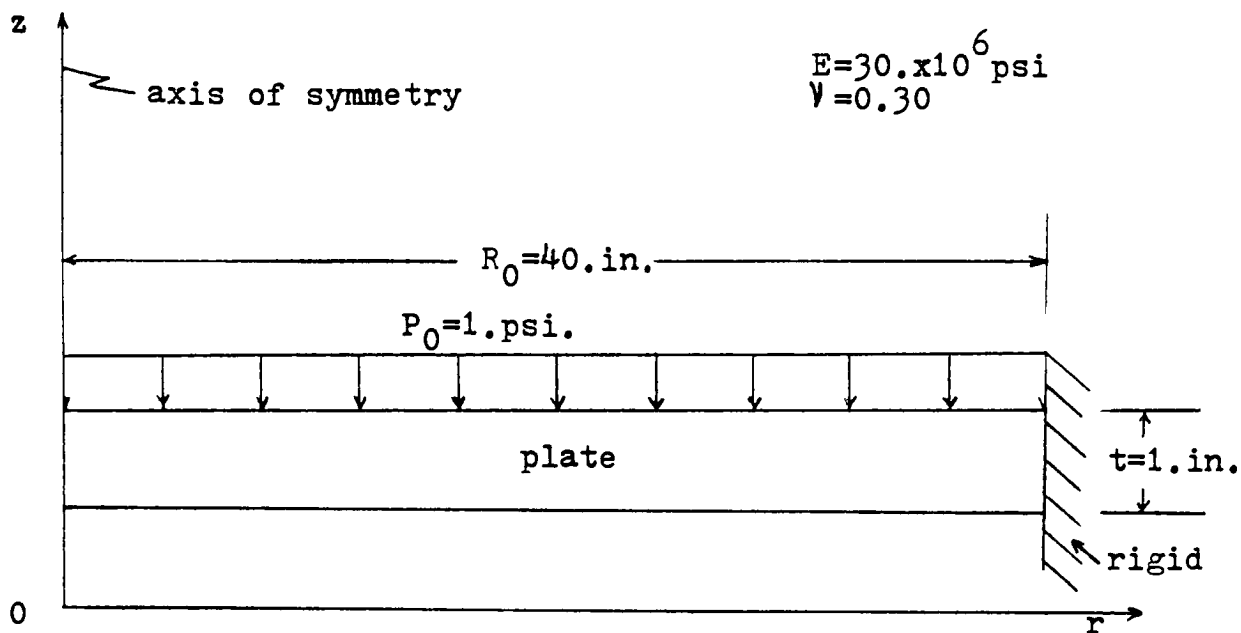
learned that this leads to retention of 5 - 6 significant figures on the Sigma 6 as opposed to 14 - 15 on the CDC 7600. The reason that this lack of significant figures should have such a pronounced effect on a plate or shell type problem as opposed to the other problems presented is suggested by Zienkiewicz [10]. Zienkiewicz states that if a plate or shell's thickness becomes small, strains normal to its middle surface are associated with very large stiffness coefficients and roundoff problems will be encountered. In the previous example problems, structure geometry did not lead to this fact.

Based on these facts it was decided that the thesis program should be run using double precision calculations which would provide 13 - 14 significant figures. However, limitations of computer core available to the author did not make this possible. Arrangements were made to make 1 computer run of the 40 element model on a Univac 1108 computer using double precision (72 bit word). Maximum displacement results for this model agreed with those predicted by the KAPL program and varied .25% from theory. Predicted displacements for this run are presented in Fig. 21. Comparisons of radial and hoop stresses on the plate surface with theory are shown in Figs.

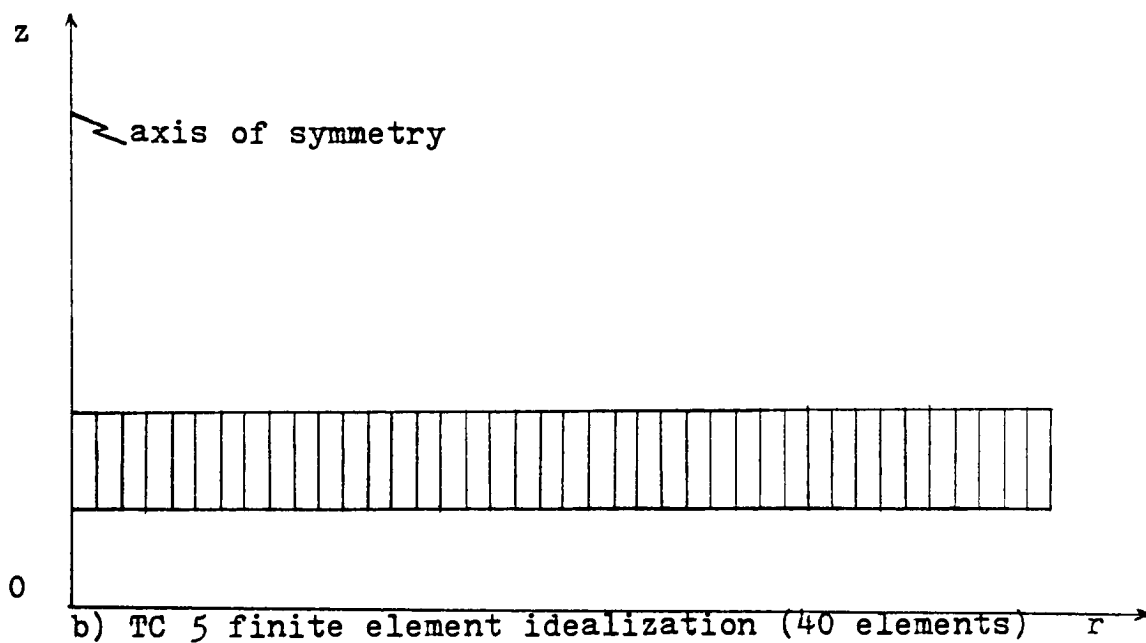
22 and 23 respectively and are within 4%.

The ability of this quadratic element to analyse flexural problems has been demonstrated.

Furthermore, the necessity of using double precision numerical calculations and obeying all assumptions of plate theory has been identified.



a) circular plate subjected to a uniform pressure load (TC 5)



b) TC 5 finite element idealization (40 elements)

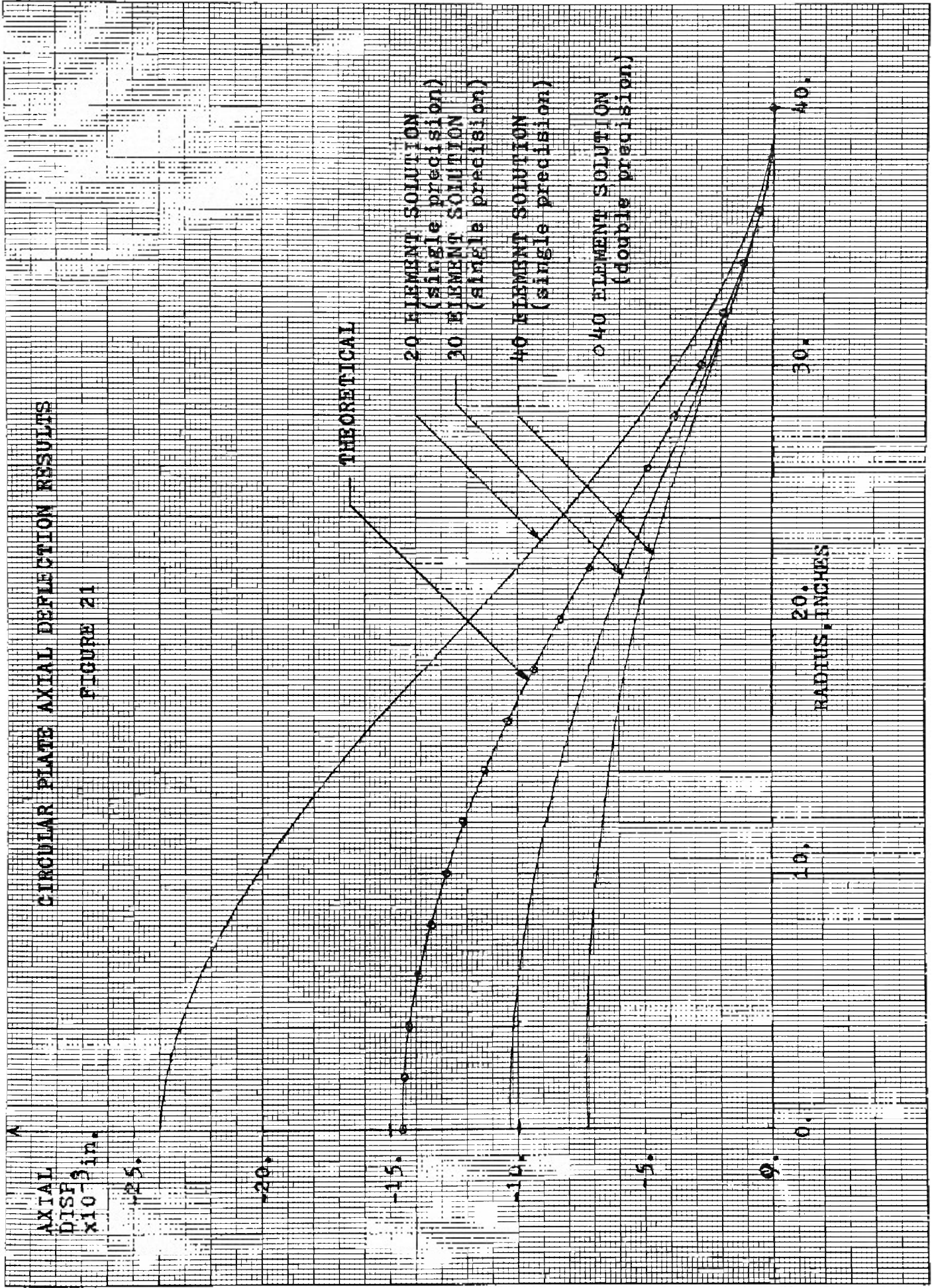
Circular Plate Subjected to Uniform Pressure

Problem and Idealization

FIGURE 20

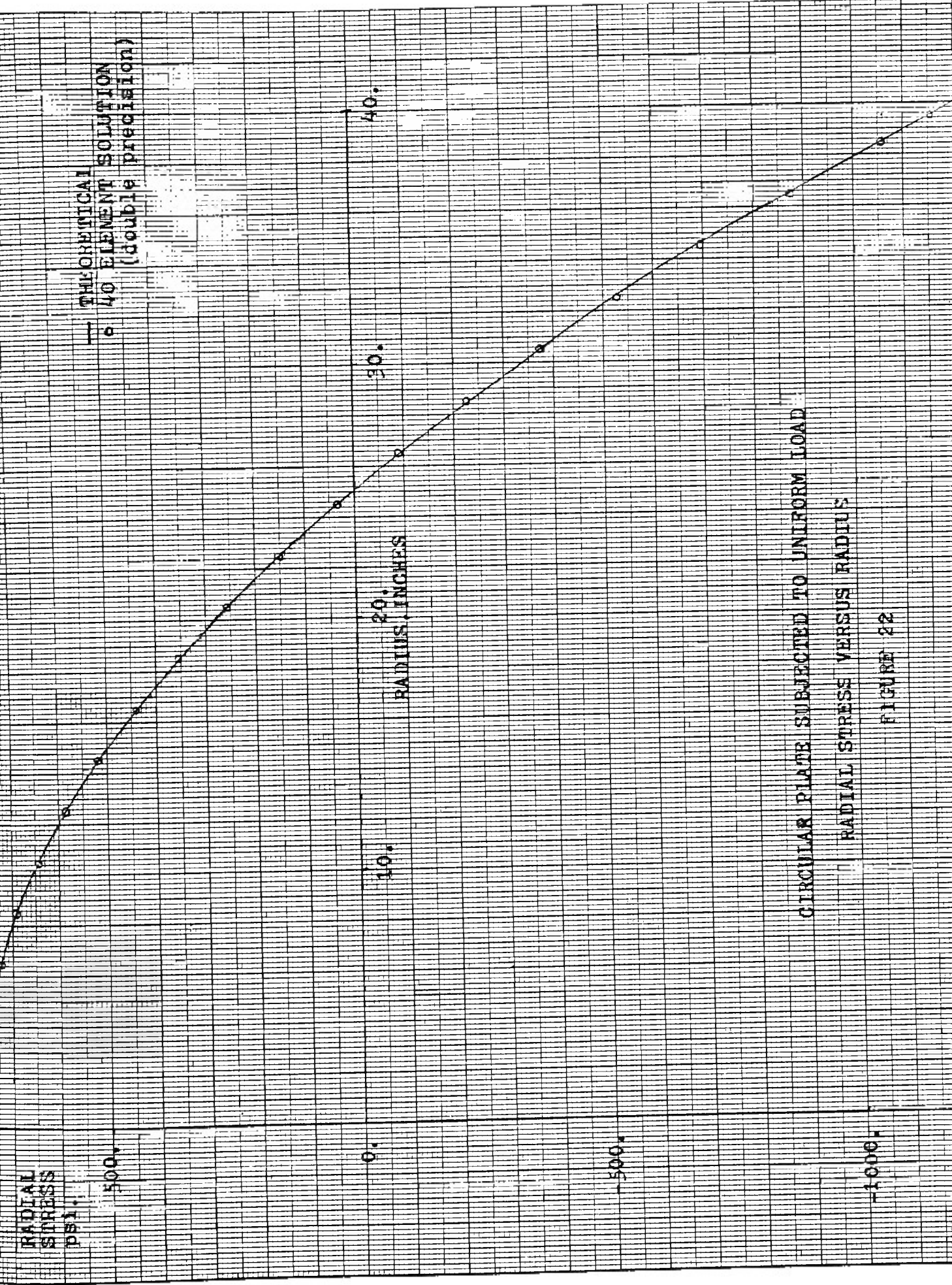
CIRCULAR PLATE AXIAL DEFLECTION RESULTS

FIGURE 21



AXIAL DISPL  $\times 10^3$  in.

RADIUS, INCHES



— THEORETICAL SOLUTION  
○ 40 ELEMENT SOLUTION  
(double precision)

CIRCULAR PLATE SUBJECTED TO UNIFORM LOAD  
RADIAL STRESS VERSUS RADIUS

FIGURE 22

HOOPE  
STRESS  
psi.

500.

0.

-500.

-1000.

THEORETICAL  
o 40 ELEMENT SOLUTION  
(double precision)

10.

20.

30.

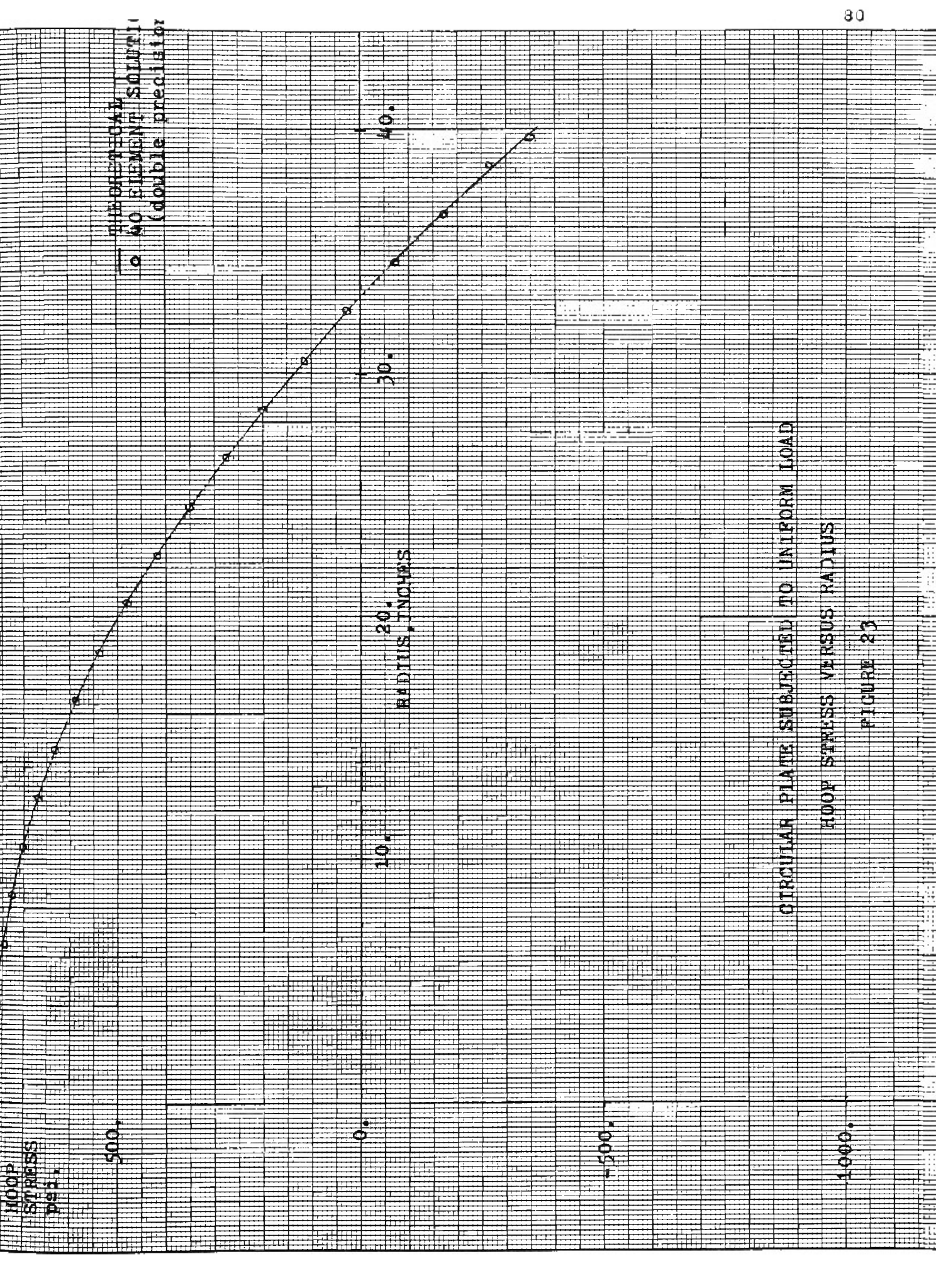
40.

RADIUS, INCHES

CIRCULAR PLATE SUBJECTED TO UNIFORM LOAD

HOOPE STRESS VERSUS RADIUS

FIGURE 23



## 9.0 DISCUSSION OF RESULTS

The theory for an axisymmetric finite element, using the isoparametric concept has been presented.

The isoparametric element requires the introduction of more sophisticated mathematical techniques than conventional straight sided elements. These mathematical sophistications lead to additional steps in element development, and to an increase in program computational time. However, it has been recognized that the curved isoparametric element will generally require fewer total elements to attain a specific degree of accuracy than will models using straight sided elements. Thus, superiority of either element type over the other is dependent on the particular area of concern. (e.g. development time, accuracy, computer time). The author believes that the isoparametric quadratic quadrilateral is an efficient element for axisymmetric analysis. Further tests of element convergence characteristics and comparisons with other elements is recommended for formal verification.

The necessity of numerical quadrature for evaluation of element stiffness matrices based on the isoparametric concept has been identified. Also, it was noted that the use of Gauss quadrature techniques as opposed to Newton-Cotes methods results in approximately a halving of the

number of sampling points required for integral evaluations, and is therefore more efficient.

The tridiagonal method developed by Levy [20] for solution of structural nodal point displacements has been found to be an efficient technique when the amount of computer core required by the program is important. By restricting the maximum allowable difference in nodal point numbers defining an element, a banded structural stiffness matrix is obtained. Considering only the stiffness coefficients within the band, the total computer core required is greatly reduced. For the program developed, utilization of its full capabilities would require computer core of  $1.44 \times 10^6$  words for a sparse stiffness matrix. Using the tridiagonal method, this problem is capable of being solved using  $10.1 \times 10^3$  words of computer core. Although this saving is impressive, several limitations of the technique have been identified which must be considered. Numerous accesses to peripheral storage devices tend to increase total computation time. Restriction of the maximum difference between element nodal points limits the number sequencing of structure nodes. This reduces flexibility in structural idealizations when large numbers of elements are necessary. When single precision computation is used (32 bit word), the round-off error or accuracy of this technique is sensitive to the form of the structural stiffness matrix.

However, no checks are provided for assessment of the error introduced.

The method presented for calculating structural element stress components by extrapolating stress matrices to element boundaries has in certain instances been found to result in stress components exhibiting finite discontinuities between adjacent elements. These discontinuities are inherent to the finite element displacement method, and are a result of interelement force equilibrium not having been satisfied. Although these discontinuities are frequently subjected to some sort of averaging, the author has chosen to identify them for use in the evaluation of the relative merit between different finite element idealizations.

The quadratic element has been found to be quite suitable for the analysis of thick pressure vessels. Both cylindrical and spherical pressure vessels have been analysed. By increasing the number of elements in the idealization, the cylindrical pressure vessel model was able to predict displacement and stress components which were within .7% of theoretical values. The spherical pressure vessel analysis resulted in a predicted maximum displacement value within 3.87% of theory but discontinuities in predicted stress values resulted in 60.% errors in stress values at boundary surfaces. This indicated that a more refined idealization was necessary using the

technique of extrapolating stress matrices to element boundaries. It is suggested that alternate methods of determining element stresses may prove more efficient. The analysis of stresses in a circular disk due to a centrifugal force loading condition has served to demonstrate both the quadratic element's ability to represent body force loading and the need for computer program capabilities to internally generate nodal point loads due to distributed surface and body forces. Predicted stress values obtained were within .1% of theoretical values. User's specification of nodal point loads was found to be possible only for regular shaped elements (defeating the purpose of elements having curved boundaries), time consuming, and susceptible to input errors.

Determination of axial stress concentrations in a cylindrical rod in tension due to a spherical inclusion resulted in accurate results being obtained with a minimum number of elements. Initial idealization resulted in predicted axial stress values in agreement with theoretical values to within 1.06%. Also demonstrated was an inability to match boundary conditions in substructure analysis of local patches of elements from the idealization. In this substructure analysis it was found that original boundary stresses were not reproduced on the boundaries of refined models. It is felt that this

discrepancy is due to violation of displacement compatibility between original and substructure models. Resolution of this problem is suggested for future study.

Investigation of the quadratic element's ability to analyse flexural problems has shown that finite element idealizations for plate bending must comply with all restrictions imposed by plate theory if reasonable results are to be expected. Also, the inadequacy of single precision calculation using Levy's tridiagonal solution technique for this type of problem has been identified. When double precision calculations were used, deflection and stress results were obtained within .25% and 4% respectively of theory.

## 10.0 CONCLUSIONS

1. A finite element for axisymmetric problems having quadratically varying boundaries has been successfully developed based on the isoparametric concept.
2. The most efficient numerical integration technique to employ for element stiffness matrix evaluation is Gauss quadrature.
3. The tridiagonal method of solving structure force displacement equations is an efficient technique to employ when computer core must be minimized and computer time is secondary. However, this technique will provide erroneous results due to round off error for plate flexural problems unless double precision calculations are used.
4. The stress discontinuities which arise at adjacent elements boundaries may be used to assess the merit of finite element idealizations.
5. The quadratic element is an efficient tool for the analysis of thick pressure vessels.
6. Axisymmetric problems involving distributed surface and body forces may be successfully analysed with the quadratic element. Computer program calculation of their equivalent nodal point forces is recommended.
7. Substructure analysis may predict erroneous boundary stress and displacement results.

8. The quadratic element will predict reliable stress and displacement results where bending deformation predominates (e.g. thin plates) providing finite element idealizations meet the assumptions of plate theory and double precision calculations are used.

## 11.0 RECOMMENDATIONS

1. Development of a routine within the program presented to calculate nodal point loads due to distributed surface and body forces.
2. Investigation of necessary conditions in sub-structure analysis to insure reproduction of original boundary stresses.
3. Investigation of alternate methods for predicting element stress components.
4. Investigation of alternate techniques for the solution of the structural equilibrium equations for one which is less sensitive to round off error or modification of the existing program to a double precision version for the Sigma 6 computer.
5. Extension of the program's options by including thermal stress calculation and two dimensional plane stress/strain analysis capabilities.
6. Provide in depth comparisons with other computer programs and convergence studies to verify program efficiency.

## 12.0 REFERENCES

1. Timoshenko, S. and Goodier, J., Theory of Elasticity (McGraw Hill Book Company, Inc., New York, 1970)
2. Timoshenko, S., Strength of Materials, Part II (Van Nostrand Reinhold Company, New York, 1958), third edition.
3. Clough, R. and Rashid, Y., "Finite Element Analysis of Axisymmetric Solids", *Journal of Engineering Mechanics*, Amer. Soc. Civil Engrs., 71-85, (Feb. 1965).
4. Wilson, E., "Structural Analysis of Axisymmetric Solids", *AIAA Journal*, Vol. 3, No. 12, 2269-2274, (Dec. 1965)
5. Crose, J., "Stress Analysis of Axisymmetric Solids with Asymmetric Properties", *AIAA Journal*, Vol. 10, No. 7, 866-871, (July 1972).
6. Ergatoudis, J., Irons, B., Zienkiewicz, O., "Curved Isoparametric 'Quadrilateral' Elements for Finite Element Analysis", *Int. Journal Solids Structures*, Vol. 4, 31-42, (1968).
7. Irons, B., "Numerical Integration Applied to Finite Element Methods", *Conference on the Use of Digital Computers in Structural Engineering*, University of Newcastle, England, July 1966, (revision from author Nov. 1973).
8. Ergatoudis, J., "Isoparametric Finite Elements in Two and Three Dimensional Stress Analysis", *PhD. Thesis*, University College of Swansea, Wales, (Oct. 1968).
9. Zienkiewicz, O., Irons, B., "The Isoparametric Finite Element System-A New Concept in Finite Element Analysis", *Conference on Recent Advances in Stress Analysis: New Concepts and Techniques and Their Practical Application*, Royal Aeronautical Society, 35-40, (March 26-29, 1968).
10. Zienkiewicz, O., Irons, B., Ergatoudis, J., Ahmad, S., Scott, F., "Isoparametric and Associated Element Families for Two and Three Dimensional Analysis", Finite Element Methods in Stress Analysis, Ivar Holand and Kolbein Bell, eds., Trondheim, Norway: Tapir Publishing, The Technical University of Norway, 383-432, (1972).

11. Zienkiewicz, O., Irons, B., "Isoparametric Elements", Finite Element Techniques in Structural Mechanics, H. Tottenham and C. Brebbia, eds., Southhampton England Stress Analysis Publishers, Southhampton University, 283-301, (1970).
12. Zienkiewicz, O., The Finite Element Method in Engineering Science, (Mc Graw Hill Book Company, Inc., London, 1971), second edition.
13. Irons, B., "Engineering Applications of Numerical Integration in Stiffness Methods, AIAA Journal Vol. 4 No. 11, 2035-2037, (Nov. 1966).
14. Irons, B., "Economical Computer Techniques for Numerically Integrated Finite Elements" Inter. Journal for Num. Meth. in Eng., Vol. 1, 201-203, (1969).
15. Irons, B., "Quadrature Rules for Brick Based Finite Elements", Inter. Journal for Num. Meth. in Eng., 293-294, (1971).
16. Gupta, A., Mohraz, B., "A Method of Computing Numerically Integrated Stiffness Matrices", Inter. Journal for Num. Meth. in Eng., Vol. 5, 83-89, (1972).
17. Desai, C., Abel, J., Introduction to the Finite Element Method, (Van Nostrand Reinhold Company, New York, 1972), first edition.
18. Archer, J., "Consistent Matrix Formulations for Structural Analysis Using Finite Element Techniques", AIAA Journal, Vol. 3, No. 10, 1911-1918, (Oct. 1965)
19. Tottenham, H., "Basic Principles", Finite Element Techniques in Structural Mechanics, H. Tottenham and C. Brebbia, eds., Southhampton England: Stress Analysis Publishers, Southhampton Univeristy, 1-30, (1970).
20. Levy, S., "ISO2D", Computer Workshop in Finite Element Methods for Stress and Other Field Problems, Schenectady, New York: Union College Graduate and Special Programs, Union College, (Aug. 1973).
21. Dario, N., Bradley, W., "A Comparison of First and Second Order Axially Symmetric Finite Elements", Inter. Journal for Num. Meth. In Eng., Vol. 5, 573-583, (1973).

22. Hildebrand, F., Introduction to Numerical Analysis, (McGraw Hill Book Company, Inc., New York, 1974), second edition.
23. Spiegel, M., Advanced Calculus, Schaum's Outline Series, (McGraw Hill Book Company, Inc., New York, 1963).
24. Oden, J., Finite Elements of Nonlinear Continua, (McGraw Hill Book Company, Inc., New York, 1972) first edition.
25. Loeber, J., Knolls Atomic Power Laboratory, Schenectady, N. Y., Private Communication.
26. McCalley, R., General Electric Company, Schenectady, N.Y., Private Communication.
27. Glasser, T., Knolls Atomic Power Laboratory, Schenectady, N.Y., Private Communication.
28. Timoshenko, S., Woinowski-Krieger, Theory of Plates and Shells (McGraw Hill Book Company, Inc., New York, 1959), second edition.
29. Cook, R., "A Note on Certain Incompatible Elements", Inter. Journal for Num. Meth. in Eng., 146-147, (1973)
30. Griffin, D., "Use of the Computer for the Elastic Analysis of Pressure Vessels", The Computer in Pressure Vessel Analysis, Papers and Discussions from ASME Computer Seminar, Dallas, Texas, September 26, 1968.
31. Ergatoudis, J., "Quadrilateral Elements in Plane Analysis and Introduction to Solid Analysis", MS Thesis, University College of Swansea, Wales, (June, 1966).
32. Wilson, E., Parsons, B., "Trapezoidal Finite Elements - Their Derivation and Use for Axisymmetric Rotating Bodies", ASME Presentation at the Design Engineering Technical Conference, Cincinnati, Ohio, September 9-12, 1973. Paper 73 - DET - 47.
33. Rieger, N., Rochester Institute of Technology, Rochester, N.Y. Private Communication.
34. Martin, H., Carey, G., Introduction to Finite Element Analysis, (McGraw Hill Book Company, Inc., New York, 1973), first edition.
35. Halbleib, W., Rochester Institute of Technology, Rochester, N.Y. Private communication.

### 13.0 APPENDIX A

It is noted that the function to be integrated in Eq. 13 was of a sufficiently complex form to necessitate the use of numerical quadrature.

Numerical quadrature is a numerical procedure for the evaluation of definite integrals. Geometrically it requires the numerical determination of the area or volume under the integrand's curve[23]. To use this procedure, sampling points are chosen within the region of interest and the integrand is evaluated at them. Based on these integrand values and the number of sampling points chosen, an approximate value of the integral may then be obtained.

Numerical quadrature techniques may be divided into two basic categories [22], those whose sampling points are equally spaced over the region of interest (Newton-Cotes), and those whose sampling point are chosen at optimal locations and have weighting functions associated with them (Gauss).

Using the Newton-Cotes formulae requires  $n$  sampling points for the exact integration of a function of order  $n-1$  whereas the Gauss technique requires  $n/2$  sampling points.

Using the finite element method, structural idealization usually involves introduction of large numbers

of elements for which stiffness matrices must be found. Efficient computing techniques rely on a minimizing of the number of mathematical operations necessary. For this reason Gaussian quadrature, which requires the fewest sampling points to integrate a function of specific order, is most frequently employed [7]. In Gaussian quadrature, the integral of a function  $f(x)$  is replaced by the summation:

$$\int_{-1}^1 f(x) dx = \sum_{i=1}^n H_i f(a_i) \quad (14)$$

$n$  is the number of sampling points

$H_i$  is the weight coefficient associated with sampling point  $i$

$a_i$  is the abscissa of sampling point  $i$

The theory for determination of optimal sampling points and weight coefficients may be found in Hildebrand [22]. Specific values for  $n = 2$  through 24 are presented in Table V.

The procedure for evaluating the element stiffness matrix,  $[K]$  is as follows:

Eq. 13 may be rewritten as:

$$[K] = \int_{-1}^1 \int_{-1}^1 f(P,Q) dP dQ \quad (15)$$

where  $f(P,Q)$  is a matrix in  $P$  and  $Q$  equal to

$$2\pi [B]^T [D] [B] [N] \{r_0\} \det [J]$$

Integration may be performed in a manner similar to the standard technique of evaluating double integrals. Substituting Eq. 14 into Eq. 15 while holding  $Q$  constant, one obtains:

$$[K] = \int_{-1}^1 \sum_{i=1}^n H_i f(a_i, Q) dQ$$

Applying Eq. 14 again but with respect to  $Q$ , the expression for  $[K]$  becomes:

$$[K] = \sum_{j=1}^n \sum_{i=1}^n H_j H_i f(a_i, a_j) \quad (16)$$

The number of sampling points in each direction used in Eq. 16 should be such that the volume of each element is exactly determined [12]. The minimum number of sampling points which are required is determined by the order of the determinant of the Jacobian matrix  $[J]$ .

For the quadratic element developed, the minimum value of  $n$  is 2. However the element developed is for  $n = 3$  for convenience in element stress calculations (Section 4.8).

Considering the case of  $n = 3$ , the element stiffness matrix is determined by the summation of the function  $f(P, Q)$  multiplied by its weight function at the nine sampling points shown in Figure 20.

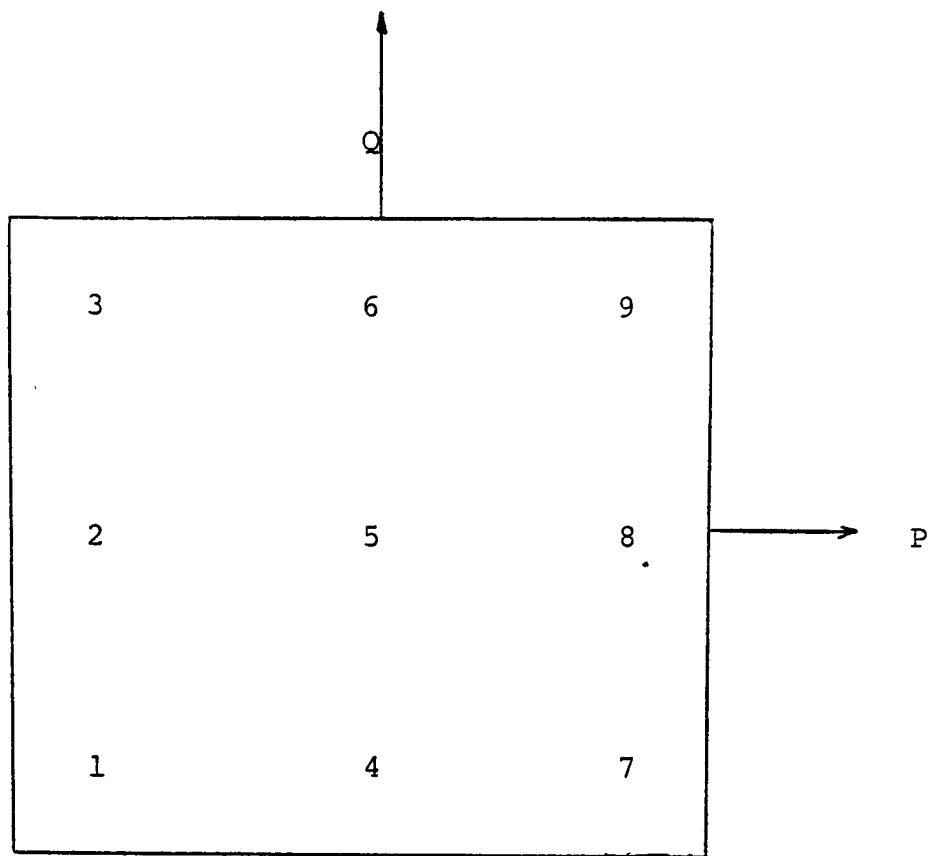


Figure 20

Sampling Point Locations  
for Gaussian Quadrature

TABLE V

ABSCISSAS AND WEIGHT FACTORS FOR GAUSSIAN INTEGRATION

$$\int_{-1}^{+1} f(x) dx = \sum_{i=1}^n w_i f(x_i)$$

Abscissas - $\pm x_i$ ; (Zeros of Legendre Polynomials)			Weight Factors - $w_i$		
$\pm x_i$		$w_i$	$\pm x_i$		$w_i$
<b>n = 2</b>			<b>n = 8</b>		
0.57735	0.2691	0.86626	0.18343	0.46424	0.95650
		1.00000	0.52553	0.24099	0.16329
		0.00000	0.77666	0.64774	0.13627
		0.00000	0.96028	0.98564	0.97536
		0.00000			
<b>n = 3</b>			<b>n = 9</b>		
0.00000	0.0000	0.30000	0.00000	0.00000	0.00000
0.77459	0.6662	0.41483	0.32425	0.34234	0.03809
		0.88888	0.61337	0.14327	0.00590
		0.55555	0.83603	0.11073	0.26636
			0.96816	0.02395	0.07626
<b>n = 4</b>			<b>n = 10</b>		
0.33998	0.10435	0.94856	0.14887	0.43389	0.81631
0.86113	0.63115	0.94053	0.43339	0.53741	0.29247
		0.65214	0.67940	0.95682	0.99024
		0.34785	0.86506	0.33666	0.88985
			0.97390	0.65285	0.17172
<b>n = 5</b>			<b>n = 12</b>		
0.00000	0.0000	0.00000	0.12523	0.34085	0.11469
0.53846	0.93101	0.05683	0.36783	0.14789	0.98180
0.90617	0.98459	0.38664	0.58731	0.79542	0.86617
		0.56888	0.76990	0.26741	0.94305
		0.47862	0.90411	0.72563	0.70475
		0.23692	0.98156	0.06342	0.46719
<b>n = 6</b>			<b>n = 16</b>		
0.23861	0.91860	0.83197	0.09501	0.25098	0.37637
0.66120	0.93864	0.66265	0.28160	0.35507	0.79258
0.93246	0.95142	0.03152	0.45801	0.67776	0.57227
			0.61787	0.62444	0.02643
			0.75540	0.44083	0.55003
			0.86563	0.12023	0.87831
			0.94457	0.50230	0.73232
			0.98940	0.09349	0.91649
					0.932596
<b>n = 7</b>			<b>n = 20</b>		
0.00000	0.00000	0.00000	0.07652	0.65211	0.33497
0.40584	0.51513	0.77397	0.22778	0.58511	0.41645
0.74153	0.11855	0.99394	0.37370	0.60887	0.15419
0.94910	0.79123	0.42759	0.51086	0.70019	0.50827
			0.63605	0.36807	0.26515
			0.74633	0.19064	0.60150
			0.83911	0.69718	0.22218
			0.91223	0.44282	0.51325
			0.96397	0.19272	0.77913
			0.99312	0.85991	0.85094
					0.924786
<b>n = 24</b>			<b>n = 24</b>		
0.06405	0.68928	0.62605	0.12793	0.81953	0.46752
0.19111	0.88674	0.73616	0.12583	0.74563	0.46828
0.31504	0.26796	0.96163	0.12167	0.04729	0.27803
0.43379	0.35076	0.26045	0.11550	0.56680	0.53725
0.54542	0.14713	0.88839	0.10744	0.42701	0.15965
0.64809	0.36519	0.36975	0.09761	0.86521	0.04113
0.74012	0.41915	0.78554	0.08619	0.01615	0.31953
0.82000	0.19859	0.73902	0.07334	0.64814	0.11080
0.88641	0.55270	0.04401	0.05929	0.85849	0.15436
0.93827	0.45520	0.2732	0.04427	0.74388	0.17419
0.97472	0.85559	0.71309	0.02853	0.13886	0.28933
0.99518	0.72199	0.97021	0.01234	0.12297	0.99987
		0.360180			0.199547

Compiled from P. Davis and P. Rabinowitz, Abscissas and weights for Gaussian quadratures of high order, J. Research NBS 56, 35-37, 1956, RP2645; P. Davis and P. Rabinowitz, Additional abscissas and weights for Gaussian quadratures of high order. Values for  $n=64, 80,$  and  $96,$  J. Research NBS 60, 613-614, 1958, RP2875; and A. N. Lowan, N. Davids, and A. Levenson, Table of the zeros of the Legendre polynomials of order 1-16 and the weight coefficients for Gauss' mechanical quadrature formula, Bull. Amer. Math. Soc. 48, 739-743, 1942 (with permission).

## 14.0 APPENDIX B COMPUTER PROGRAM ISOAXI

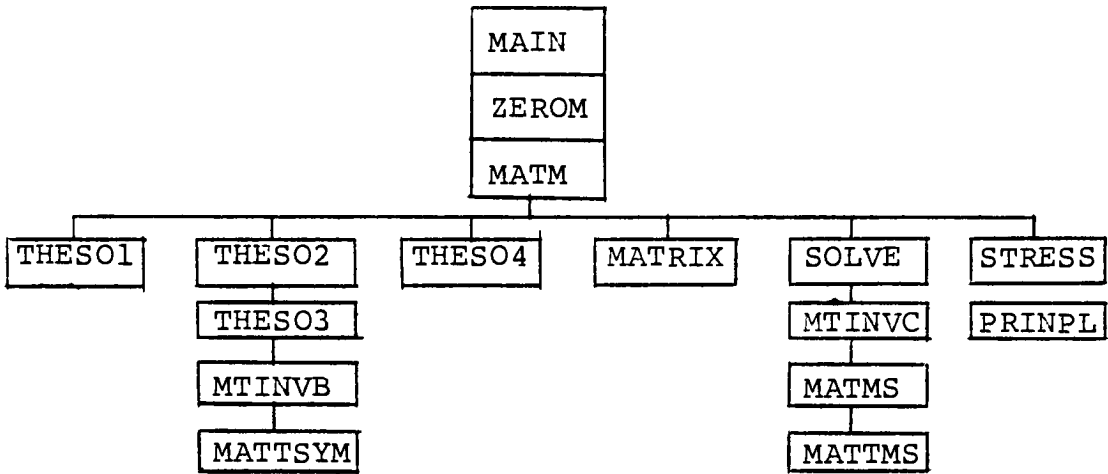
### B1. General Analyst's Information

ISOAXI is a finite element computer program for the static stress analysis of axisymmetric structures having axisymmetric boundary conditions. The element used is a quadratic axisymmetric quadrilateral capable of representing geometric boundaries of quadratic variation. The assumed element displacement function is also quadratic. Element stress-strain relations are for a homogeneous isotropic material. Up to ten different materials may be specified per problem. Options not included at present are internal calculations of body forces and surface forces, thermal stress capabilities, and pre and post processors for mesh generation and computer plotting.

### B2. Programmer's Information

Program development was accomplished using a Xerox Sigma 6 computer. ISOAXI is written in Fortran IV and makes use of three temporary files (2,3,4) for data storage and retrieval during execution. Data input is from a card reader (F:105) and output is to a line printer

(F:108). The program is overlaid as shown in B3. and required 10.1K words of main computer core for execution.

B3. COMPUTER PROGRAM STRUCTURE

#### B4. SUBROUTINE DESCRIPTIONS

The functions of the subroutines shown in B3. are as follows:

1. MAIN executive routine for calling subroutines
2. ZEROM\* initializes a matrix to zero
3. MATM\* multiplies two matrices
4. THES01 calculates the shape functions and their partial derivatives at the nine sampling points.
5. THES02 reads the majority of input data and writes it out for checking.
6. THES03 calculates the element stiffness matrices and stress matrices at the sampling points of each element
7. MTINVB\* finds the inverse of a matrix and also the value of its determinant
8. MTTSYM\* multiplies two matrices, first transposed times the other and insures resulting matrix is symmetric
9. THES04 extrapolates the stress matrices at the sampling points of each element to its midside nodes.
10. MATRIX\* reads nodal point prescribed displacements and external forces, assembles the structural stiffness matrix and modifies it to accomodate prescribed displacements.

11. SOLVE\* solves the structural equilibrium relations for displacement using a modified Gauss elimination technique
12. MTINVC\* inverts a matrix using the Gauss technique with pivoting
13. MATMS\* multiplies two matrices
14. MATTMS\* multiplies the transpose of a matrix with a second matrix
15. STRESS writes nodal point displacements, calculates and writes element stresses.
16. PRINPL\* calculates principal stresses and direction cosines

\*Subroutines obtained from Levy [20].

B5 INPUT DATA FORMAT

Data input to ISOAXI is in the form of punched cards. Data required may be generalized as consisting of seven sets, (A-G) with the number of cards required in each set depending on the particular problem being solved. The order in which input data should appear, its format, and definition is presented below.

DATA SET A PROBLEM PARAMETERS (FORMAT 7I4)

KPNT - number of nodal points in problem (max. 600)

KELM - number of elements in problem

NGEO - number of nodes having geometric constraints

NMAT - number of different materials in problem  
(max. 10)

NFREE- degrees of freedom per node (always 2)

NFOR - number of nodes subjected to external force

NPART - number of partitions in problem (max. 45)

DATA SET B NODAL POINT LOCATIONS (FORMAT 2F16.8)

X(1,J) - radial distance from origin of nodal  
point J

X(2,J) - axial distance from origin of nodal  
point J

(This set contains KPNT cards in sequential order from 1 through KPNT.)

DATA SET C MATERIAL PROPERTIES (FORMAT 2F16.4)

E(I) - Young's modulus of material I

P(I) - Poisson's ratio of material I

(This set contains NMAT cards in sequential order from 1 through NMAT)

DATA SET D ELEMENT DEFINITION (FORMAT 9I4)

N1,N2,...N8 the eight nodal points defining an element specified counter-clockwise with respect to coordinate axes and started at a corner node.

NM - the number I in data set C which corresponds to the material properties of the element

(This set contains KELM cards in sequential order from 1 through KELM)

DATA SET E PARTITION INFORMATION (FORMAT 4I4)

NSTART(I) - first element in partition I

NEND(I) - last element in partition I

NFIRST(I) - first node in partition I

NLAST(I) - last node in partition I

(This set contains NPART cards in sequential order from 1 through NPART)

DATA SET F PRESCRIBED NODAL DISPLACEMENTS (FORMAT 3I4, 2F16.8)

NO - the node having prescribed displacements

NA - 0 if radial displacement is specified, 1  
if not

NB - 0 if axial displacement is specified, 1,  
if not

U - magnitude of specified radial displacement

V - magnitude of specified axial displacement

(This set contains NCEO cards)

DATA SET G EXTERNAL NODAL POINT FORCES (FORMAT  
I4,2F16.4)

NODE - the node at which external force acts

FORR - the radial component of force acting at  
the node\*

FORZ - the axial component of force acting at  
the node\*

\* the total force through  $2\pi$  radians

(This set contains NFOR cards)

## B6 EXAMPLE OF COMPUTER INPUT-OUTPUT DATA

An example of computer program output is presented in Fig.24 and corresponds to the cylindrical pressure vessel problem (1 element solution) presented in section 8.1, Fig. 7. A sample listing of input data is not presented since computer output includes this information.

First output by the program is all input data information. This is done to facilitate data checking and also provide model documentation. Printout of this information is in the same order as presented in section B5 and is noted in Fig. 24. Following this information, displacement components of all structural nodal points are output. Displacement output in Fig.24 for nodal point 1 indicates that radial and axial displacement components are:

$$u = -.43032356 \times 10^{-2} \text{in.}$$

$$v = .37970068 \times 10^{-3} \text{in.}$$

Following displacement output, element stress information is printed. Four sets of stress information are provided for each element's midside nodes. Each set contains the following information:

EL           - Element number

NODES       - The 8 nodes defining element EL

STRPT - Midside node to which stress components correspond.

SIGR - Normal component of stress in the radial direction

SIGTHETA - Normal component of stress in the theta direction

SIGZ - Normal stress component in the axial direction .

TAURZ - Shear stress in the rz plane

PS - Principal stress value

L - Direction cosine between PS and r axis

M - Direction cosine between PS and z axis

N - Direction cosine between Ps and the  $\theta$  axis

An example of interpretation of this information for element 1, defined by nodes 1 2 3 5 8 7 6 4, the stress components acting at node 4 (STRP 4) are:

$$\sigma_r = -12188.5 \text{ psi}$$

$$\sigma_\theta = -21995.3 \text{ psi}$$

$$\sigma_z = -15.5 \text{ psi}$$

$$\tau_{rz} = -3.2 \text{ psi}$$

These stress components correspond to principal stresses of:

15.5 psi in the  $-z$  direction (L=0.,M=-1.,N=0.)

-12188.4 psi in the  $\underline{r}$ direction (L=-1.,M=0.,N=0.)

-21995.3 psi in the  $+\underline{\theta}$  direction (L=0.,M=0.,N=1)

FIGURE 24  
COMPUTER OUTPUT - ISOAXI

RUN (LUN, THERIC)  
 TOTAL NUMBER OF NODAL POINTS..... 8  
 TOTAL NUMBER OF ELEMENTS..... 1  
 NUMBER OF GEOMETRIC CONSTRAINTS..... 0  
 NUMBER OF DIFFERENT MATERIALS..... 1  
 DEGREES OF FREEDOM PER NODE..... 2  
 NUMBER OF NODES SUBJECTED TO FORCE..... 6  
 NUMBER OF PARTITIONS..... 1

NODE	R CO-ORDINATE	Z CO-ORDINATE
1	5.0000	1.0000
2	5.0000	.5000
3	5.0000	.0000
4	7.5000	1.0000
5	7.5000	.5000
6	10.0000	1.0000
7	10.0000	.5000
8	10.0000	.0000

MATERIAL MODULUS OF ELASTICITY POISSONS RATIO

1 30000000.0000 .3000  
 ELEMENT ELEMENT NODES MATERIAL

	1	2	3	5	8	7	6	4	1
3	1	1	.00000000				.00000000		1
7	1	0	.00000000				.00000000		
1		37123.8906				.0000			
2		148495.5625				.0000			
3		37123.8906				.0000			
6		-157079.6250				.0000			
7		-628319.5000				.0000			
8		-157079.6250				.0000			

\* \* \* \*DISPLACEMENTS\* \* \* \* \* \*

NO DE RADIAL (R) AXIAL (Z)

1	-.43032356E-02	.37970068E-03
2	-.43273158E-02	.19016737E-03
3	-.43445453E-02	.00000000E-00
4	-.45335413E-02	.26179291E-03
5	-.46213232E-02	-.80375456E-04
6	-.52341036E-02	.19534706E-03
7	-.52484572E-02	.00000000E-00
8	-.52689308E-02	-.18555872E-03

EL 1 NODES 1 2 3 5 8 7 6 4 STPRT 0

STGR -9594.0SIGTHETA -28376.7SIGZ -. STAUP7 -. .E

PC -.2L -.0000644-1.000000N .000000

Figure 24 (Continued)

```

PC      -9594.5L  -.9999928M  -.112642M  .0000000
PC      -22376.7L  .0000000M  .1000000N  1.0000000
EL      1  NODES   1    2    3    5    8    7    6    4 STOPT   7
SIGD    -12193.2SIGTHETA  -22146.7SIGZ      -11.5 STAUPT   4.0
PC      -1145L  -.0001324M -1.000000N  .0000000
PC      -12193.2L  -.999997M  -.102433M  .0000000
PC      -22146.7L  .0000000M  .0000000N  1.0000000
EL      1  NODES   1    2    3    5    8    7    6    4 STOPT   7
SIGD    -16223.5SIGTHETA  -20843.0SIGZ      7. STAUPT   1.0
PC      7.3L  .0000018M -1.000000N  .0000000
PC      -16223.5L  .999998M  -.113614M  .0000000
PC      -20843.0L  .0000000M  .0000000N  1.0000000
EL      1  NODES   1    2    3    5    8    7    6    4 STOPT   4
SIGD    -12188.5SIGTHETA  -21995.3SIGZ      -15. STAUPT   1.0
PC      -15.5L  -.0002654M -1.000000N  .0000000
PC      -12188.4L  -.999999M  -.101209M  .0000000
PC      -21995.3L  .0000000M  .0000000N  1.0000000
** TO P* 0

```



10  
 20  
 30  
 40  
 50  
 60  
 70  
 80  
 90  
 100  
 110  
 120  
 130  
 140  
 150  
 160  
 170  
 180  
 190  
 200  
 210  
 220  
 230  
 240  
 250  
 260  
 270  
 280  
 290  
 300  
 310  
 320  
 330  
 340  
 350  
 360  
 370  
 380  
 390  
 400  
 410  
 420  
 430  
 440  
 450  
 460  
 470  
 480  
 490  
 500  
 510  
 520  
 530  
 540  
 550  
 560  
 570  
 580  
 590  
 600  
 610  
 620  
 630  
 640  
 650  
 660  
 670  
 680  
 690  
 700  
 710  
 720  
 730  
 740  
 750  
 760  
 770  
 780  
 790  
 800  
 810  
 820  
 830  
 840  
 850  
 860  
 870  
 880  
 890  
 900  
 910  
 920  
 930  
 940  
 950  
 960  
 970  
 980  
 990  
 1000

SUBROUTINE MATM(D,B,DB,L,M,N)  
 DIMENSION D(L,M),B(M,N),DB(L,N)  
 DO 110 J=1,N  
 DO 120 I=1,L  
 DB(I,J)=0.  
 DO 130 K=1,M  
 DB(I,J)=DB(I,J)+D(I,K)\*B(K,J)  
 RETURN  
 END

1  
 2  
 3  
 4  
 5  
 6  
 7  
 8  
 9  
 10  
 11  
 12  
 13  
 14  
 15  
 16  
 17  
 18  
 19  
 20  
 21  
 22  
 23  
 24  
 25  
 26  
 27  
 28  
 29  
 30  
 31  
 32  
 33  
 34  
 35  
 36  
 37  
 38  
 39  
 40  
 41  
 42  
 43  
 44  
 45  
 46  
 47  
 48  
 49  
 50  
 51  
 52  
 53  
 54  
 55  
 56  
 57  
 58  
 59  
 60  
 61  
 62  
 63  
 64  
 65  
 66  
 67  
 68  
 69  
 70  
 71  
 72  
 73  
 74  
 75  
 76  
 77  
 78  
 79  
 80  
 81  
 82  
 83  
 84  
 85  
 86  
 87  
 88  
 89  
 90  
 91  
 92  
 93  
 94  
 95  
 96  
 97  
 98  
 99  
 100  
 101  
 102  
 103  
 104  
 105  
 106  
 107  
 108  
 109  
 110  
 111  
 112  
 113  
 114  
 115  
 116  
 117  
 118  
 119  
 120  
 121  
 122  
 123  
 124  
 125  
 126  
 127  
 128  
 129  
 130  
 131  
 132  
 133  
 134  
 135  
 136  
 137  
 138  
 139  
 140  
 141  
 142  
 143  
 144  
 145  
 146  
 147  
 148  
 149  
 150  
 151  
 152  
 153  
 154  
 155  
 156  
 157  
 158  
 159  
 160  
 161  
 162  
 163  
 164  
 165  
 166  
 167  
 168  
 169  
 170  
 171  
 172  
 173  
 174  
 175  
 176  
 177  
 178  
 179  
 180  
 181  
 182  
 183  
 184  
 185  
 186  
 187  
 188  
 189  
 190  
 191  
 192  
 193  
 194  
 195  
 196  
 197  
 198  
 199  
 200  
 201  
 202  
 203  
 204  
 205  
 206  
 207  
 208  
 209  
 210  
 211  
 212  
 213  
 214  
 215  
 216  
 217  
 218  
 219  
 220  
 221  
 222  
 223  
 224  
 225  
 226  
 227  
 228  
 229  
 230  
 231  
 232  
 233  
 234  
 235  
 236  
 237  
 238  
 239  
 240  
 241  
 242  
 243  
 244  
 245  
 246  
 247  
 248  
 249  
 250  
 251  
 252  
 253  
 254  
 255  
 256  
 257  
 258  
 259  
 260  
 261  
 262  
 263  
 264  
 265  
 266  
 267  
 268  
 269  
 270  
 271  
 272  
 273  
 274  
 275  
 276  
 277  
 278  
 279  
 280  
 281  
 282  
 283  
 284  
 285  
 286  
 287  
 288  
 289  
 290  
 291  
 292  
 293  
 294  
 295  
 296  
 297  
 298  
 299  
 300  
 301  
 302  
 303  
 304  
 305  
 306  
 307  
 308  
 309  
 310  
 311  
 312  
 313  
 314  
 315  
 316  
 317  
 318  
 319  
 320  
 321  
 322  
 323  
 324  
 325  
 326  
 327  
 328  
 329  
 330  
 331  
 332  
 333  
 334  
 335  
 336  
 337  
 338  
 339  
 340  
 341  
 342  
 343  
 344  
 345  
 346  
 347  
 348  
 349  
 350  
 351  
 352  
 353  
 354  
 355  
 356  
 357  
 358  
 359  
 360  
 361  
 362  
 363  
 364  
 365  
 366  
 367  
 368  
 369  
 370  
 371  
 372  
 373  
 374  
 375  
 376  
 377  
 378  
 379  
 380  
 381  
 382  
 383  
 384  
 385  
 386  
 387  
 388  
 389  
 390  
 391  
 392  
 393  
 394  
 395  
 396  
 397  
 398  
 399  
 400  
 401  
 402  
 403  
 404  
 405  
 406  
 407  
 408  
 409  
 410  
 411  
 412  
 413  
 414  
 415  
 416  
 417  
 418  
 419  
 420  
 421  
 422  
 423  
 424  
 425  
 426  
 427  
 428  
 429  
 430  
 431  
 432  
 433  
 434  
 435  
 436  
 437  
 438  
 439  
 440  
 441  
 442  
 443  
 444  
 445  
 446  
 447  
 448  
 449  
 450  
 451  
 452  
 453  
 454  
 455  
 456  
 457  
 458  
 459  
 460  
 461  
 462  
 463  
 464  
 465  
 466  
 467  
 468  
 469  
 470  
 471  
 472  
 473  
 474  
 475  
 476  
 477  
 478  
 479  
 480  
 481  
 482  
 483  
 484  
 485  
 486  
 487  
 488  
 489  
 490  
 491  
 492  
 493  
 494  
 495  
 496  
 497  
 498  
 499  
 500  
 501  
 502  
 503  
 504  
 505  
 506  
 507  
 508  
 509  
 510  
 511  
 512  
 513  
 514  
 515  
 516  
 517  
 518  
 519  
 520  
 521  
 522  
 523  
 524  
 525  
 526  
 527  
 528  
 529  
 530  
 531  
 532  
 533  
 534  
 535  
 536  
 537  
 538  
 539  
 540  
 541  
 542  
 543  
 544  
 545  
 546  
 547  
 548  
 549  
 550  
 551  
 552  
 553  
 554  
 555  
 556  
 557  
 558  
 559  
 560  
 561  
 562  
 563  
 564  
 565  
 566  
 567  
 568  
 569  
 570  
 571  
 572  
 573  
 574  
 575  
 576  
 577  
 578  
 579  
 580  
 581  
 582  
 583  
 584  
 585  
 586  
 587  
 588  
 589  
 590  
 591  
 592  
 593  
 594  
 595  
 596  
 597  
 598  
 599  
 600  
 601  
 602  
 603  
 604  
 605  
 606  
 607  
 608  
 609  
 610  
 611  
 612  
 613  
 614  
 615  
 616  
 617  
 618  
 619  
 620  
 621  
 622  
 623  
 624  
 625  
 626  
 627  
 628  
 629  
 630  
 631  
 632  
 633  
 634  
 635  
 636  
 637  
 638  
 639  
 640  
 641  
 642  
 643  
 644  
 645  
 646  
 647  
 648  
 649  
 650  
 651  
 652  
 653  
 654  
 655  
 656  
 657  
 658  
 659  
 660  
 661  
 662  
 663  
 664  
 665  
 666  
 667  
 668  
 669  
 670  
 671  
 672  
 673  
 674  
 675  
 676  
 677  
 678  
 679  
 680  
 681  
 682  
 683  
 684  
 685  
 686  
 687  
 688  
 689  
 690  
 691  
 692  
 693  
 694  
 695  
 696  
 697  
 698  
 699  
 700  
 701  
 702  
 703  
 704  
 705  
 706  
 707  
 708  
 709  
 710  
 711  
 712  
 713  
 714  
 715  
 716  
 717  
 718  
 719  
 720  
 721  
 722  
 723  
 724  
 725  
 726  
 727  
 728  
 729  
 730  
 731  
 732  
 733  
 734  
 735  
 736  
 737  
 738  
 739  
 740  
 741  
 742  
 743  
 744  
 745  
 746  
 747  
 748  
 749  
 750  
 751  
 752  
 753  
 754  
 755  
 756  
 757  
 758  
 759  
 760  
 761  
 762  
 763  
 764  
 765  
 766  
 767  
 768  
 769  
 770  
 771  
 772  
 773  
 774  
 775  
 776  
 777  
 778  
 779  
 780  
 781  
 782  
 783  
 784  
 785  
 786  
 787  
 788  
 789  
 790  
 791  
 792  
 793  
 794  
 795  
 796  
 797  
 798  
 799  
 800  
 801  
 802  
 803  
 804  
 805  
 806  
 807  
 808  
 809  
 810  
 811  
 812  
 813  
 814  
 815  
 816  
 817  
 818  
 819  
 820  
 821  
 822  
 823  
 824  
 825  
 826  
 827  
 828  
 829  
 830  
 831  
 832  
 833  
 834  
 835  
 836  
 837  
 838  
 839  
 840  
 841  
 842  
 843  
 844  
 845  
 846  
 847  
 848  
 849  
 850  
 851  
 852  
 853  
 854  
 855  
 856  
 857  
 858  
 859  
 860  
 861  
 862  
 863  
 864  
 865  
 866  
 867  
 868  
 869  
 870  
 871  
 872  
 873  
 874  
 875  
 876  
 877  
 878  
 879  
 880  
 881  
 882  
 883  
 884  
 885  
 886  
 887  
 888  
 889  
 890  
 891  
 892  
 893  
 894  
 895  
 896  
 897  
 898  
 899  
 900  
 901  
 902  
 903  
 904  
 905  
 906  
 907  
 908  
 909  
 910  
 911  
 912  
 913  
 914  
 915  
 916  
 917  
 918  
 919  
 920  
 921  
 922  
 923  
 924  
 925  
 926  
 927  
 928  
 929  
 930  
 931  
 932  
 933  
 934  
 935  
 936  
 937  
 938  
 939  
 940  
 941  
 942  
 943  
 944  
 945  
 946  
 947  
 948  
 949  
 950  
 951  
 952  
 953  
 954  
 955  
 956  
 957  
 958  
 959  
 960  
 961  
 962  
 963  
 964  
 965  
 966  
 967  
 968  
 969  
 970  
 971  
 972  
 973  
 974  
 975  
 976  
 977  
 978  
 979  
 980  
 981  
 982  
 983  
 984  
 985  
 986  
 987  
 988  
 989  
 990  
 991  
 992  
 993  
 994  
 995  
 996  
 997  
 998  
 999  
 1000

C SUBROUTINE ZEROM  
 SUBROUTINE ZEROM(A,I,K)  
 DIMENSION A(1)  
 II=I\*K  
 DO 10 J=1,II  
 10 A(J)=0.0  
 RETURN  
 END





```

1. C **** SUBROUTINE THES02
2. C SUBROUTINE THES02
3.
4. C COMMON NPART,KPNT,KELM,NGEO,NMAT,NFREE,NFOR
5. C 1,NSTART(45),NEND(45),NFIRST(45),NLAST(45)
6.
7. C DIMENSION NOD(8),EMOD(10),P(10),XE(8,2)
8. C 1,APJ(2,8,9),RFUN(9,8),X(600,2)
9.
10. C REWIND 2
11.
12. C **** READ SHAPE FUNCTIONS RFUN AND THEIR PARTIAL DERIVATIVES FROM FILE
13. C READ(2)((APJ(J,K,L),J=1,2),K=1,8),L=1,9),
14. C 1((RFUN(I,M),I=1,9),M=1,8)
15. C REWIND 4
16. C REWIND 4
17.
18. C **** READ DATA SET A
19. C READ(105,10)KPNT,KELM,NGEO,NMAT,NFREE,NFOR,NPART
20. C WRITE(108,20)KPNT,KELM,NGEO,NMAT,NFREE,NFOR,NPART
21. C WRITE(108,41)
22.
23. C **** READ DATA SET B
24. C DO 30 I=1,KPNT
25. C READ(105,40)(X(I,J),J=1,2)
26. C WRITE(108,50)I,(X(I,J),J=1,2)
27. C 30 CONTINUE
28. C WRITE(108,79)
29.
30. C **** READ DATA SET C
31. C DO 60 J=1,NMAT
32. C READ(105,70)EMOD(J),P(J)
33. C WRITE(108,80)J,EMOD(J),P(J)
34. C 60 CONTINUE
35. C REWIND 3
36. C WRITE(108,109)
37.
38. C **** READ DATA SET D
39. C DO 90 NX=1,KELM
40. C READ(105,100)(NOD(J),J=1,8),NEP
41. C WRITE(108,110)NX,(NOD(J),J=1,8),NEP
42. C DO 120 I=1,8
43. C JJ=200(I)
44. C DO 120 IX=1,NFREE
45. C XE(I,IX)=X(JJ,IX)
46. C 120
47.
48. C **** COMPUTE ELEMENT STIFFNESS MATRIX
49. C CALL THES03(APJ,RFUN,NX,EMOD(NEP),P(NEP),XE,NOD)
50. C 90 CONTINUE
51.
52. C 10 FORMAT(7I4)
53. C 20 FORMAT(1X,39HTOTAL NUMBER OF NODAL POINTS.....,I4/
54. C 11X,39HTOTAL NUMBER OF ELEMENTS.....,I4/
55. C 21X,39HNUMBER OF GEOMETRIC CONSTRAINTS.....,I4/
56. C 31X,39HNUMBER OF DIFFERENT MATERIALS.....,I4/
57. C 41X,39HNUMBER OF FREEDOM PER NOOE.....,I4/
58. C 51X,39HNUMBER OF NODES SUBJECTED TO FORCE.....,I4/
59. C 61X,39HNUMBER OF PARTITIONS.....,I4//)
60.
61. C 40 FORMAT(2F16.8)
62. C 41 FORMAT(10X,4HNODE,10X,13HR CO-ORDINATE,10X,13HZ CO-ORDINATE/)
63. C 50 FORMAT(10X,I4,7X,F16.4,7X,F16.4)
64. C 70 FORMAT(2F16.4)
65. C 79 FORMAT(1X,8HMATERIAL,2X,21HMODULUS OF ELASTICITY,2X,14HPDISSNS R
66. C 1TIO/)
67. C 80 FORMAT(1X,4X,I4,7X,F16.4,2X,F14.4)
68. C 100 FORMAT(9I4)
69. C 109 FORMAT(1X,7HELEMENT,9X,14HELEMENT NODES,9X,8HMATERIAL/)
70. C 110 FORMAT(1X,3X,I4,8I4,2X,I2)
71.
72. C **** READ DATA SET E
73. C DO 2000 J=1,NPART
74. C READ(105,2001)NSTART(J),NEND(J),NFIRST(J),NLAST(J)
75. C 2001 FORMAT(4I4)

```

81.  
82.  
83.  
84.  
85.  
86.

```
2002 WRITE(108,2002)NSTART(J),NEND(J),NFIRST(J),NLAST(J)  
2000 FORMAT(10X,4(I4,10X))  
C CONTINUE  
RETURN  
END
```

```

1. C**** SUBROUTINE THES03 SEPTEMBER 18,1973 F. X. JANUCIK
2. SUBROUTINE THES03(APJ,RFUN,NKO,E,P1,X,NODE)
3. C
4. COMMON NGPNT,KPNT,KELM,NGEO,MMAT,NFREE,NFOR
5. 1, NSTART(45),NEND(45),NFIRST(45),NLAST(45)
6. C
7. DIMENSION RFUN(9,8),APJ(2,8,9),CE(16,16),B(4,16),SCR(2,8),NODE(8
8. 1,X(8,2),AJO(2,2),C(9),D(4,4),AINT(4,16,9),CIN(16,16)
9. 1,RR(1,1),CFUN(1,8)
10. C
11. C**** DEFINE GAUSS QUADRATURE WEIGHT COEFFICIENTS
12. C
13. W1=0.55555556
14. W2=0.88888889
15. C
16. C(1)=W1**2
17. C(2)=W1**2
18. C(3)=W1**2
19. C(4)=W1**2
20. C(5)=W2**2
21. C(6)=W2**2
22. C(7)=W2**2
23. C(8)=W2**2
24. C(9)=W1**2
25. C
26. C**** INITIALIZE ELEMENT STIFFNESS MATRIX CE TO ZERO
27. CALL ZEROM(CE,16,16)
28. C
29. C**** CALCULATE ELASTICITY MATRIX D
30. C
31. C**** SET ELEMENT ELASTICITY MATRIX TO ZERO
32. CALL ZEROM(D,4,4)
33. EC1=P1/(1.+P1)
34. EC2=(1.-2.*P1)/(2.*(1.+P1))
35. EC3=(1.-P1)/((1.+P1)*(1.+2.*P1))
36. EC4=EC1*EC3
37. C
38. D(1,1)=EC3
39. D(1,2)=EC4
40. D(1,3)=EC4
41. C
42. D(2,1)=D(1,2)
43. D(2,2)=EC3
44. D(2,3)=EC4
45. C
46. D(3,1)=D(1,3)
47. D(3,2)=D(2,3)
48. D(3,3)=EC3
49. C
50. D(4,4)=EC2*EC3
51. C
52. C**** CALCULATE ELEMENT STIFFNESS MATRIX
53. C
54. DO 100 NGP=1,9
55. C**** CALCULATE JACOBIAN
56. CALL MATM(APJ(1,1,NGP),X,AJO,2,8,2)
57. DO 30 J=1,8
58. CFUN(1,J)=RFUN(NGP,J)
59. 30 CONTINUE
60. C**** CALCULATE RADIAL DISTANCE TO GAUSS SAMPLING POINT
61. CALL MATM(CFUN,X,RR,1,8,1)
62. C**** CALCULATE JACOBIAN INVERSE AND THE VALUE OF ITS DETERMINANT
63. CALL MTINVB(AJO,2,AREA)
64. C**** CALCULATE VOLUME ASSOCIATED WITH SAMPLING POINT NGP
65. VOL=6.283185*C(NGP)*RR(1,1)*AREA
66. CALL MATM(AJO,APJ(1,1,NGP),SCR,2,2,8)
67. C**** INITIALIZE THE B MATRIX TO ZERO
68. CALL ZEROM(B,4,16)
69. C**** CALCULATE THE B MATRIX AT SAMPLING POINT NGP
70. DO 200 I=1,8
71. X=2*I
72. J=2*I-1
73. B(1,J)=SCR(1,I)
74. B(2,J)=RFUN(NGP,I)/RR(1,1)
75. B(3,K)=SCR(2,I)
76. B(4,J)=SCR(2,I)
77. B(4,K)=SCR(1,I)
78.
79.
80.

```

```

200 CONTINUE
*** INITIALIZE MATRIX CIN TO ZERO
CALL ZEROX(CIN,16,16)
*** CALCULATE STIFFNESS CONTRIBUTION OF SAMPLING POINT NGP MATRIX CIN
*** MULTIPLY MATRIX B TIMES O TO GET STRESS MATRIX AINT AT POINT NGP
CALL MATM(O,B,AINT(1,1,NGP),4,4,16)
*** MULTIPLY MATRIX AINT TIMES THE B MATRIX TRANSPOSED TO GET CIN AT POINT NGP
CALL MTTSYM(S,AINT(1,1,NGP),CIN,16,4,16)
DO 400 J=1,16
DO 400 X=1,16
CE(J,X)=CE(J,X)+VOL*CIN(J,X)
400 CONTINUE
100 CONTINUE
*** WRITE THE ELEMENT STIFFNESS MATRIX, NODES, AND NUMBER TO TEMPORARY FILE 3
WRITE(3)((CE(J,I),J=1,16),I=1,16),(NODE(I),I=1,8),NKO
*** WRITE THE STRESS MATRICES AT THE NINE SAMPLING POINTS OF EACH ELEMENT TO 4
WRITE(4)((AINT(I,J,K),I=1,4),J=1,16),K=1,9)
1,(NODE(L),L=1,8)
RETURN
END

```

```

SUBROUTINE MTTSYM(O,B,OB,L,M,N)
DIMENSION D(M,L),B(M,N),OB(L,N)
DO 110 J=1,N
DO 110 I=1,L
IF(I.LT.J) OB(I,J)=OB(J,I)
IF(I.LT.L) GO TO 110
OB(I,J)=0.000000000
DO 120 K=1,M
OB(I,J)=OB(I,J)+O(K,I)*B(K,J)
120 CONTINUE
RETURN
END

```



## SUBROUTINE THES04

```

C *** EXTRAPOLATES STRESS MATRICES AT SAMPLING POINTS TO ELEMENT MIDSIDE NODE
COMMON NPART,KPNT,KELM,NGEO,NMAT,NFREE,NFOR
1,NSTART(45),NEND(45),NFIRST(45),NLAST(45)
C
C DIMENSION STR(4,16,4),NA(4),NODE(8),OB(4,16,9)
C
C REWIND 4
C *** DEFINE WEIGHT COEFFICIENTS
AA=1.47883056
AB=0.66666667
AC=0.18723611
C *** READ ELEMENT STRESS MATRICES AT GAUSS SAMPLING POINTS
C *** ALSO ELEMENT NODAL POINT NUMBERS
READ(4)((OB(I,J,K),I=1,4),J=1,16),K=1,9)
1,(NODE(L),L=1,8)
C
C *** INITIALIZE MIDSIDE NODE STRESS MATRICES TO ZERO
DO 2 I1=1,16
DO 2 J1=1,4
DO 2 K1=1,4
2 STR(J1,I1,K1)=0.0000000
C *** CALCULATE STRESS MATRICES AT MIDSIDE NODES
DO 3 I2=1,4
DO 3 J2=1,16
STR(I2,J2,1)=AC*OB(I2,J2,4)+AB*OB(I2,J2,5)+AA*OB(I2,J2,6)
STR(I2,J2,2)=AA*OB(I2,J2,2)+AB*OB(I2,J2,5)+AC*OB(I2,J2,8)
STR(I2,J2,3)=AA*OB(I2,J2,4)+AB*OB(I2,J2,5)+AC*OB(I2,J2,6)
STR(I2,J2,4)=AC*OB(I2,J2,2)+AB*OB(I2,J2,5)+AA*OB(I2,J2,8)
3 CONTINUE
C *** DEFINE MIDSIDE NODES ASSOCIATED WITH CALCULATED STRESS MATRICES
DO 4 J6=1,4
J7=2*J6
NA(J6)=NODE(J7)
4 CONTINUE
C
C *** WRITE STRESS MATRICES AND THE NODE ASSOCIATED WITH EACH AND ALSO ELEMENT
C *** NODES TO TEMPORARY FILE 2
WRITE(2)((STR(I,J,K),I=1,4),J=1,16),K=1,4)
1,(NA(L),L=1,4),(NODE(L),L=1,8)
1 CONTINUE
RETURN
END

```

```

1
2
3
4
5
6
7
8
9
10
11
12
13
14
15
16
17
18
19
20
21
22
23
24
25
26
27
28
29
30
31
32
33
34
35
36
37
38
39
40
41
42
43
44
45
46
47
48
49
50
51
52
53
54
55
56
57
58
59
60
61
62
63
64
65
66
67
68
69
70
71
72
73
74
75
76
77
78
79
80
81
82
83
84
85
86
87
88
89
90
91
92
93
94
95
96
97
98
99
100
101
102
103
104
105
106
107
108
109
110
111
112
113
114
115
116
117
118
119
120
121
122
123
124
125
126
127
128
129
130
131
132
133
134
135
136
137
138
139
140
141
142
143
144
145
146
147
148
149
150
151
152
153
154
155
156
157
158
159
160
161
162
163
164
165
166
167
168
169
170
171
172
173
174
175
176
177
178
179
180
181
182
183
184
185
186
187
188
189
190
191
192
193
194
195
196
197
198
199
200
201
202
203
204
205
206
207
208
209
210
211
212
213
214
215
216
217
218
219
220
221
222
223
224
225
226
227
228
229
230
231
232
233
234
235
236
237
238
239
240
241
242
243
244
245
246
247
248
249
250
251
252
253
254
255
256
257
258
259
260
261
262
263
264
265
266
267
268
269
270
271
272
273
274
275
276
277
278
279
280
281
282
283
284
285
286
287
288
289
290
291
292
293
294
295
296
297
298
299
300
301
302
303
304
305
306
307
308
309
310
311
312
313
314
315
316
317
318
319
320
321
322
323
324
325
326
327
328
329
330
331
332
333
334
335
336
337
338
339
340
341
342
343
344
345
346
347
348
349
350
351
352
353
354
355
356
357
358
359
360
361
362
363
364
365
366
367
368
369
370
371
372
373
374
375
376
377
378
379
380
381
382
383
384
385
386
387
388
389
390
391
392
393
394
395
396
397
398
399
400
401
402
403
404
405
406
407
408
409
410
411
412
413
414
415
416
417
418
419
420
421
422
423
424
425
426
427
428
429
430
431
432
433
434
435
436
437
438
439
440
441
442
443
444
445
446
447
448
449
450
451
452
453
454
455
456
457
458
459
460
461
462
463
464
465
466
467
468
469
470
471
472
473
474
475
476
477
478
479
480
481
482
483
484
485
486
487
488
489
490
491
492
493
494
495
496
497
498
499
500
501
502
503
504
505
506
507
508
509
510
511
512
513
514
515
516
517
518
519
520
521
522
523
524
525
526
527
528
529
530
531
532
533
534
535
536
537
538
539
540
541
542
543
544
545
546
547
548
549
550
551
552
553
554
555
556
557
558
559
560
561
562
563
564
565
566
567
568
569
570
571
572
573
574
575
576
577
578
579
580
581
582
583
584
585
586
587
588
589
590
591
592
593
594
595
596
597
598
599
600
601
602
603
604
605
606
607
608
609
610
611
612
613
614
615
616
617
618
619
620
621
622
623
624
625
626
627
628
629
630
631
632
633
634
635
636
637
638
639
640
641
642
643
644
645
646
647
648
649
650
651
652
653
654
655
656
657
658
659
660
661
662
663
664
665
666
667
668
669
670
671
672
673
674
675
676
677
678
679
680
681
682
683
684
685
686
687
688
689
690
691
692
693
694
695
696
697
698
699
700
701
702
703
704
705
706
707
708
709
710
711
712
713
714
715
716
717
718
719
720
721
722
723
724
725
726
727
728
729
730
731
732
733
734
735
736
737
738
739
740
741
742
743
744
745
746
747
748
749
750
751
752
753
754
755
756
757
758
759
760
761
762
763
764
765
766
767
768
769
770
771
772
773
774
775
776
777
778
779
780
781
782
783
784
785
786
787
788
789
790
791
792
793
794
795
796
797
798
799
800
801
802
803
804
805
806
807
808
809
810
811
812
813
814
815
816
817
818
819
820
821
822
823
824
825
826
827
828
829
830
831
832
833
834
835
836
837
838
839
840
841
842
843
844
845
846
847
848
849
850
851
852
853
854
855
856
857
858
859
860
861
862
863
864
865
866
867
868
869
870
871
872
873
874
875
876
877
878
879
880
881
882
883
884
885
886
887
888
889
890
891
892
893
894
895
896
897
898
899
900
901
902
903
904
905
906
907
908
909
910
911
912
913
914
915
916
917
918
919
920
921
922
923
924
925
926
927
928
929
930
931
932
933
934
935
936
937
938
939
940
941
942
943
944
945
946
947
948
949
950
951
952
953
954
955
956
957
958
959
960
961
962
963
964
965
966
967
968
969
970
971
972
973
974
975
976
977
978
979
980
981
982
983
984
985
986
987
988
989
990
991
992
993
994
995
996
997
998
999
1000

```





```

1. MATRIX INVERSION, MODIFIED 2/4/72 BY S. LEVY
2. SUBROUTINE INVC(A,N,N,SIZE)
3. A IS MATRIX BEING INVERTED
4. N IS MATRIX SIZE
5. SIZE IS MEMORY SIZE
6. DIMENSION A(40), IPIVOT(40), INDEX(40,2), PIVOT(40)
7. * * * * *
8. * * * * *
9. * * * * *
10. * * * * *
11. * * * * *
12. * * * * *
13. * * * * *
14. * * * * *
15. DO 200 J=1,N
16. IPIVOT(J)=0
17. DO 550 I=1,N
18. * * * * *
19. * * * * *
20. * * * * *
21. * * * * *
22. * * * * *
23. * * * * *
24. * * * * *
25. * * * * *
26. * * * * *
27. * * * * *
28. * * * * *
29. * * * * *
30. * * * * *
31. * * * * *
32. * * * * *
33. * * * * *
34. * * * * *
35. * * * * *
36. * * * * *
37. * * * * *
38. * * * * *
39. * * * * *
40. * * * * *
41. * * * * *
42. * * * * *
43. * * * * *
44. * * * * *
45. * * * * *
46. * * * * *
47. * * * * *
48. * * * * *
49. * * * * *
50. * * * * *
51. * * * * *
52. * * * * *
53. * * * * *
54. * * * * *
55. * * * * *
56. * * * * *
57. * * * * *
58. * * * * *
59. * * * * *
60. * * * * *
61. * * * * *
62. * * * * *
63. * * * * *
64. * * * * *
65. * * * * *
66. * * * * *
67. * * * * *
68. * * * * *
69. * * * * *
70. * * * * *
71. * * * * *
72. * * * * *

```





